



**HAL**  
open science

## $\sigma$ -H–H, $\sigma$ -C–H, and $\sigma$ -Si–H Bond Activation Catalyzed by Metal Nanoparticles

Juan Manuel Asensio, Donia Bouzouita, Piet W N M van Leeuwen, Bruno  
Chaudret

► **To cite this version:**

Juan Manuel Asensio, Donia Bouzouita, Piet W N M van Leeuwen, Bruno Chaudret.  $\sigma$ -H–H,  $\sigma$ -C–H, and  $\sigma$ -Si–H Bond Activation Catalyzed by Metal Nanoparticles. *Chemical Reviews*, 2019, 10.1021/acs.chemrev.9b00368 . hal-02337400

**HAL Id: hal-02337400**

**<https://hal.science/hal-02337400>**

Submitted on 29 Oct 2019

**HAL** is a multi-disciplinary open access archive for the deposit and dissemination of scientific research documents, whether they are published or not. The documents may come from teaching and research institutions in France or abroad, or from public or private research centers.

L'archive ouverte pluridisciplinaire **HAL**, est destinée au dépôt et à la diffusion de documents scientifiques de niveau recherche, publiés ou non, émanant des établissements d'enseignement et de recherche français ou étrangers, des laboratoires publics ou privés.

# $\sigma$ -H-H, $\sigma$ -C-H and $\sigma$ -Si-H Bond Activation catalyzed by Metal Nanoparticles

*Juan M. Asensio,\* Donia Bouzouita, Piet W. N. M. van Leeuwen and Bruno Chaudret.\**

LPCNO, Université de Toulouse, CNRS, INSA, UPS, 135 avenue de Rangueil, 31077 Toulouse, France.

Juan M. Asensio: asensior@insa-toulouse.fr

Bruno Chaudret: chaudret@insa-toulouse.fr

## **Abstract**

Activation of H–H, Si–H and C–H bonds through  $\sigma$ -bond coordination has grown in the past 30 years from a scientific curiosity to an important tool in the functionalization of hydrocarbons. Several mechanisms were discovered via which the initially  $\sigma$ -bonded substrate could be converted: oxidative addition, heterolytic cleavage,  $\sigma$ -bond metathesis, electrophilic attack, etc. The use of metal nanoparticles (NPs) in this area is a more recent development, but obviously nanoparticles offer a much richer basis than classical homogeneous and heterogeneous catalysts for tuning reactivity for such a demanding process as C–H functionalization. Here, we will review the surface chemistry of nanoparticles and catalytic reactions occurring in the liquid phase, catalyzed either by colloidal or supported metal NPs. We consider nanoparticles prepared in solution, which are stabilized and tuned by polymers, ligands and supports. The question we have addressed concerns the differences and similarities between molecular complexes and metal NPs in their reactivity towards  $\sigma$ -bond activation and functionalization.

## **Table of Contents:**

Table of Contents:.....	1
1. Introduction.....	2
2. H-H and D-D activation on metal NPs.....	4
2.1. Ru NPs in the H-H activation. Surface hydrides characterization.....	5
2.2. Other metal NPs in the H-H activation.....	11
2.2.1. Subsurface hydrides.....	11
2.2.2. Ligand effects: ligand assisted H-H cleavage.....	14

2.2.3. $\sigma$ -H activation promoted by light. ....	15
3. C-H activation by metal NPs. ....	16
3.1. H-D exchange catalyzed by metal NPs. ....	17
3.2. C-C bond formation. ....	28
3.2.1. Pd NPs for the C-H activation/C-C bond formation. Leached active species vs. surface-catalysis. ....	29
3.2.2. Au NPs in the C-H functionalization of C(sp)-H bonds and beyond. ....	37
3.2.3. Other metal NPs in C(sp)-H activation. ....	39
3.3. C-X Bond formation. ....	42
3.3.1. Oxidative C-H activation to afford C-O bonds. ....	42
3.3.2 C-H bond activation in the formation of other bonds. ....	45
3.3.2.1 C-H bond activation for C-N formation. ....	46
3.3.2.2 C-H bond activation for chalcogenation and halogenation. ....	47
4. Si-H activation by metal NPs. ....	49
4.1. Hydrosilylation. ....	50
4.1.1. Platinum NPs as catalysts for hydrosilylation of C-C multiple bonds. ....	51
4.1.2. Other metallic nanoparticles as catalysts for hydrosilylation of functional groups. ....	56
4.1.2.1 Au. ....	56
4.1.2.2. Pd. ....	57
4.1.2.3. Rh. ....	61
4.1.2.4. Ni. ....	62
4.1.3. Bimetallic NPs as new catalytic systems for hydrosilylation reactions. ....	64
4.2. Silane oxidation. ....	69
4.2.1. Silanol formation catalyzed by metal NPs. ....	69
4.2.2. Other catalytic reactions involving oxidation of silanes. ....	73
5. Conclusions. ....	75
6. Acknowledgements. ....	76
7. Bibliography. ....	76
8. Biography of authors. ....	94
Table of Content: ....	95

## 1. Introduction.

Activation of H-H, Si-H and C-H bonds through  $\sigma$ -bond coordination has attracted a lot of interest and experienced spectacular developments in organometallic chemistry for the past 30 years. Reactions of dihydrogen and metal complexes have a long history, from heterolytic cleavage on copper acetate<sup>1</sup> to the first observation of dihydrogen oxidative addition by Vaska in 1962<sup>2</sup> and oxidative addition to rhodium for catalytic hydrogenation of olefins,<sup>3</sup> but at this time, for these reactions no metal-H<sub>2</sub>  $\sigma$ -bonds were invoked. Since the first demonstration by Kubas of the existence

of a stable dihydrogen complex,<sup>4</sup> numerous examples of such species have been discovered,<sup>5-9</sup> including bis(dihydrogen) derivatives.<sup>10</sup> Stable silane complexes have also been known and discussed either as  $\sigma$ -bond complexes or as complexes containing a bridging hydride since the seminal works of Schubert<sup>11</sup> and Kubas.<sup>12</sup> Although C-H activation has been widely studied by Crabtree and many others,<sup>13</sup> only a limited number of  $\sigma$ -C-H bond complexes has been observed or isolated.<sup>14-19</sup> These species are important in terms of reactivity since, for example, they have contributed to the understanding of important catalytic reactions such as low barrier exchange reactions in the coordination sphere of a complex, C-H functionalization, heterolytic cleavage of dihydrogen, and hydrogenation of polar substrates such as ketones. From a mere curiosity  $\sigma$ -C-H-bond activation has therefore become a major tool in organic synthesis nowadays that avoids in several instances the use of toxic reagents and production of salts.<sup>20</sup>

In heterogeneous catalysis, dihydrogen activation has been known ever since Sabatier described the catalytic hydrogenation of unsaturated substrates using “finely divided metals” which led to his Nobel Prize in 1913.<sup>21</sup> Heterogeneous catalysis has developed numerous processes involving activation of hydrogen or hydrocarbons, but in this review we will look at similar processes occurring on the surface of nanoparticles. Surfaces show a much richer coordination chemistry towards substrates, while nanoparticles have a much higher number of atoms exposed than the particles occurring in heterogenous catalysis.

Here, we will focus on the surface chemistry of nanoparticles and catalytic reactions occurring in the liquid phase under mild conditions, catalyzed either by colloidal or supported NPs, which have emerged in the past 20 years. We consider nanoparticles prepared in solution stabilized by polymers, ligands or inorganic supports and the reactivity of which is analyzed by combining those techniques derived from molecular chemistry and those typical of material chemistry and heterogeneous catalysis. The question we want to address concerns the specificity, or not, of the reactivity of such nano-objects compared to traditional heterogeneous catalysts and the possible correspondence between the mode of coordination observed in molecular complexes and the interactions of substrates and ligands with nanoparticles.

On the other hand, several catalysts that initially were supposed to be homogeneous, have later been shown to be decomposed under the reaction conditions to give metal NPs.<sup>22</sup> However, the nature of the active species in many cases remains unclear, as NPs, intermediate species formed during the decomposition process (i.e. “naked” atoms, clusters, etc.) or leached species could be responsible for the catalytic activity. Here, we will discuss those cases in which the nature of the active species has been studied in detail or at least proposed based on experimental evidences.

In this review, we will therefore consider the interaction of  $\sigma$ -bonds with the surface of metal nanoparticles. This will be divided into:

- Surface studies concerning the interactions of H-H, C-H and Si-H bonds with the surface of nanoparticles defined as separate objects amenable to studies in solution or after deposition on a support. We exclude the literature concerning surface studies in vacuo or heterogeneous catalysts prepared according to classical methods.

- Transformations involving H-H, C-H and Si-H catalyzed by nanoparticles. We will exclude hydrogenation since many recent reviews have been dedicated to this reaction;<sup>23</sup> we will just give their references. C-H functionalization by metal NPs was reviewed by Gómez and Pla in 2016,<sup>24</sup> but this topic will be revisited in the present work. However, hydrosilylations by nanoparticles have not been recently reviewed and these reactions will be discussed in detail.

## 2. H-H and D-D activation on metal NPs.

Catalytic hydrogenation is probably the most studied reaction and includes substrates such as N<sub>2</sub>, CO, CO<sub>2</sub>, as well as unsaturated organic compounds. A review by Zaera described recently the surface chemistry of heterogeneous hydrogenation catalysts.<sup>23</sup> Here we will consider the interaction of metal nanoparticles in solution with hydrogen, which are synthesized in the presence of organic ligands that act as stabilizers because otherwise the NPs would agglomerate to give metallic deposits. We will further study the modes of coordination of hydrogen on these nanoparticles and, when available, the dynamics of coordinated hydrogen.

As mentioned above, formation of stable dihydrogen complexes has been known for more than 30 years.<sup>25</sup> These complexes contain a 3-center-2-electron bond<sup>26</sup> as a result of the interaction between the  $\sigma$ -molecular orbital of the H<sub>2</sub> molecule and an empty orbital of the metal center. In addition, back-donation from the d orbitals of the metal to the  $\sigma^*$ -H-H molecular orbital can also participate in bonding (Figure 1). These complexes can exist as an equilibrium between the  $\sigma$ -complex and the dihydride complex that formally involves an oxidative addition to the metal center.<sup>6</sup> On the other hand, metal NPs are well-known to activate H-H  $\sigma$ -bonds, and solid-state NMR studies suggest that  $\sigma$ -H<sub>2</sub> species can exist at the surface of metal NPs.<sup>27</sup> Therefore, the classical organometallic understanding of these chemical bonds can be used as model to understand  $\sigma$ -H-H activation with metal NPs to give surface hydrides.

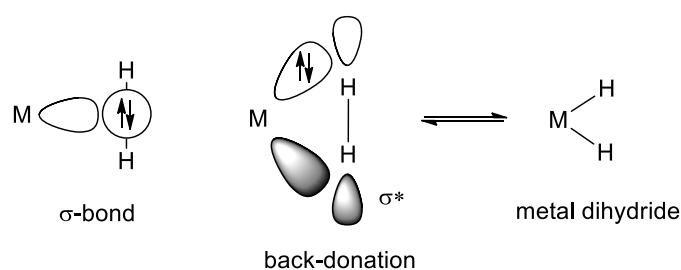


**Figure 1.** Bonding in a  $\sigma$ -H<sub>2</sub> complex and oxidative addition

Hydrogen activation has been explored for many metal NPs, either dispersed in solution or after deposition on a support, of which the most widely studied have been Pd, Pt, Ru and Rh NPs. Characterization of the coordination mode of hydrogen molecules at the surface of the NPs can help to understand their behavior and reactivity. However, direct characterization of surface hydrides is a challenging task. Many efforts to quantify the amount of surface hydrogen have been undertaken, which involve hydrogen evolution after thermal desorption or other indirect methods,<sup>28-29</sup> but direct detection of hydrides has been less explored.

The main application of the  $\sigma$ -bond activation of H-H is the catalytic hydrogenation of organic molecules, although there are other promising applications such as hydrogen storage.<sup>23,30-39</sup> Herein, we will focus on the characterization of hydrogen and deuterium at the surface of metal NPs and on their direct observation, mainly through Nuclear Magnetic Resonance. Last, we will briefly discuss how ligands can modulate the homolytic or heterolytic nature of the H-H cleavage, which can lead to different catalytic activity and selectivity.

### **2.1. Ru NPs in the H-H activation. Surface hydrides characterization.**

Ru is a very well-known catalyst for the activation of H-H bonds in both homogeneous and heterogeneous phase,<sup>40-42</sup> and has been widely used in hydrogenation catalysis.<sup>43-46</sup> In addition, several model molecular ruthenium compounds were prepared, accommodating different modes of coordination of hydrogen, namely terminal,  $\mu_2$ -bridging,  $\mu_3$ -bridging,  $\eta^2$ -dihydrogen and even interstitial (see Figure 2).<sup>27,47-48</sup> Our research group has a large experience in the synthesis of Ru NPs after decomposition of organometallic precursors under a reductive atmosphere of hydrogen. Ru NPs stabilized by different ligands such as alcohols,<sup>49</sup> N-heterocyclic carbenes,<sup>50</sup> phosphines,<sup>51</sup> carboxylates<sup>52</sup> or amines<sup>53</sup> have been prepared by this methodology. Therefore, qualitative and quantitative analyses of surface hydrides is essential for understanding spectroscopic features and reactivity of these NPs.

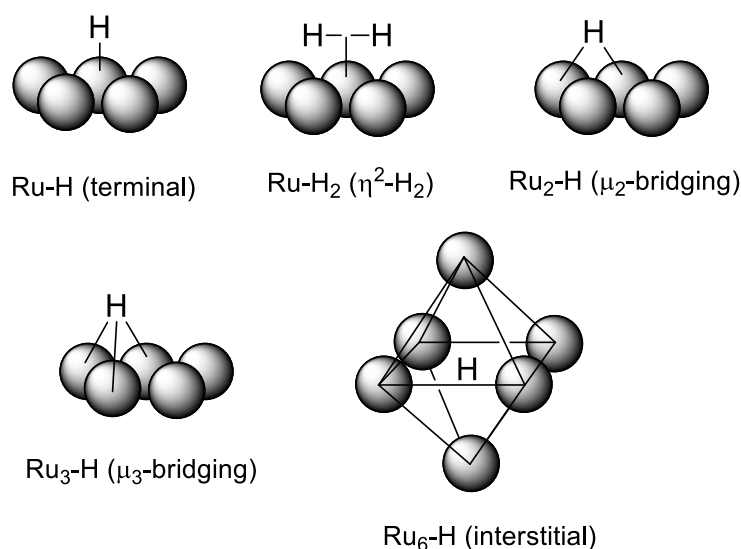


**Figure 2.** Different coordination modes of H/H<sub>2</sub> to Ru NPs.

Initially it was suggested that Ru NPs prepared through decomposition of an organometallic precursor in the presence of H<sub>2</sub> and stabilized by hexadecylamine ligands (HDA), contained surface hydrides that were released as H<sub>2</sub> into the solution as observed by <sup>1</sup>H NMR.<sup>53</sup> However, direct characterization of hydride coordination to Ru was not possible, neither by liquid nor solid state NMR. In 2005, Buntkowsky, Limbach, and co-workers studied the presence of surface hydrides in Ru NPs by the use of NMR.<sup>54</sup> Thus, Ru NPs initially treated with molecular H<sub>2</sub> were, after removal of the gas phase under vacuum, subjected to a D<sub>2</sub> atmosphere. Gas phase <sup>1</sup>H NMR monitoring evidenced the appearance of a signal corresponding to H-D and allowed the titration of surface hydrides. Later, in 2008, the amount of hydrides at the surface of various *hcp*-Ru NPs, stabilized by polyvinylpyrrolidone (PVP), hexadecylamine (HDA) and bis(diphenylphosphino)decane (dppd), was quantified by titration with an olefin (1-octene and norbornene) taking advantage of the high reactivity of Ru NPs as a hydrogenation catalyst.<sup>55</sup> Knowing the conversions and the size of the NPs, the number of surface hydrides per surface Ru atom could be estimated as 1.3, 1.3 and 1.1 for Ru/PVP, Ru/HDA and Ru/dppd respectively. Similarly, Berthoud et al. determined the number of hydrogens per surface Ru atom in Ru NPs of 2 nm supported on SiO<sub>2</sub> through adsorption measurements.<sup>56</sup> In this work, the authors determined that the NPs were able to adsorb approximately 2 H atoms per surface Ru. The higher capacity to adsorb H atoms at the surface of these NPs may be related to the absence of coordinating ligands and hence to a more available surface. Surface hydrides were also quantified on nanoparticles stabilized by ionic liquids.<sup>57-58</sup> In this case, it was found that the size of the nanoparticles was determined by the size of the lipophilic domains present in the nanostructured

ionic liquids. This demonstrated that naked ruthenium hydride nanoparticles are lipophilic, in agreement with the very low polarization of the Ru-H bond.

Direct detection of adsorbed deuterium was carried out by static solid state  $^2\text{H}$  NMR.<sup>59-60</sup> By analysis of the quadrupolar coupling constants ( $Q_{cc}$ ), which are characteristic of the degree of anisotropy experienced by a quadrupolar nucleus, solid state NMR can help to understand all the possible coordination modes of deuterium that can co-exist on a metal NP. Hence, measurements on Ru/PVP, Ru/HDA and Ru/dppb evidenced the presence of the fluxionality of deuterium on the surface of the particles (see Figure 3). After freezing this mobility at 200 K, the presence of mostly bridging deuterides and possibly dideuterium coordination was established. Interstitial hydrogen atoms have not been observed and DFT calculations confirm that all hydrogen atoms are located at the surface.<sup>61</sup> In the case of Ru NPs stabilized by metal-organic frameworks (MOFs),<sup>62</sup> surface-adsorbed D atoms were observed by solid state NMR spectroscopy, which in this case displayed high mobility even down to 40 K. This effect was attributed to the weak interaction between the MOF and the Ru NPs in comparison to stabilizing ligands such as HDA.

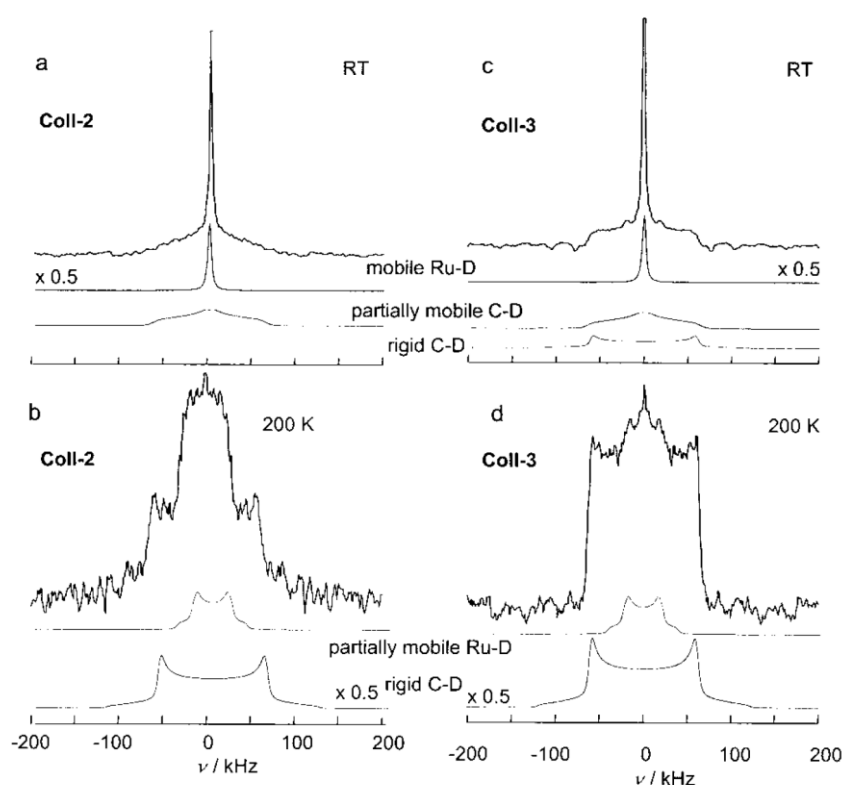


**Figure 3.** Solid-state 45.7 MHz  $^2\text{H}$  NMR spectra of static samples of Ru/HDA particles after H–D exchange performed in the solid state (**Coll-2**) and in solution (**Coll-3**) at room temperature (a and c) or at 200 K (b and d). The experimental spectra correspond to the sum of the corresponding subspectra. Reprinted with permission from ref 54. Copyright 2005 John Wiley and Sons.



In 2009, Truflandier et al. performed both DFT calculations to understand the coordination mode of H to Ru (1000) surfaces with more than 1 H per Ru atom,<sup>63</sup> and simulations to fit the results previously obtained by <sup>2</sup>H solid state NMR by Pery et al.<sup>54</sup> The authors proposed the existence of different types of surface hydrides (terminal and  $\mu_3$ -bridging), which were mobile in all cases. One-fold sites (terminal or on-top coordination, labeled in green in Figure 4) are not energetically favored at low hydrogen coverage, where H binds preferentially at three-fold sites ( $\mu_3$ -bridging *fcc* coordination, labeled in blue in Figure 4). When the coverage was higher than 1 H per Ru surface atom, and the surface saturated in three-fold sites, the hydrides occupy the on-top sites, leading to the most stable systems. In other words, the on-top coordination of hydrides, which has a transition-state nature at low coverage values, becomes stabilized after saturation of the Ru surface, i.e. when the number of H atoms per surface Ru is larger than 1.

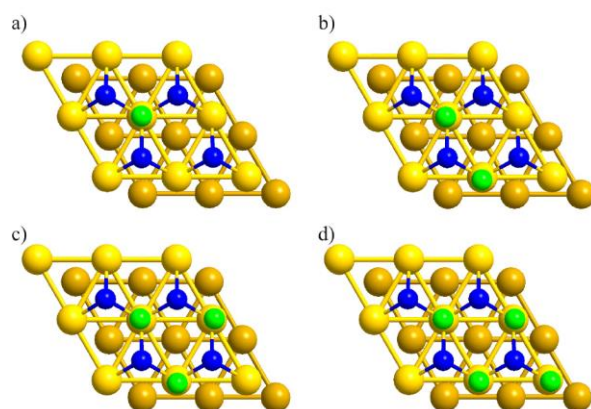


**Figure 4.** Surface hydrides preferentially bind as  $\mu_3$ -bridging species (blue). After full coverage of the three-fold sites, surface hydrides adopt the less energetically favoured terminal coordination (green). The image shows the on-top coordination of (a) 1, (b) 2, (c) 3 or (d) 4 hydrides after saturation of the three-fold sites. Reprinted with permission from ref 63. Copyright 2009 John Wiley and Sons.

A further development of DFT calculations for Ru-carbonyl clusters with different amounts of D permitted to effectively calculate the energy levels for the d orbital of each surface atom in its chemical environment.<sup>61</sup> This model led to a better understanding of the coordination mode of D to the surface of Ru NPs and corroborated the <sup>2</sup>H NMR observations. The co-existence of different surface adsorbed deuterides contrasts with the model proposed above for a Ru (1000) surface that contained only terminal and  $\mu_3$ -bridging D. This can be expected as the NPs surface is more diverse than a Ru (1000) surface. The presence of more energetic sites located at the edges and corners and

the exposure of different crystallographic facets makes the NPs more complex systems. However, a model that incorporates all different coordination modes of hydrogen is compatible with the presence of more than 1 H per Ru surface atom. For instance, Lara et al. reported a space-filling model of 1.8 nm *hcp*-Ru NPs stabilized by an N-Heterocyclic Carbene (NHC) ligand that was able to accommodate 1.5 hydrides per surface Ru.<sup>50</sup>

Bumüller and co-workers have recently reported on DFT calculations of H<sub>2</sub> adsorption onto Ru nanoclusters of 19 Ru atoms.<sup>64</sup> In contrast to large Ru NPs, which present an *hcp* structure, Ru<sub>19</sub><sup>-</sup> possesses a closed-shell octahedral *fcc* structure. Interestingly, in the Ru<sub>19</sub>D<sub>x</sub><sup>-</sup> nanocluster range containing 0 to 40 D atoms, there is a transition from the octahedral *fcc* to a bi-icosahedral structure at 20 D atoms, to maximize the adsorption energy of D. In addition, hydrogen atoms coordinate at two-fold sites on both cluster core motifs, in contrast to flat surfaces where a three-fold coordination is preferred.

Recently, Limbach et al. described a new approach to understand the D<sub>2</sub> activation mechanism by Ru NPs covered with H<sub>2</sub> using gas phase <sup>1</sup>H NMR.<sup>65</sup> The authors compared two possible mechanistic routes: a dissociative vs. an associative exchange (see Figure 5). In the latter mechanism a molecule of D<sub>2</sub> coordinates to Ru, forms a D–D–H intermediate, that releases HD.<sup>66</sup> In this work, the authors observed the formation of only H-D and no H<sub>2</sub> at the beginning of the reaction when using Ru/PVP and Ru/HDA NPs. This agrees with an associative exchange model, which prevails around room temperature and normal pressures, the conditions used for catalytic hydrogenation with Ru NPs. In addition, the associative exchange mechanism is coherent with the kinetic profile of the reaction.

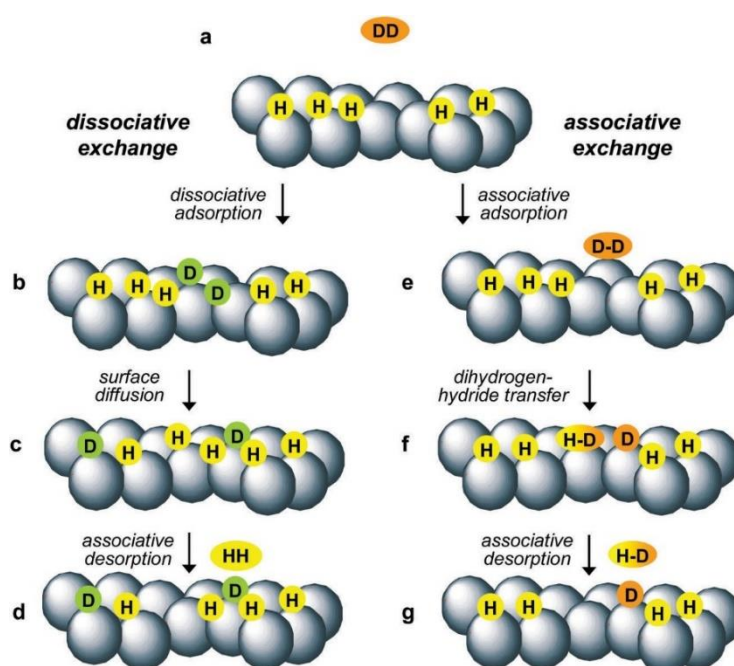


**Figure. 5.** Mechanisms of equilibration of gaseous D<sub>2</sub> in contact with a Ru surface covered with H<sub>2</sub>. Left side: Dissociative exchange model that consists in dissociative adsorption, surface diffusion and associative desorption, which operates at low temperatures and low pressures. Right side: Associative exchange model that consists in an associative adsorption, followed by hydride transfer and associative desorption. Reprinted with permission from ref 65. Copyright 2018 Royal Society of Chemistry.

Rothermel et al. have extended the characterization of surface hydrides coordinated to monometallic and bimetal NPs.<sup>67</sup> Three different systems were prepared in this work: Ru/dppb, Pt/dppb and RuPt/dppb (dppb=1,4-bis(diphenylphosphino)butane). After treatment with D<sub>2</sub>, the authors carried out the characterization of the products via gas-phase NMR, GC-MS and <sup>13</sup>C and <sup>31</sup>P solid-state NMR. An interesting finding of this work was that several deuterated aliphatic products namely deuterated butane and cyclohexane together with H-D were formed. These molecules arise from the decomposition of the dppb ligand through the cleavage of C-P bonds.

Another important field is the comprehension of the  $\sigma$ -bond activation of H<sub>2</sub> in the presence of CO molecules, which is highly relevant for the understanding of the mechanism of the Fischer-Tropsch reaction. Thus, the competition between the coordination of H<sub>2</sub> and CO at the surface of Ru/PVP and Ru/dppb was investigated by Novio et al. in 2010.<sup>68</sup> Titration of hydrides was carried out after exposure to a CO atmosphere for 15 min (Ru/PVP/CO and Ru/dppb/CO), or after exposure to a CO atmosphere and followed by a H<sub>2</sub> atmosphere during 6 h (Ru/PVP/CO/H<sub>2</sub> and Ru/dppb/CO/H<sub>2</sub>). It was observed that after exposure to CO the amount of surface hydrides decreased to 0, due to the complete coverage of the NPs surface by CO molecules. Exposure to H<sub>2</sub> of these NPs did not lead to the initial number of hydrides per surface Ru, 0.3 and 0.2 in Ru/PVP and Ru/dppb respectively, because only a part of the adsorbed CO molecules was replaced by H<sub>2</sub> under the conditions applied. The competition between CO and H<sub>2</sub> coordination to Ru NPs was further studied in 2016 by Cusinato et al.<sup>69</sup> The authors performed a comparison between theoretical calculations and experimental results to understand the surface composition of Ru NPs of 1 nm size in the presence of a *syngas* mixture (CO:H<sub>2</sub>). In this report it was shown that under FT reaction conditions (~450 K and 1-3 bar of *syngas*) the NPs were saturated with surface adsorbed CO and that no co-adsorption of H<sub>2</sub> took place. The onset of the FT reaction with H<sub>2</sub> likely involved the exothermic, simultaneous CO dissociation and water formation.

Finally, a few studies of supported Ru NPs have been reported, in which the nature of the support has shown to be important for H diffusion from the particle (the so-called hydrogen spillover). For example, theoretical studies of Ru NPs supported on TiO<sub>2</sub> or tetragonal ZrO<sub>2</sub> showed that  $\sigma$ -H<sub>2</sub> activation occurs at the Ru NP surface, whereas the nature of the support determines the energetic

barrier for H spillover.<sup>70</sup> In another study, Fernandez et al. reported on the kinetics of H<sub>2</sub> adsorption and the mobility in Ru/ $\gamma$ -Al<sub>2</sub>O<sub>3</sub>.<sup>71</sup> The authors concluded that larger Ru NPs (of ~10 nm) can activate H<sub>2</sub> and that the adsorbed hydrides were highly mobile on the Al<sub>2</sub>O<sub>3</sub> surface. In contrast, in the case of smaller Ru NPs (of ~3 nm), hydrogen adsorption led to strongly coordinated hydrides with low diffusivity towards the support. Comprehension of the coordination mode and the mobility of the hydrides allowed the authors to propose a more accurate kinetic model for the low-temperature ammonia synthesis.

## 2.2. Other metal NPs in the H-H activation.

Characterization of surface hydrides has been mainly performed on Ru NPs, but there are a few works exploring the surface coordination of dihydrogen to other metallic systems. Hydrogen activation catalyzed by supported metal NPs has been widely explored and it is well-known that hydrides can migrate from the NPs surface to the support, the so-called hydrogen spillover, or to the interior of the NPs.<sup>70,72-73</sup> This topic presents interesting applications in the fields of hydrogen storage, catalytic hydrogenation or isotopic exchange,<sup>73</sup> but will not be discussed herein.

Unlike Ru, Pd shows the formation of bulk hydrides and thus Pd can be used for hydrogen storage. Numerous studies have been devoted to bulk Pd and Pd NPs immobilized on many supports. A variety of sophisticated surface analysis techniques has been applied to identify surface and sub-surface hydrogen. To the best of our knowledge, few examples of H<sub>2</sub> activation by soluble metal NPs have been reported in which the presence of surface hydrides has been directly observed, as many surface science spectroscopic techniques cannot be used in solution. Notably, the formation of weakly bonded surface hydrides in Pd NPs makes them more active than clean Pd surfaces in catalytic hydrogenation of alkenes at low H<sub>2</sub> pressures.<sup>74</sup> Pd NPs have been widely studied for hydrogen storage applications<sup>75</sup> and thus several techniques for indirect detection of the formation of Pd hydrides have been explored. For instance, hydride formation has been determined by luminescence,<sup>76</sup> or by plasmonic shifting of Au NPs in contact with Pd nanocubes.<sup>77</sup> However, direct characterization of surface hydrides on Pd NPs has been less explored. As an example, one experimental proof of the formation of metal-hydrides in Pd NPs was provided by Zlotea et al. in 2010. The authors used *in situ* X-Ray Diffraction (XRD) to characterize the adsorbed hydrogens on Pd NPs of ca. 2 nm encapsulated in Metal-Organic Frameworks (MOFs).<sup>78</sup> This composite displayed higher hydrogen uptake than the pristine material, which was attributed to the presence of palladium hydrides, as demonstrated by *in situ* XRD. After exposure of the system to different H<sub>2</sub> pressures up to 10 kPa, the authors observed the formation a palladium hydride phase in the XRD diffractogram, which progressively transformed into a different phase upon increasing the H<sub>2</sub> pressure.

### 2.2.1. Subsurface hydrides.

In the case of Pd NPs, sub-surface hydrides<sup>79-80</sup> are particularly important in the determination of the reactivity of the system. For instance, Ludwig et al. have shown that, in the stereoselective *syn*-hydrogenation of alkenes catalyzed by Pd NPs supported on Fe<sub>3</sub>O<sub>4</sub>, the presence of subsurface hydrogens was a key factor to maintain a good catalytic activity at the steady state of the catalyst (see Figure 6).<sup>81</sup> The formation of subsurface hydrogens was characterized by a combination of kinetic analysis and nuclear reaction analysis (NRA).<sup>82</sup> Furthermore, the authors observed that deposition of carbon at the lower coordination sites of the NPs, i.e. the corners and the edges, favors the diffusion of the surface hydrides inside the NPs enhancing the long-term catalytic performance of the system. The easier diffusion of subsurface hydrides promoted by interstitial carbon was predicted by Neyman et al. in 2010, who showed that the incorporation of carbon slightly increased the lattice parameters thus facilitating the transfer of hydrogen from the inner octahedral sites to the surface.<sup>83</sup> This fact also explains why Pd NPs were more active in alkene hydrogenation than Pd surfaces. Thus, this work constitutes a good example of the need of more realistic models to explain the H<sub>2</sub> cleavage on metal NPs, where the classical models based on crystal surfaces are not consistent with the experimental results.

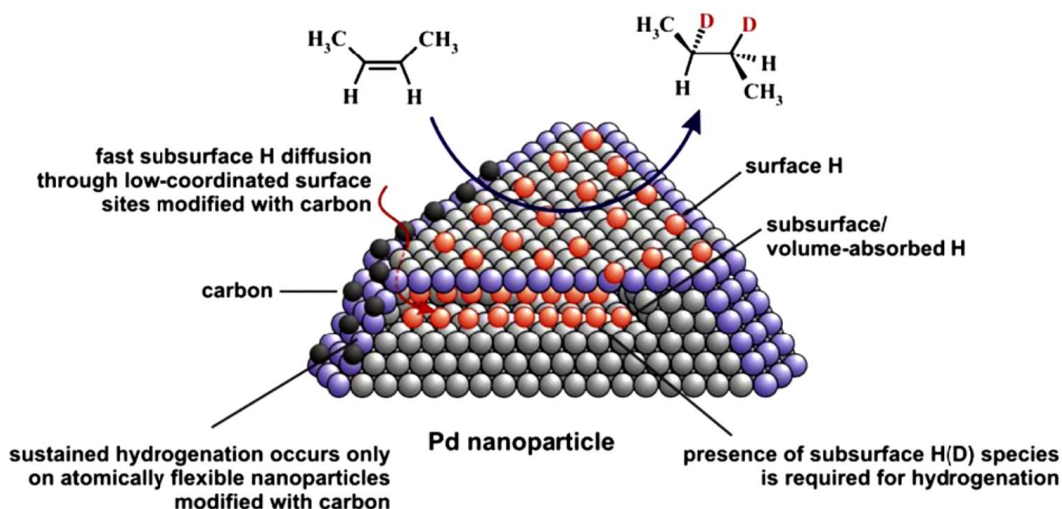


**Figure 6.** The presence of C atoms at the corners of the Pd NPs facilitates the diffusion of the hydrides and the formation of subsurface H(D) species, which enhance the catalytic performance.

Reprinted with permission from ref 81. Copyright 2011 Elsevier.

A theoretical study comparing the role of subsurface hydrides in NPs and single crystals of different transition metals in the catalytic hydrogenation of ethylene was reported by Aleksandrov et al.<sup>84</sup> In the case of Pd and Pt, the subsurface hydrides can destabilize the surface adsorbed H, promoting the occupation of antibonding Pd-H<sup>ad</sup> or Pt-H<sup>ad</sup> states. This effect is remarkably stronger for NPs than for metallic surfaces, and, in the case of Pd, it can increase the rate constant of the

reaction by several orders of magnitude (see Figure 7). On the other hand, in the case of Ni and Rh, the subsurface hydrides help to stabilize the surface adsorbed H due to the more polar character of the Rh-H and Ni-H bonds. As a result, the calculated reaction rates were lower at higher hydrogen loadings. This work evidenced how the nature of the M-H bond can affect the nature of the subsurface hydrides and their role in the catalytic hydrogenation.

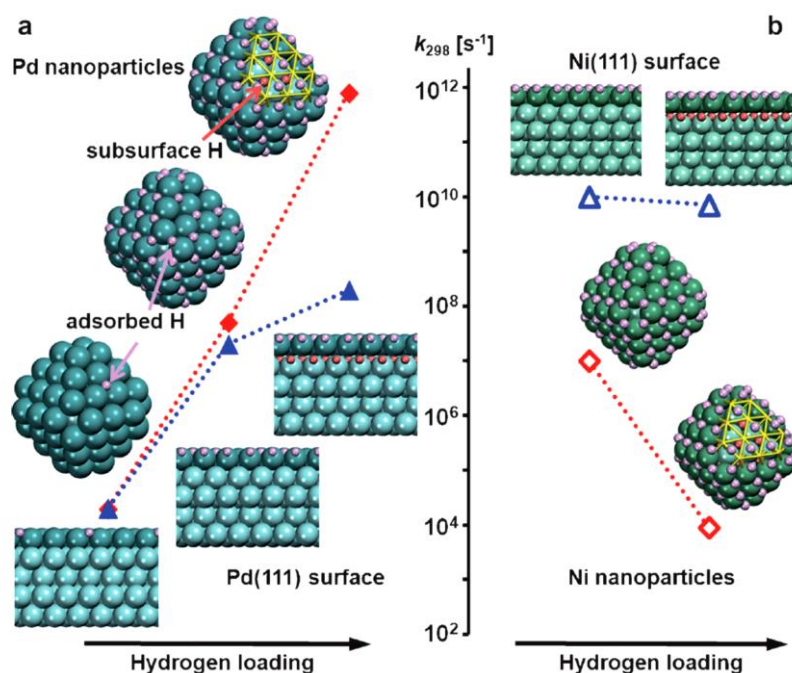


**Figure 7.** The subsurface hydrogens destabilize the surface hydrides on Pd NPs, and this can increase the reaction rate of hydrogenation reactions by several orders of magnitude in comparison to Pd surfaces (left). In contrast, in the case of Ni NPs, the presence of subsurface hydrides stabilizes the surface hydrides, which decreases the catalytic activity of Ni NPs in hydrogenation reactions. Reprinted with permission from ref 84. Copyright 2014 John Wiley and Sons.

Subsequently, Neyman and co-workers determined by theoretical calculations that in Pd and Pt nanoparticles, which contain more edges than the bulk material, the energy barrier to allow the formation of subsurface hydrides is smaller.<sup>85</sup> Interestingly, it was also demonstrated that H absorption was exothermic for H-covered Pd NPs, whereas it was endothermic for pristine Pd NPs.<sup>86</sup> This led the authors to conclude that not only structural considerations, but also the presence of surface hydrides must be taken into account to understand  $\text{H}_2$  activation by transition metals.

In summary, the presence of subsurface hydrides in metal NPs can affect the reactivity of Pd, Pt or Ni based NPs. The characterization of these species and the studies of their role in the catalytic reactions are therefore crucial to understand and to predict the reactivity of the NPs, especially in hydrogenation reactions. Thus, both surface hydrides and subsurface hydrides function not only as

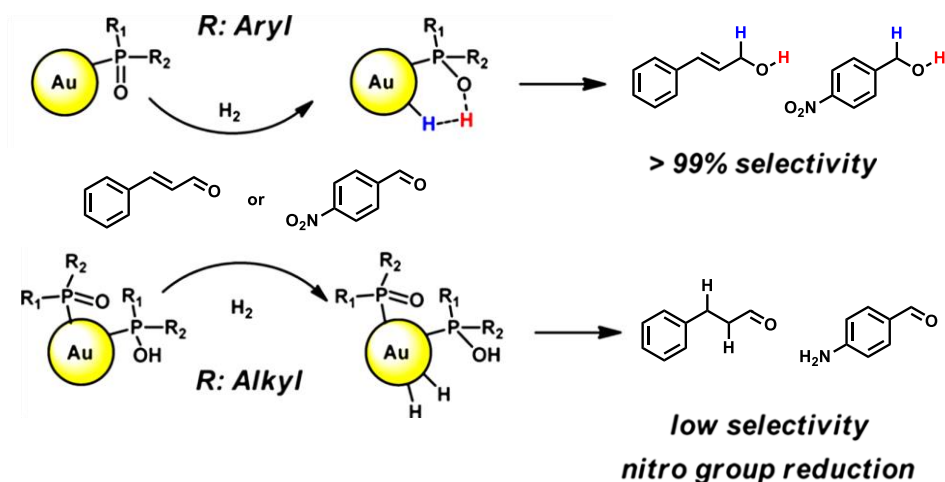
reactants but also as ligands and as such exert “ligand effects”. It should be noted that the works that have been discussed in this section are based on non-functionalized NPs.

### 2.2.2. Ligand effects: ligand assisted H-H cleavage.

Organic ligands are common stabilizers of NPs in solution. These ligands influence the size, properties and reactivity of the NPs, but in many cases the nature of the ligand effects remains unknown. An interesting ligand effect has been evidenced on Au NPs stabilized by secondary phosphine oxides (SPOs) displaying different electronic and steric features. Thus, depending on the SPO's nature, these NPs can catalyze the homolytic or the heterolytic cleavage of the H-H bond, hence leading to different reactivity in catalytic hydrogenation.<sup>87</sup> In this work, the catalytic activity had permitted to elucidate the nature of the H-H activation process. Aryl SPO ligands favored heterolytic cleavage of H<sub>2</sub> and hydrogenation of aldehydes (See Scheme 1), whereas aliphatic SPOs favored hydrogenation of nitro groups, a typical reactivity of Au(0) NPs. DFT calculations on Au<sub>55</sub>(Ph<sub>2</sub>PO)<sub>27</sub> showed preference for heterolytic cleavage and outer-sphere hydrogen transfer to the C=O bond of acrolein.<sup>88</sup> No gold hydrides could be observed for these Au NPs, but exposure to a mixture of H<sub>2</sub> and D<sub>2</sub> slowly produced HD indicating the intermediacy of chemisorbed H<sub>2</sub>. Similarly, the good selectivity of Ir NPs functionalized with SPO ligands towards the aldehyde hydrogenation in cinnamaldehyde suggests a heterolytic H-H cleavage.<sup>89</sup> This contrasts with the results obtained for Ir NPs supported on SiO<sub>2</sub>, where both the alkene and the aldehyde are equally hydrogenated.<sup>90</sup>

In summary, ligand effects can play an important role on the heterolytic or homolytic nature of H<sub>2</sub> activation. Although deeper studies are still needed to better understand the reaction mechanisms, the reactivity and selectivity of metal NPs in catalytic hydrogenation can serve as a model to understand the nature of the homolytic or heterolytic H-H cleavage. This approach can pave the way to develop new catalytic systems based on metal NPs, in which the nature of the ligand may enable to modulate the H<sub>2</sub> activation and thus to tune the reaction selectivity.

**Scheme 1.** Aryl SPOs favor the heterolytic cleavage of the H<sub>2</sub> molecule, which enhances the selectivity of Au NPs towards the hydrogenation of aldehydes (upper). Alkyl SPOs favor the homolytic activation of the H<sub>2</sub> molecule, which results in low selectivity to aldehyde hydrogenation (lower). Reprinted after modifications with permission from ref 87. Copyright 2015 American Chemical Society.



### 2.2.3. $\sigma$ -H activation promoted by light.

A new approach that is gaining attention is the activation of  $\sigma$ -H<sub>2</sub> by metal NPs displaying plasmonic properties promoted by light. It has been proposed that, under laser irradiation, the excited “hot-electrons” can be transferred to the  $\sigma^*$ -H-H orbital of the molecule, which weakens the H-H bond decreasing the barrier for its activation. An interesting feature of this process is its reversibility, so the surface hydrides are desorbed when the irradiation with the laser stops. This activation and its mechanism have been studied by the group of Halas, Nordlander and co-workers, and has been supported by theoretical calculations.<sup>91-92</sup> The authors first studied this activation with plasmonic Au NPs after irradiation at different wavelengths (450-800 nm). It was observed that the support played an important role in this activation. When the Au NPs were supported on dielectric materials such as SiO<sub>2</sub> or Al<sub>2</sub>O<sub>3</sub>, the reaction rate was enhanced by 2 orders of magnitude compared to TiO<sub>2</sub>. This was attributed by the authors to the semi-conductor nature of TiO<sub>2</sub> and the transfer of hot electrons into TiO<sub>2</sub>.

In a recent work, Halas, Nordlander, Carter and co-workers demonstrated that Al nano-cubes can activate H<sub>2</sub> in the presence of a laser.<sup>93</sup> Due to the plasmonic nature of the Al cubes, the authors observed that irradiation with laser promotes the activation of the H-H bond. A screening of wavelength was performed (from 350 to 1000 nm), showing that H<sub>2</sub> activation rate was maximized at those wavelengths matching with the surface plasmon (461 nm) or with the interband transition (800 nm). The mechanism of this reaction was studied using theoretical calculations, supporting the above-described mechanism of the “hot-electron” transfer to the  $\sigma^*$ -H-H orbital facilitating the  $\sigma$ -bond activation. The mechanism was further experimentally supported by simultaneous activation of H<sub>2</sub> and D<sub>2</sub>. First,  $\sigma$ -bond activation of both species under laser irradiation afforded surface-adsorbed



hydrides and deuterides. Then, when the laser irradiation stopped, recombination of the surface adsorbed species led to the formation of H-D molecules. (see Fig 8).

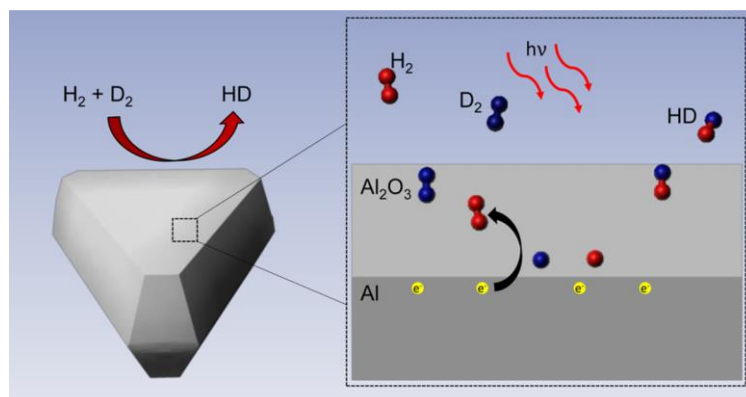


**Figure 8.** In the presence of laser irradiation on Al nano-cubes, “hot-electrons” are transferred to the  $\sigma^*$ -H-H and  $\sigma^*$ -D-D orbitals reducing the energetic barrier for the  $\sigma$ -bond activation. This process is reversible and when the laser irradiation stops, the surface hydrides and deuterides recombine to generate H-D species. Reprinted with permission from ref 93. Copyright 2016 American Chemical Society.

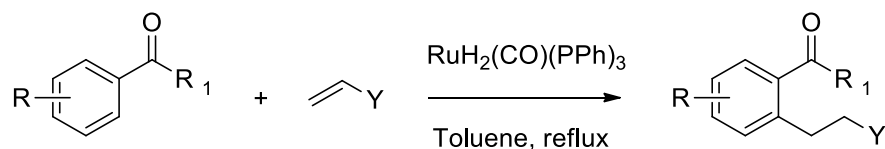
In conclusion,  $\sigma$ -H<sub>2</sub> activation promoted by light is an interesting topic that has been experimentally proved, but to the best of our knowledge, the existence of surface hydrides has only been proposed by theoretical calculations. Thus, further developments in surface characterization may enable to determine the mechanism of this  $\sigma$ -H<sub>2</sub> activation, as well as the different hydride species that can exist at the surface of the NPs.

### 3. C-H activation by metal NPs.

Catalytic C-H activation in solution has attracted a considerable interest for the past thirty years in view of potential applications in the synthesis of valuable organic molecules.<sup>13,20,94-98</sup> This is now a reality and the number of processes involving a C-H activation/functionalization step keep growing.<sup>99-101</sup> In molecular chemistry, several mechanisms have been described: oxidative addition,  $\sigma$ -bond metathesis, and electrophilic displacement, depending on the nature of the metal used.<sup>102-103</sup> For late transition metals, prone to undergo oxidative additions but also able to coordinate to C-H bonds, the most studied are the heavier group 8-10 metals, namely Ru, Rh, Pd, Ir, Pt.<sup>104</sup> The first demonstration of C-H bond oxidative addition goes back to Chatt on a Ru(dppe)<sub>2</sub> complex in 1965<sup>105</sup> whereas Rh and Ir have allowed the first demonstrations that alkane C-H bonds could be cleaved to lead to alkane dehydrogenation or to a stable alkyl complex.<sup>106</sup> As far as catalysis is concerned the most spectacular alkane functionalization involving C-H activation besides dehydrogenation is the

Murai reaction (see Scheme 2), which consists of the alkylation of aromatic ketones through a C-H bond activation in the *ortho* position that is catalyzed by ruthenium organometallic complexes.<sup>107-109</sup>

**Scheme 2.** Murai reaction catalyzed in homogeneous phase by a Ru complex.



However, C-H activation in homogeneous phase displays some limitations related to harsh reaction conditions, difficulty to isolate the reaction products or absence of possibility to recycle the catalyst. NPs could constitute a good alternative due to their high reactivity, adjustable size which can give them higher surface areas than traditional heterogeneous catalysts, and ability to be immobilized on a support to allow their recycling.<sup>24</sup>

In this chapter we outline C-H activation by metal NPs in solution under mild conditions. First, we will discuss H/D exchange reactions, which involve both C-H and D-D  $\sigma$ -bond activations. Then, we will summarize C-H functionalization for C-C bond formation catalyzed by metal NPs. Finally, C-X bond formation through oxidative C-H bond activation will be considered.

### 3.1. H-D exchange catalyzed by metal NPs.

During these last decades, the application of hydrogen isotopes has significantly increased in several areas.<sup>110</sup> Deuterium-labeled compounds are of high interest in life sciences, and particularly in pharmacology and drug discovery.<sup>111</sup> In addition, kinetic isotopic effects can significantly enhance the pharmacokinetic properties of drugs or reduce their toxicology.<sup>112</sup> On the other hand, deuterium-labeled molecules have shown to be very useful in other applications such as nuclear magnetic resonance, mass spectrometry or as tracers in mechanistic studies.<sup>113-114</sup> Therefore, the development of efficient H/D exchange reactions via C-H exchange having a good control over reaction selectivity is a topic of great interest.<sup>115</sup> Several methods to perform H/D exchange through homogeneous catalysis have been developed using different metal complexes. Although in some cases H/D exchange can be performed at high temperatures in acid or basic medium without the need for any metal catalyst,<sup>116</sup> in this review we will focus on H/D exchange catalyzed by metal NPs.

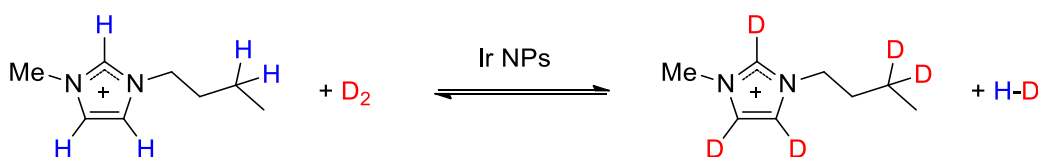
Metal complexes in homogeneous phase have been explored as catalysts in H/D exchange. For instance, iridium complexes such as the Crabtree catalyst [Ir(cod)(PCy<sub>3</sub>)(py)]PF<sub>6</sub>, are well known to afford efficient deuterium incorporation in many substrates (benzoic acids, benzamides, ...).<sup>117-118</sup> Another metal that has been used in H/D exchange reactions is ruthenium. Some examples are the Shvo catalyst, which gave good chemoselectivities towards the deuteration of amines in the  $\alpha$  and  $\beta$

positions of the nitrogen atom,<sup>119</sup> or the Ru pincer catalyst described by Khaskin et al. that catalyzes the regioselective deuteration of alcohols with D<sub>2</sub>O.<sup>120-121</sup> Additionally, rhodium,<sup>122</sup> palladium<sup>123</sup> and platinum<sup>124</sup> complexes have also been described in literature to catalyze H/D exchange in homogeneous phase. The mechanism of these reactions is known and generally involves heterolytic cleavage of the H-H and C-H bonds.

On the other hand, heterogeneous catalysis has also shown high efficiencies in H/D exchange, with the advantage of the easy removal and recyclability of the catalyst. Amongst them, the most employed heterogeneous catalysts are palladium, platinum and ruthenium supported on carbon (Pd/C, Pt/C and Ru/C).<sup>125</sup> As an example, Ru/C is known to catalyze the H/D exchange of amino acids and amino alcohols.<sup>126</sup> However, other metals have also been studied in the H/D exchange in heterogeneous phase, such as nickel, cobalt, etc.<sup>115</sup> As discussed above, in this review we focus on the deuteration reactions catalyzed by metallic nanoparticles in solution.

In 2005, Ott et al reported an example of H/D exchange catalyzed by metal NPs.<sup>127</sup> In this work, Ir NPs of 2.1 ± 0.6 nm were prepared in ionic liquids based on imidazolium salts, and they were able to catalyze the H-D exchange of 1-butyl-3-methylimidazolium in the imidazolium cation as well as in the alkyl chain (see Scheme 3). In addition, due to the higher deuteration degree in position 2 of the imidazole ring, the authors introduced the hypothesis that imidazolium salts were coordinating to the NPs surface as N-Heterocyclic Carbene (NHC) ligands, opening the door to NPs stabilization by such molecules. Since then, some examples have been reported in the literature showing the efficiency of nanoparticles to perform catalytic deuteration in solution.

**Scheme 3.** Ir NPs can deuterate different aromatic and aliphatic positions of imidazolium salts. The higher deuteration degree of the 2-position of the imidazole ring was attributed to the coordination of the NHC ligand to the surface of the NPs.



In 2008, Sullivan et al. reported the use of 3.4 nm Pd NPs immobilized on multi-walled carbon nanotubes (MWCNTs) for catalyzing in aqueous medium H-D exchange on aromatic C-H bonds of 4-dimethylaminopyridine (DMAP) with a selectivity for the  $\alpha$  position to N.<sup>128</sup> The authors studied the effect of the temperature on the reaction and showed that at higher temperatures (80 °C), the reaction rate increased but led to a higher deuteration degree in the  $\beta$  position as a side reaction. Other substrates containing a pyridine ring were tested in the H/D exchange reaction at 50 °C (see table 1). The deuteration of 4-aminopyridine proceeded similarly but the reaction of 4-hydroxypyridine

showed an inversion in the selectivity with a higher deuteration for the  $\beta$  protons. This is likely due to a different coordination mode of the substrate to the NPs surface leading to a different selectivity, suggesting that coordination of the substrate determines the selectivity. One possible explanation may be the presence of Pd(II) species at the surface of the catalyst, which enhances its affinity for the coordination of O atoms. Thus, when the substrate contains an -OH group, coordination through the O would direct the H/D reaction towards the  $\beta$  position. Otherwise, the substrate preferentially coordinates through the aromatic N leading to deuteration in the  $\alpha$  position.

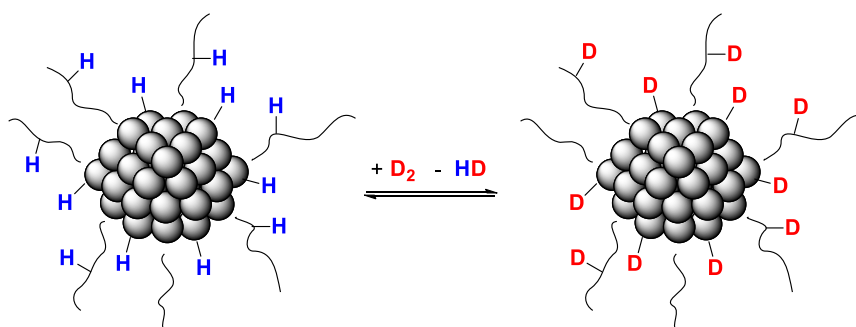


Substrate	$\alpha$ exchange (%)	$\beta$ exchange (%)
4-dimethylaminopyridine (DMAP)	87	13
4-aminopyridine	76	17
4-hydroxypyridine	6	34

**Table 1.** Pd NPs supported on MWCNTs can deuterate the  $\alpha$  and  $\beta$  positions of different 4-substituted pyridines. The selectivity of the deuteration depends on the nature of the 4-substituent, suggesting that the coordination mode of the substrate determines the reactivity of the NPs.

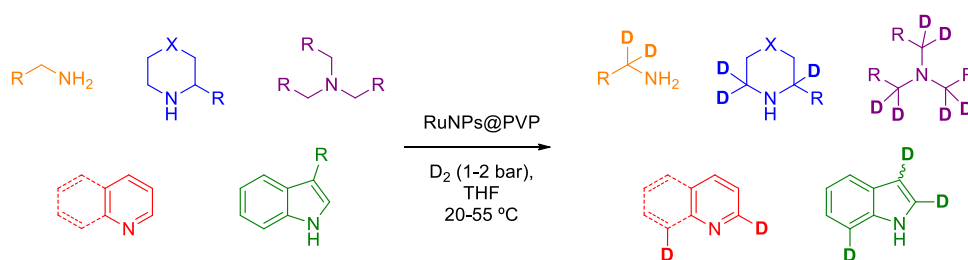
Our group has been interested during the past 15 years in the interaction of ruthenium nanoparticles with H<sub>2</sub> (see discussion above). Hydrogen substitution by deuterium at the surface of Ru NPs was studied by Pery et al. in 2005 in order to determine the number of hydrides present at the surface.<sup>54</sup> In this work, H/D exchange was observed both at the surface of the NPs and in the stabilizing hexadecylamine (HDA) ligands (see Scheme 4), evidencing a combination of C-H, H-H and D-D activations assisted by Ru NPs. The detection of H<sub>2</sub> and HD was performed through gas-phase <sup>1</sup>H NMR as the direct detection of the particles in solid phase did not give satisfactory results. The incorporation of D in HDA was also demonstrated but no information on the deuterated positions could be obtained. These preliminary results were a proof of concept of the viability of the system for isotopic labelling reactions. Since then, further development in the scope and mechanistic comprehension of H/D exchange reactions catalyzed by Ru NPs has been performed.

**Scheme 4.** When Ru/HDA NPs are treated with D<sub>2</sub>, D not only is present at the surface of the NPs but it is also incorporated in HDA, demonstrating that Ru NPs are able to activate H-H, D-D and C-H bonds.



In 2014, Pieters et al. reported the use of Ru nanoparticles stabilized by polyvinylpyrrolidone (Ru@PVP) for the selective H-D exchange of bioactive *aza* compounds.<sup>129</sup> Small ruthenium nanoparticles of 1.1 nm were obtained through decomposition of Ru(*cod*)(*cot*) (*cod* = 1,5-cyclooctadiene, *cot* = 1,3,5 cyclooctatriene) in the presence of the polymer. Ru@PVP NPs behave as “naked” nanoparticles since they are only sterically stabilized. Good regioselectivities for the deuteration of the  $\alpha$  position to the N atom were observed in the isotopic labeling of molecules of biological interest such as pyridines, indoles and amines (see Scheme 5). The catalytic reactions were performed under mild conditions, 55 °C or at room temperature, using 1-2 bar of deuterium gas as the isotopic source and 3% Ru loading. Additionally, the labeling of eight biologically active compounds containing at least one nitrogen atom was performed (Figure 9). Differences in the regioselectivity of the reaction could be explained through the coordination mode and the accessibility of the different positions, the  $\alpha$  positions to N being most prone to deuteration. For example, in a molecule containing an aliphatic secondary amine and a pyridine ring (Figure 9a-b), the positions  $\alpha$  to the aromatic N were preferentially deuterated. Another interesting observation was the moderate deuteration in position C7 of the indole ring (40%, Figure 9d).

**Scheme 5.** Ru@PVP NPs can selectively deuterate molecules of biological interest such as pyridines, indoles and amines under mild reaction conditions.



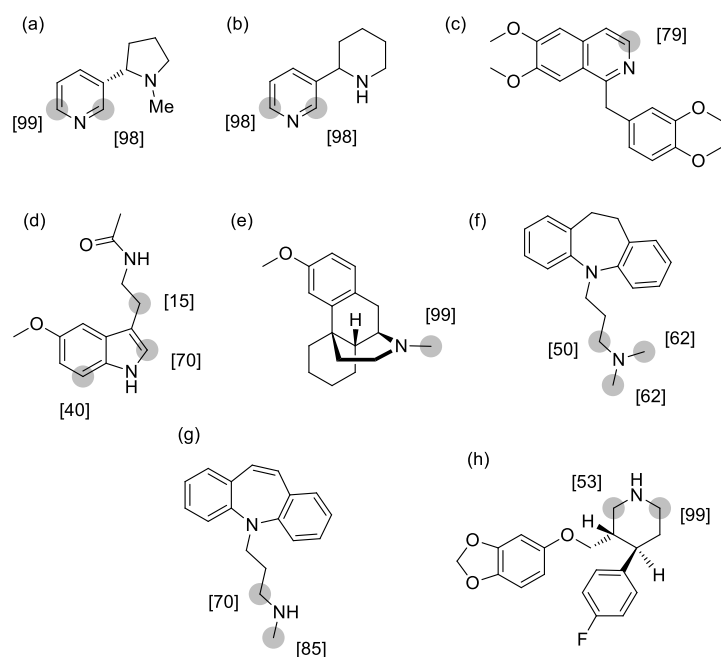


**Figure 9.** Scope of substrates that were deuterated using Ru@PVP NPs showing the position and the percentage of deuterium incorporation.

In 2015, the authors expanded their work to the deuteration of molecules of biological interest catalyzed by Ru NPs.<sup>130</sup> An enantiospecific H/D exchange was observed on chiral amines using the same Ru@PVP system, leading to high yields in the deuteration of the  $\alpha$  positions to the N atoms of the molecules in mild reaction conditions (55 °C and 2 bar of deuterium gas). Retention of the configuration was always observed. Then, the reaction was extended to amino acids and other peptides (see Figure 10). A good deuteration degree was observed for hydrogens  $\alpha$  to nitrogen in almost all the cases, although lower deuterium incorporation was observed in compounds containing three coordination sites. This effect was attributed to a tridentate coordination of the substrate to the nanoparticle surface, which would decrease the flexibility of the molecule hindering the deuteration process. The reaction mechanism was also studied in this work through DFT calculations and the transition state for the C-H activation step is shown in Figure 11. The first step of the reaction consists in the coordination of the substrate through the N atom, followed by rotation of the amine to orient the C-H bond towards the Ru center. Then, C-H activation occurs at the surface of the NPs in the  $\alpha$  position of the substrate to form a four-membered dimetallacycle intermediate. Further H-D exchange at the surface atoms followed by reductive elimination and decoordination of the substrate completed the reaction mechanism to afford the deuterated product.

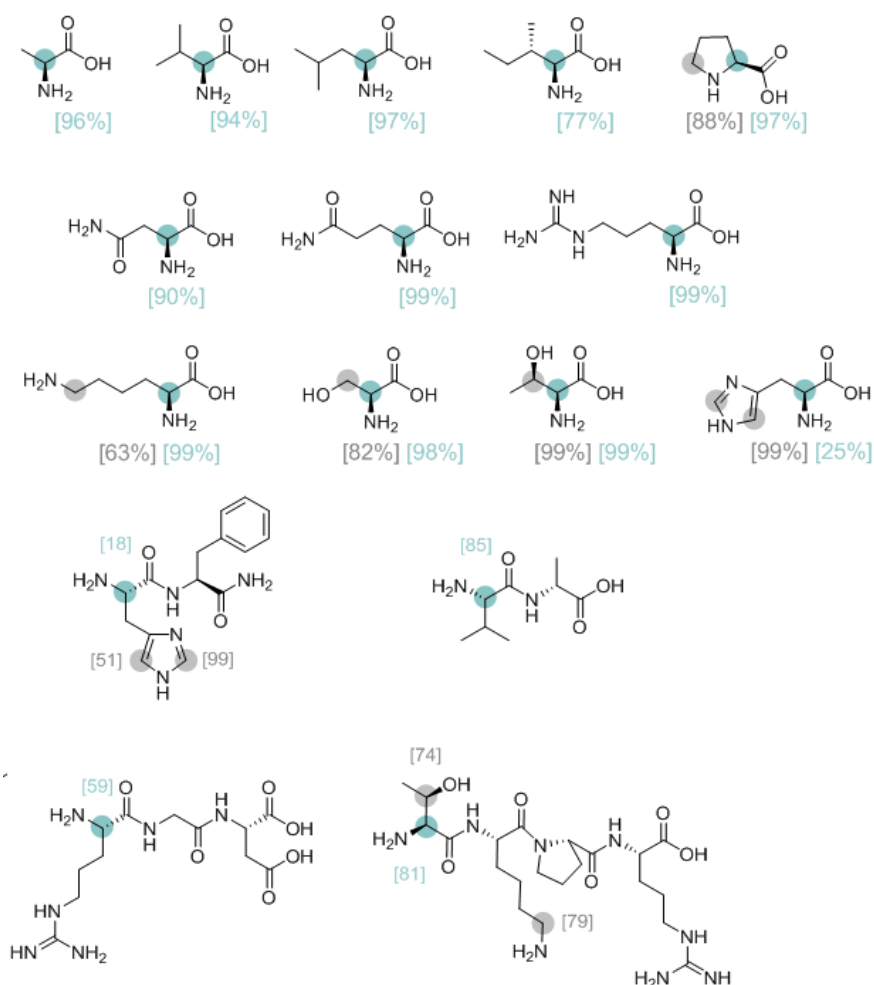


**Figure 10.** Scope of H/D exchange on chiral amines catalyzed Ru@PVP NPs showing the position and the percentage of deuterium incorporation. Reprinted with permission from ref 130. Copyright 2015 John Wiley and Sons.

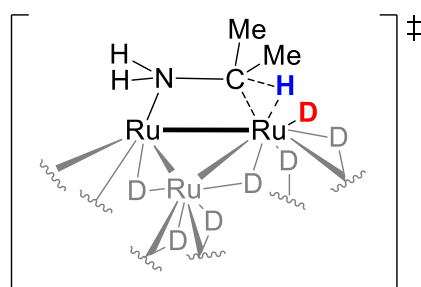


**Figure 11.** Transition state in the C-H activation step for the Langmuir–Hinshelwood-type H/D exchange mechanism calculated by DFT for 1 nm Ru<sub>55</sub>D<sub>n</sub> clusters. Activation of the C-H bond leads to the formation of a four-member metallacycle containing a Ru-Ru moiety.

Ru NPs are also active in the deuteration of organic ligands that do not contain N atoms. Bresó-Femenia et al. reported the deuteration of phosphorus compounds using Ru NPs stabilized by PVP in

mild conditions (2 bar  $D_2$ , 55 °C).<sup>131</sup> Three different type of P ligands were tested in the H/D exchange: triphenylphosphine, triphenylphosphine oxide and triphenyl phosphite. Selective deuteration of the *ortho* positions of the aromatic rings was observed for triphenylphosphine with incorporation of 1 to 6 deuterium atoms depending on the reaction time, without any evidence for the reduction of the aromatic rings (see Figure 12-a). However, RuNPs@PVP were not able to deuterate the aliphatic groups of  $Ph_2MeP$  and  $dppb$ , and only the phenyl groups were deuterated at the 2,6-positions. Triphenylphosphine oxide also led to deuterium incorporation under the same conditions, but in this case reduction of the aromatic ring was observed even at low temperatures, which was explained by a  $\pi$ -coordination mode of the substrate through the phenyl ring (see Figure 12-b). Finally, triphenyl phosphite was not deuterated under the same conditions. In this case, the presence of O atoms prohibits the desired orientation of the aromatic ring to two adjacent Ru atoms, thus disfavoring H/D exchange (see Figure 12-c). Note that monometallic molecular Ru complexes readily metallate triphenyl phosphite, one of which is a catalyst for H/D exchange of phenols.<sup>132</sup>

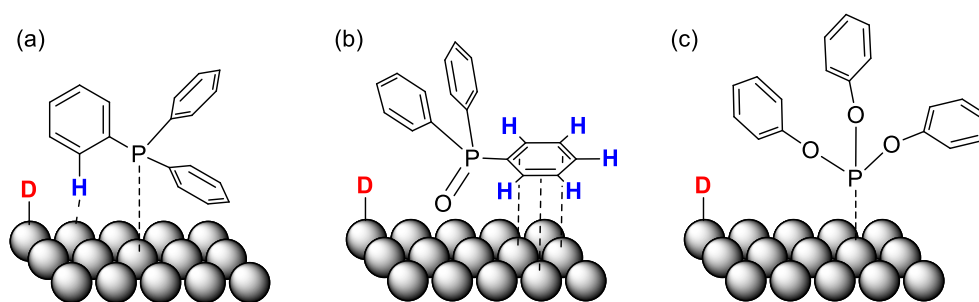


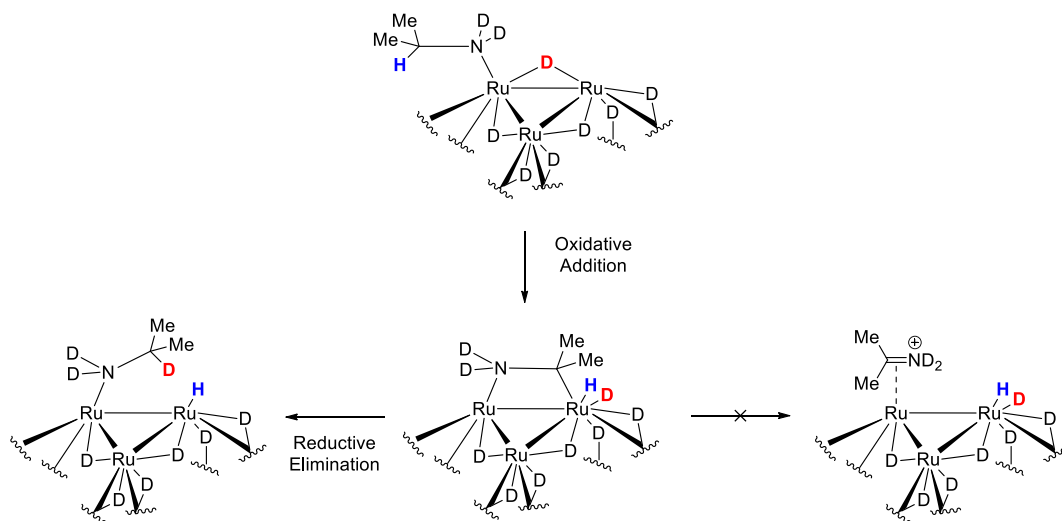
**Figure 12.** Phosphine deuteration catalyzed by Ru@PVP NPs. (a)  $PPh_3$  is selectively deuterated in the 2-position of the phenyl substituent. (b)  $OPPh_3$  cannot coordinate through the P atom, and  $\pi$ -coordination of the aromatic ring affords the reduction of the phenyl substituents. (c) With  $P(OPh)_3$ , the coordination mode prohibits the deuteration of the aromatic rings.

In 2016, Bathia et al. reported the use of Ru NPs supported on an activated carbon cloth (RuNPs/ACC) for stereoretentive H/D exchange on sites vicinal to amines and alcohols groups through electrocatalysis.<sup>133</sup> This methodology of deuteration using  $D_2O$  with a supply of steady state current without  $D_2$  gas, afforded a high percentage of deuteration on 2-aminobutane as model substrate. The anode is a platinum wire which plays the role of counter electrode and the reaction occurs on the cathode comprised of RuNPs/ACC. Then, the authors explored the deuteration of various substrates in this reaction. Alcohols generally showed better deuteration degree in the  $\alpha$  position to the heteroatom than amines, which was proved after deuteration of amino-alcohol

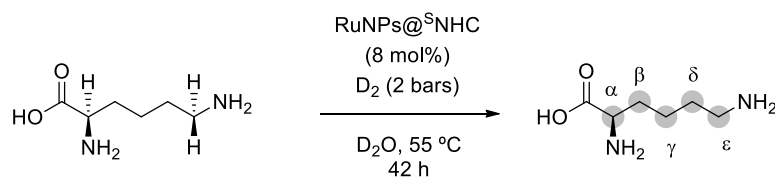


substrates containing both functional groups. A mechanism for the reaction similar to the one given by Taglang et al.<sup>130</sup> was proposed. (see Scheme 6)

**Scheme 6.** Proposed mechanism for the electrocatalytic H/D exchange catalyzed by Ru/ACC NPs.



NHC ligands have recently received a lot of attention as stabilizers of metal NPs. This family of ligands provides a strong coordination to the NPs surface, enhancing the stability of the NPs. In addition, they can allow tuning the solubility of the NPs through modification of the substituents. A methodology to synthesize water-soluble Ru NPs stabilized by sulfonated N-heterocyclic carbene ligands (<sup>S</sup>NHC) was reported by Martínez-Prieto et al. in 2017.<sup>134</sup> The RuNPs@<sup>S</sup>NHC were studied in the H/D exchange of L-lysine at different pHs (Table 2). This catalytic system allowed a direct NMR monitoring of the H/D exchange. Variation of the pH in the medium had an important influence on the coordination mode of L-lysine to the NPs, affecting the rate and selectivity of the H/D exchange. At the pH value provided by L-lysine (10.4), two positions were mainly deuterated, the positions  $\alpha$  and  $\epsilon$  (although a slight deuteration of 12.5% was also observed in position  $\gamma$ ). Decreasing the pH slowed down the reaction rate, so at a pH of 2.2 there was almost no deuteration of the substrate. This is probably since at low pH, the  $\text{NH}_2$  groups are protonated preventing amino acid coordination to the surface of the NPs (see Figure 13). On the other hand, higher deuterium incorporation was found at basic pH values. For example, at a pH of 13.2 where L-lysine is in the  $\text{Lys}^-$  form, the two amino groups can coordinate to the NPs surface, providing almost complete deuteration of the positions  $\alpha$ ,  $\gamma$  and  $\epsilon$  (99%, 98.5% and 89.5% respectively). At a pH of 13.8, selectivity deuteration of the positions  $\alpha$  and  $\gamma$  decreases, likely due to passivation of the NPs surface in the presence of high concentration of  $\text{OD}^-$ . Figure 13 visualizes the exchange at C- $\gamma$ . The coordination mode of the substrate to the NPs was also proven by chemical shift perturbation (CSP) in the  $^1\text{H}$ - $^{13}\text{C}$  HSQC NMR.



pH	$\alpha$ (%)	$\epsilon$ (%)	$\gamma$ (%)	$\beta$ (%)	$\delta$ (%)
2.2	6	2	-	-	-
6.9	95	70	-	-	-
8.4	97	92	-	-	-
10.4	99	98,5	12,5	-	-
11.0	99	98,5	45	-	-
13.2	99	98,5	89,5	10	-
13.8	76	98	31,5	-	-

**Table 2.** % of deuterium incorporation in L-lysine catalyzed by Ru NPs stabilized by sulfonated NHCs as a function of the pH of the aqueous solution.

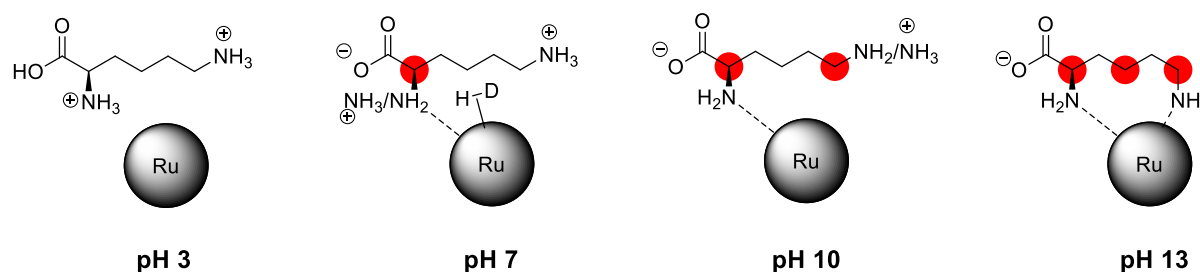


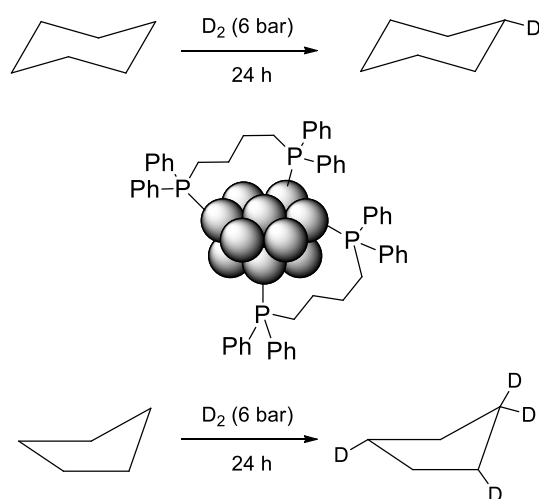
**Figure 13.** At a pH value of 3, all the amino groups are protonated, and L-lysine does not react with Ru NPs. After progressively augmenting the pH values, deprotonation of the amino groups facilitates the coordination of the substrate enhancing the D incorporation at the different positions of the molecule.

The reactivity of Ru NPs towards the deuteration of alkanes, which bind very weakly to the Ru surface, has been recently explored. To this end, Rothermel, et al. synthesized Ru NPs stabilized by bis(diphenylphosphino)butane (dppb) ligands.<sup>135</sup> A surprisingly high reactivity was observed for cyclopentane as compared to cyclohexane and other alkanes, the initial rate of exchange being about 20 times higher for cyclopentane (60 °C, 6 bars of D<sub>2</sub>) (See Scheme 7). As cyclohexane and cyclopentane have similar bond cleavage energies (400 kJ/mol and 395-403 kJ/mol respectively), the

origin of such a different reactivity was difficult to understand. The ligand influence was explored, and similar results were obtained even in the absence of dppb as stabilizing ligand. DFT calculations using a ligand-free Ru<sub>13</sub>H<sub>17</sub> model cluster as catalyst indicated that the rate-limiting reaction step was the oxidative C-H cleavage of the bound substrates. Also, comparable binding and activation enthalpies were found for the two alkanes. These results seem to indicate that the NPs surface shows a specific recognition for the cyclopentane substrate. Although the reason is not yet understood, it may be caused by a subtle interplay of various intra- and intermolecular surface-substrate interactions, entropies included.

**Scheme 7.** Ru NPs stabilized by dppb can efficiently deuterate cycloalkanes under mild conditions.

Surprisingly, the initial rate of exchange was about 20 times higher for cyclopentane than for cyclohexane, which resulted in higher deuteration degree of the former.



Recently, Palazzolo et al. have reported the selective deuteration and tritiation of pharmaceuticals and oligonucleotides catalyzed by Ru NPs.<sup>136</sup> The reactivity of two different catalysts was compared: Ru NPs stabilized by PVP (Ru@PVP) and by a N-heterocyclic carbene ligand (1,3-bis(cyclohexyl)-1,3-dihydro-2*H*-imidazol-2-ylidene, Ru@ICy). It was observed that Ru@ICy showed improved catalytic activities in some of the cases, which was attributed to their higher dispersibility in organic solvents than that of Ru@PVP. Both systems showed a remarkably broad scope of substrates under mild reaction conditions, 55 °C and 2 bar of D<sub>2</sub> (see Figure 14). It must be highlighted that no reduction of the aromatic rings was detected. In addition, 6-mer and 12-mer oligonucleotides were successfully deuterated by Ru NPs stabilized by water-soluble NHCs, using 1 equivalent of catalyst and 2 bar of D<sub>2</sub>. The isotopic labelling was accompanied by total conservation of the structure, and no reduction of the pyrimidine bases was observed.

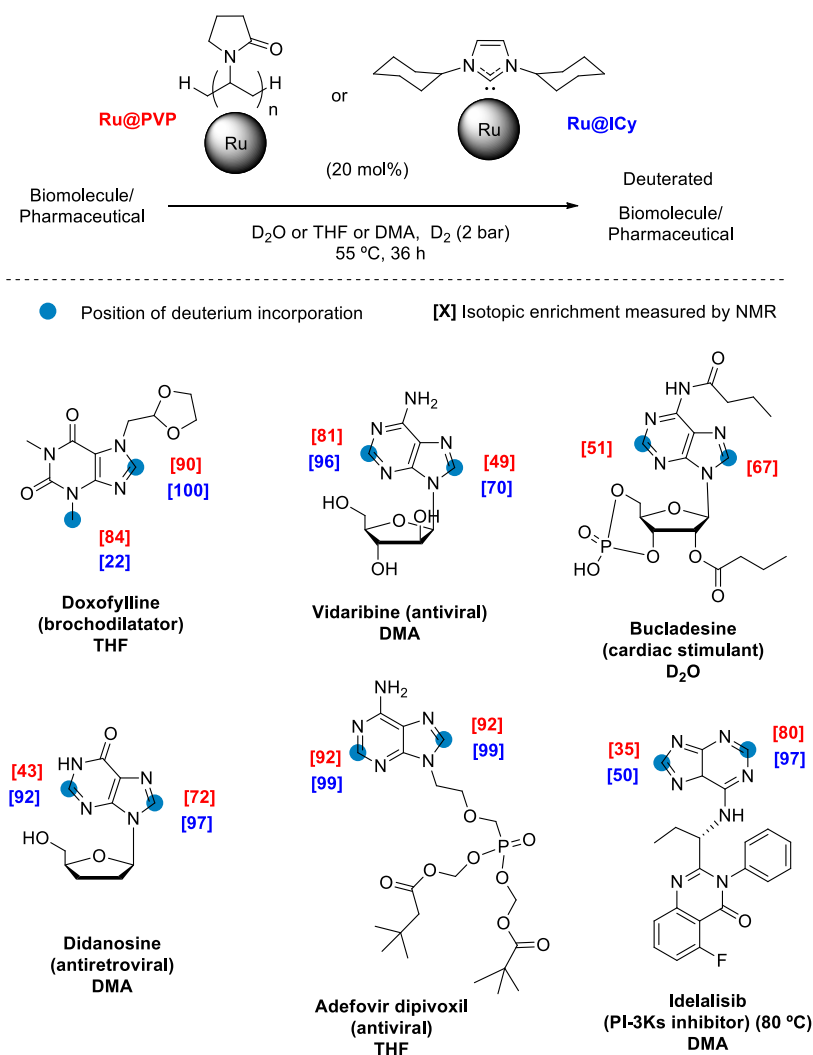


**Figure 14.** Scope of substrates for the deuteriation of pharmaceuticals and biomolecules catalyzed by Ru@PVP (in red, %) and Ru@ICy (in blue, %)

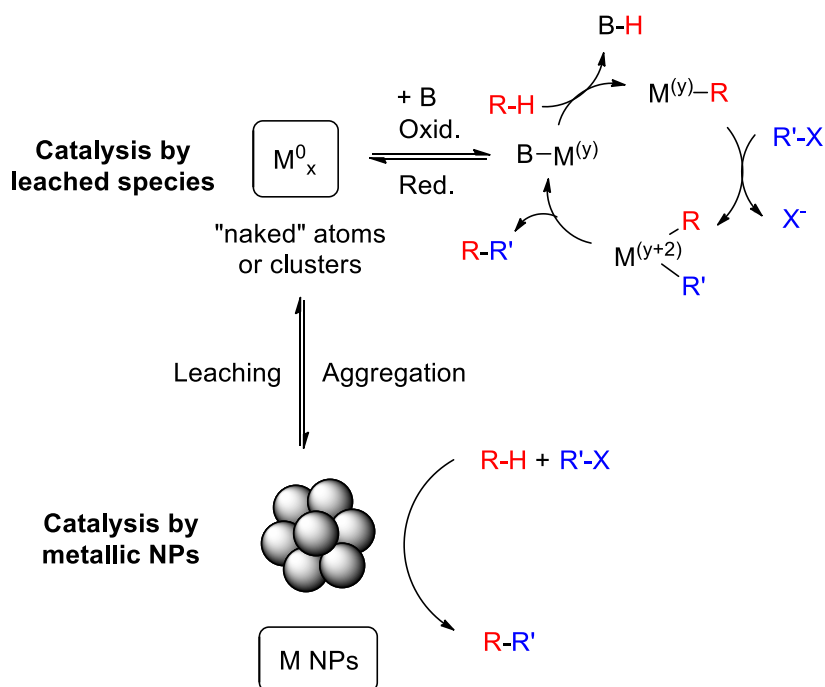
To conclude, in this section we have shown that metal NPs, especially Ru NPs, are good catalysts for H-D exchange reactions since they are very active systems in C-H, H-H and D-D activation. Thus, a wide variety of organic substrates could be selectively deuterated under mild conditions. Notably, the possibility of functionalizing the NPs surface makes these systems very promising catalysts as their activity, selectivity and solubility, among other properties, can be easily tuned by modification of the ligands. This constitutes an advantage of NPs over the classical heterogeneous catalysts. Also, important efforts to understand the reaction mechanisms have been developed. Interestingly, the mechanisms involve the same types of species observed in molecular complexes, namely, hydrides or alkyl/aryl metal bonds, dihydrogen or  $\sigma$ -C-H bonds, but NPs benefit from the presence of adjacent ruthenium atoms, facilitating the formation of a four-center metallacycle together with H and D diffusion, and therefore H/D exchange.

### 3.2. C-C bond formation.

During the past few years, systems based on metal NPs have been developed extensively in the field of catalytic C-H activation followed by C-C bond formation. NPs display a multiplicity and a variety of surface sites able to activate organic molecules but, the reaction mechanisms are not as precisely known as in molecular chemistry, and, in some cases, doubts remain concerning the nature of the active species. Thus, studying the reaction mechanism for each particular system is important in order to optimize the reaction conditions and to improve the recyclability of the catalysts. In some catalytic systems, several observations suggest that catalysis may be performed by solution-stable catalytically active molecular species that are leached from NPs surface, and in this case the NPs would act as a reservoir for these species that may be either “naked” atoms or metallic clusters (see Scheme 8).<sup>137</sup> This is particularly true for Pd which is prone to oscillate between the molecular and the nanoparticulate states in solution. At an early stage already De Vries and Reetz proposed that leached Pd species were responsible for the catalytic activity of Pd NPs in C-C coupling reactions.<sup>138</sup>

In this chapter we will describe the state-of-the-art productive C-H activation leading to the formation of C-C bonds. Most of the literature concerns three metals, Pd, Au and Cu. It is interesting to note that, although Lohr et al. proposed in 2013 that *in situ* formed platinum nanoparticles were able to activate C-D bonds from the deuterated solvent,<sup>139</sup> other metals studied in molecular chemistry, namely Ru, Rh, Ir, Pt are not used or not active as NP catalysts and therefore not present in this study,

**Scheme 8.** In some cases, C-H functionalization can take place at the surface of the NPs. Nevertheless, for some catalytic systems, several observations suggest that catalysis may be performed by solution-stable catalytically active molecular species that are leached from NPs surface.



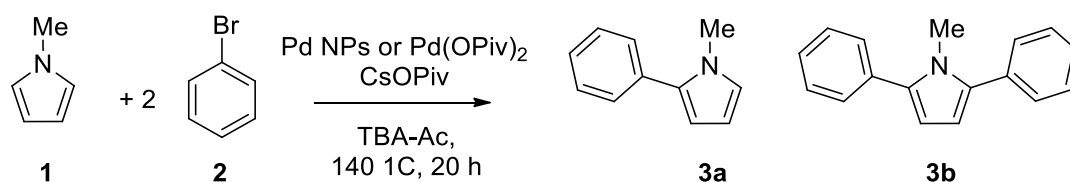
### 3.2.1. Pd NPs for the C-H activation/C-C bond formation. Leached active species vs. surface-catalysis.

Palladium is one of the most employed catalysts in C-H activation thanks to its electronic characteristics and coordination possibilities.<sup>140</sup> Pd complexes have long been used in arylation reactions through C-H activation, but amongst them, Pd(OAc)<sub>2</sub> has been the most widely studied.<sup>141-142</sup> In addition, Pd heterogeneous catalysts have been used in C-H functionalization of aromatic substrates, and amongst them Pd/C has been the one most explored.<sup>143-145</sup> Aromatic substrates such as indoles, pyrroles, furans or thiophenes have been used as substrates in C2 arylation reactions through C(sp<sup>2</sup>)-H activation catalyzed by Pd NPs. It is well-known that homogeneous C(sp<sup>2</sup>)-H activation of arenes followed by C-C formation is catalyzed by Pd(II) species.<sup>141,146</sup> In this context, it has been observed that the use of O<sub>2</sub> enhances the activity of homogeneous Pd complexes in the C-H activation of arenes.<sup>147</sup> Thus, the use of oxygen or oxidants in the C2 arylation catalyzed by Pd NPs probably suggests that oxidation of superficial atoms from Pd(0) to Pd(II) may be the first step in the catalytic cycle. Note that surface oxygen atoms may act as acceptors of both electrons and protons that are generated in the process, as proposed for Au NPs (see discussion below).<sup>148</sup> In this context many authors present their work as C-H activation, but it should be borne in mind that

mechanistically, a  $\text{Pd}^{2+}$  complex does an electrophilic attack on the aromatic ring after which deprotonation of the  $\text{C}(\text{sp}^2)\text{-H}$  unit occurs, often assisted by acetate ions.<sup>149</sup> There is also experimental and theoretical evidence that the latter is more important and that electrophilic attack does not have to be invoked.<sup>150</sup>

In 2011, Zinovyeva et al. prepared a nanocomposite material that consisted of Pd NPs of 2.4 nm supported in polypyrrole (PdNPs@PPy), which was synthesized by sonication of  $\text{Pd}(\text{NH}_3)_4\text{Cl}_2$  in the presence of pyrrole in water.<sup>151</sup> The NPs gave good activities in the C5 arylation of 2-butylfuran and 2-butylthiophene with bromoarenes in dimethylacetamide (DMAc) at 150 °C. When performing recycling experiments, the authors observed a significant growth of the NPs from 2 to 7 nm. However, the NPs were still well-dispersed through the support and there was no significant agglomeration. Thus, the authors proposed that the active species in the reaction were leached palladium species that were re-deposited at the end of the reaction and were responsible of the NPs growth.

In 2013, Langer and co-workers reported the use of a ligand-free catalytic system composed of Pd NPs supported on polyvinylpyrrolidone (Pd/PVP) for the C-H activation of pyrroles in ionic liquids, and they compared its activity with the one obtained from homogeneous  $\text{Pd}(\text{OPiv})_2$ .<sup>152</sup> The PdNPs/PVP system was active only when tetrabutylammonium acetate (TBA-Ac) was used as solvent, whereas in other solvents there was no reaction (see Table 3). An effect of the NPs size was observed, leading to higher activities with the smaller NPs and higher selectivity towards the formation of the diarylated product. However,  $\text{Pd}(\text{OPiv})_2$  exhibited higher activities. Since it was reported that PdNPs/PVP are oxidized in the presence of ammonium salts,<sup>153</sup> the authors proposed that the reaction mechanism evolved by formation of Pd(II) species that leached from the NPs surface and that were stabilized by TBA-Ac. After the catalysis the species would be re-deposited on the NPs, and the TBA-Ac would prevent their aggregation into “palladium black”.



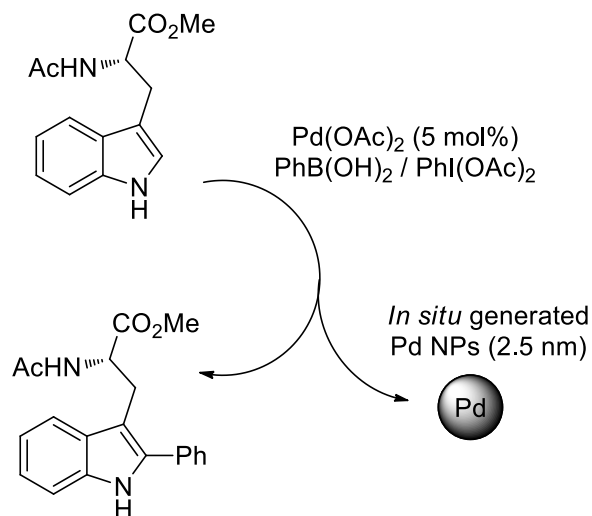
Entry	Catalyst	Ratio 3a/3b	Yield
1 <sup>a</sup>	Pd NPs (1.1 nm)	0.0:1.0	49
2 <sup>a</sup>	Pd NPs (2.4 nm)	1.0:1.1	23
3 <sup>a</sup>	Pd NPs (3.1 nm)	1.0:0.8	17
4 <sup>b</sup>	Pd(OPiv) <sub>2</sub>	0.0:1.0	79

**Table 3.** <sup>a</sup>Reaction conditions: Pd NPs (1 mol%), **1** (1 mmol), CsOPiv (3.0 equiv.), **2** (3.0 equiv.), TBA-Ac (1.5 g). <sup>b</sup>Reaction conditions: Pd(OPiv)<sub>2</sub> (1 mol%), **1** (0.5 mmol), CsOPiv (3.0 equiv.), **2** (3.0 equiv.), TBA-Ac (1.5 g).

Yang et al. found a three-dimensional system interconnected network with graphene oxide (GO) and carbon nanotubes (CNTs) supported on Fe<sub>3</sub>O<sub>4</sub> that was stable towards aggregation.<sup>154</sup> Pd NPs were supported on GO/CNTs-Fe<sub>3</sub>O<sub>4</sub>, and used in C2 arylation of benzoxazole with iodobenzene in DMF at 140 °C, and in the Glaser reaction (homocoupling of phenylacetylene) in THF at 60 °C. Fairlamb and co-workers observed that in the C2 arylation of protected tryptophan with PhB(OH)<sub>2</sub> and PhI(OAc)<sub>2</sub> catalyzed by Pd(OAc)<sub>2</sub>, Pd NPs of 2.5 nm were formed at the beginning of the reaction (see Scheme 9).<sup>155</sup> The authors compared the activity of Pd(OAc)<sub>2</sub> with pre-formed NPs of 1.8 nm stabilized by polyvinylpyrrolidone (PVP), showing that the latter NPs were also active in this reaction. Although no further mechanistic studies were performed, the authors proposed that the Pd NPs were acting as a reservoir for Pd(0) active species, as was proposed for the Heck arylation processes.<sup>138</sup> Similarly, the authors also found the formation of Pd NPs in the C2 arylation of benzoxazoles catalyzed by Pd(OAc)<sub>2</sub> and suggested that the NPs acted as a reservoir for the active species.<sup>156</sup> The authors studied the reaction mechanism of the C2 arylation of indoles and other substrates (imidazole, benzoxazole or adenosine, amongst others) catalyzed by Pd(OAc)<sub>2</sub> using ArI as aryl source and hydrocarbyl transfer agents such as CuI.<sup>157</sup> It was shown that Pd NPs were generated in all cases but, depending on the substrate, they appeared at the beginning of the reaction or after few hours. However, in all the arylations that were carried out in this work, Pd NPs stabilized by PVP were also active in the reaction and, in some cases, they were even more active than the Pd(OAc)<sub>2</sub> system, thus allowing to perform the catalysis under milder conditions. Through a three-phase experiment, the authors concluded that the reaction would proceed through formation of Pd leached species, but it was not possible to determine whether the active species were Pd clusters or monoatomic Pd.

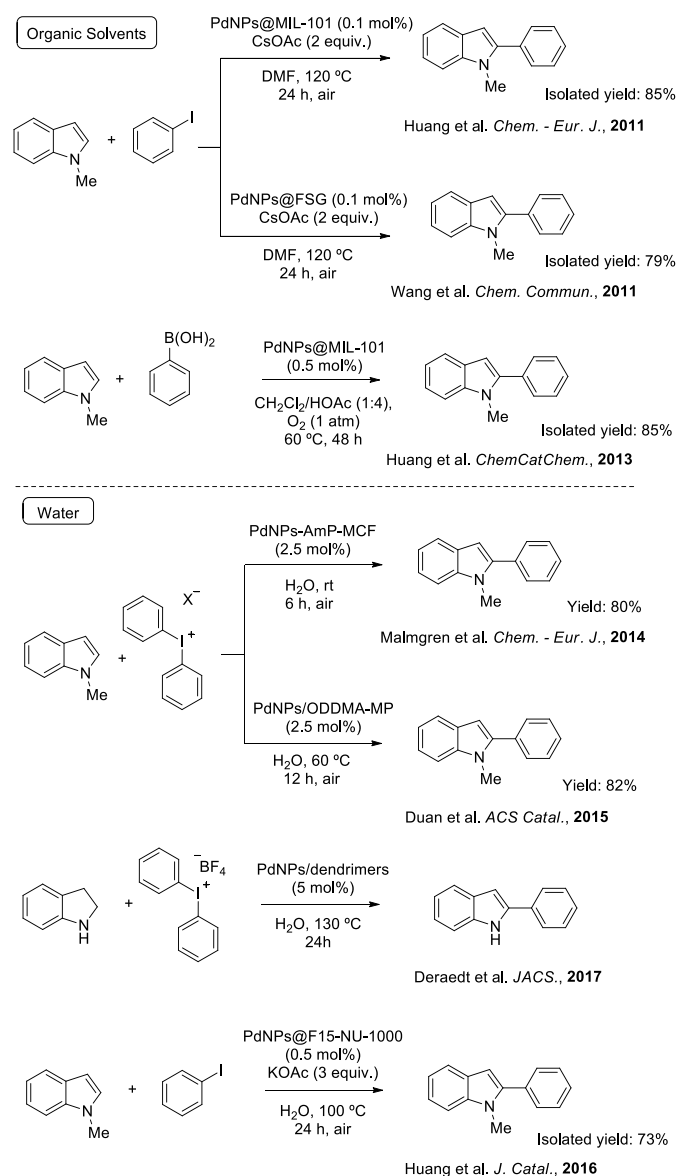


**Scheme 9.** In the C2 arylation of protected tryptophan with  $\text{PhB(OH)}_2$  and  $\text{PhI(OAc)}_2$  catalyzed by  $\text{Pd(OAc)}_2$ , Pd NPs of 2.5 nm were being formed at the beginning of the reaction, which were also active.



C2 arylation of indoles is commonly performed in the presence of oxygen or air (see Scheme 10). Cao and co-workers reported in 2011 the use of Pd NPs with a mean diameter of 2.6 nm encapsulated in mesoporous metal-organic frameworks (MOFs, more concretely  $\text{MIL-101(Cr)}$ <sup>158</sup>) for the C2 arylation of indoles with haloarenes.<sup>159</sup> The authors observed very low values of both Pd (0.4 ppm) and Cr (which is a component of the MOF material) leaching in the solution, which was attributed to the fact that encapsulation of the MOF did not allow the NPs escaping through the microporous windows. Hot filtration experiments also indicated that there was probably no Pd leaching, and the catalyst was recyclable up to 5 times without decreasing its activity. With these results, the authors proposed that catalysis was taking place at the surface of the NP. In the same year, the same reaction of C2 arylation with iodobenzene was explored by Wang et al. using 2 nm Pd NPs supported on a fluorosilica gel (FSG)<sup>160</sup> which led to similar conversions. Again, the absence of leached Pd in the solution determined by ICP, the absence of conversion after a hot filtration test and the good recyclability of the catalyst, led the authors to propose that catalysis was likely to occur at the surface of the NPs.

**Scheme 10.** C2-arylation of indole in solution catalyzed by Pd NPs performed in organic solvents (above) or in water (below). It should be noted that in all cases, the reactions were carried out in the presence of O<sub>2</sub> or air.



Cao and co-workers also reported the C2 arylation of indoles catalyzed by the same Pd NPs encapsulated in MIL-101(Cr) system above mentioned<sup>159</sup> using phenylboronic acids and oxygen instead of haloarenes.<sup>161</sup> Thanks to their high specific surface area and porosity, the MOFs allowed the reusability of the Pd NPs without loss of activity. The reaction was performed using CH<sub>2</sub>Cl<sub>2</sub>/HOAc as solvent 0.5 mol% of Pd loading and relatively low temperatures (60 °C) in the presence of 1 atm of O<sub>2</sub>. Commercial Pd/C gave only 19% yield in this reaction whereas the Pd NPs/MOF system afforded more than 90% yield. Since the reactions with indoles containing electron-withdrawing groups did not work when using O<sub>2</sub> as oxidant, the reactions were carried out using KF and TEMPO. The authors performed a hot filtration test, which led them to propose that the reaction

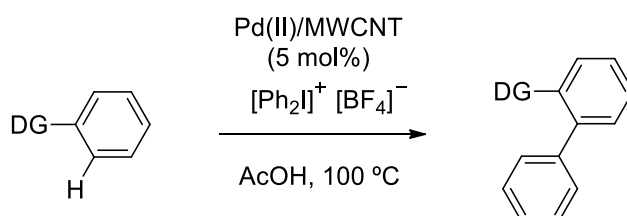
is likely taking place at the surface of the catalyst. In addition, there were very small amounts of leached Pd in solution (0.9 ppm). Interestingly, the C-H activation was preferred even in the presence of -Br or -I groups in the indole substrate.

Pd nanoparticles are also able to activate C-H bonds of indoles in water. Although the reactions generally require high catalyst loadings, they were carried out under milder conditions. In 2014, Malmgren et al. reported the use of Pd NPs supported on amino-functionalized mesocellular foam (PdNP-AmP-MCF) in the C2 arylation of indoles with diaryliodonium salts.<sup>162</sup> Commercial Pd/C was not active in the reaction. An analogous Pd(II) heterogeneous catalyst (Pd<sup>II</sup>-AmP-MCF) prepared in the same work was less active than the Pd NPs. This observation, together with the very low leaching determined by ICP, is in agreement with the hypothesis that Pd NPs are indeed participating as active species in the arylation process. However, the catalyst showed a gradual decrease in its activity through subsequent cycles, and that was attributed to the fact that Pd(II) species were removed from the NPs and dispersed through the support.

Duan et al. also reported the use of Pd NPs supported on a mesoporous resin material for the catalytic arylation of indoles with diaryliodonium salts in aqueous media.<sup>163</sup> Pd NPs with an average size of 1.5 nm were supported on a reusable mesoporous hybrid polymer-material modified with nitrogen containing groups. The polymeric material was synthesized through a surfactant-templating method and using octadecylmethyl[3-(trimethoxysilyl)-propyl] ammonium chloride as a linker between the support and the NPs (PdNPs/ODDMA-MP). The role of the support was to disperse the Pd NPs avoiding their agglomeration during the reaction and to facilitate the diffusion of the organic substrates inside the pores. The catalytic system was used in the C2 arylation of N-methylindole in water at 60 °C under air. The catalyst was more active than commercially available Pd/C, but the use of iodonium salts may limit their application on industrial scale. The catalyst could be re-used up to eight times maintaining its activity. The absence of Pd leaching was proposed by the authors after performing a hot-filtration test and analyzing the reaction mixture by ICP-AES (Pd content in the solution was less than 0.05 ppm). In 2016, Cao and co-workers also used Pd NPs with an average size of 2.5 nm, supported on hydrophobic mesoporous MOFs (NU-1000, a Zr composed MOF with mesopores of 3.0 nm<sup>164</sup>) for the C-H arylation of indoles in water with iodoarenes.<sup>165</sup> The NPs were synthesized through reduction of Pd(acac)<sub>2</sub> in the presence of the activated support under a H<sub>2</sub>/N<sub>2</sub> flow. Perfluoroalkane (F15) chains were introduced into the pores of the MOF to immobilize the NPs and to provide the hydrophobic environment. These PdNPs@F15-NU-1000 were more active and selective towards the formation of the C2 arylated product than Pd(acac)<sub>2</sub>. A hot filtration experiment indicated that the reaction probably took place at the surface of the catalyst. In 2017, Somorjai, Toste and co-workers observed that Pd NPs stabilized by dendrimers and supported on mesoporous silica, could also be active catalysts for C-H activation in H<sub>2</sub>O.<sup>166</sup> Thus, when indoline was treated with

diphenyliodonium tetrafluoroborate at 130 °C in H<sub>2</sub>O in the presence of the catalyst, 2-phenylindole was observed as the major reaction product. The authors proposed that the reaction mechanism started from dehydrogenation of indoline followed by C-H activation and C-C coupling.

Besides C2 arylation, Pd NPs have also been demonstrated to be active catalysts in the activation of C(sp<sup>2</sup>)-H activation of aromatic rings that do not contain heteroatoms, in the presence of a directing group. Korwar et al. have reported the synthesis of Pd NPs supported on multiwalled carbon nanotubes. XPS analyses evidenced the presence of a mixture of Pd(II) and Pd(0) atoms at the surface of the NPs. Thus, assuming that the active species are Pd(II) atoms, the authors named their catalyst Pd(II)/MWCNT. It showed high activity in the selective N-chelation-directed C-H activation/C-C bond formation with diaryliodonium salts.<sup>167</sup> Its performances were comparable to those of homogeneous Pd(OAc)<sub>2</sub> (see Table 4). Hot filtration experiments suggested however that the reaction was taking place heterogeneously, and the catalyst was recycled three times without deactivation.

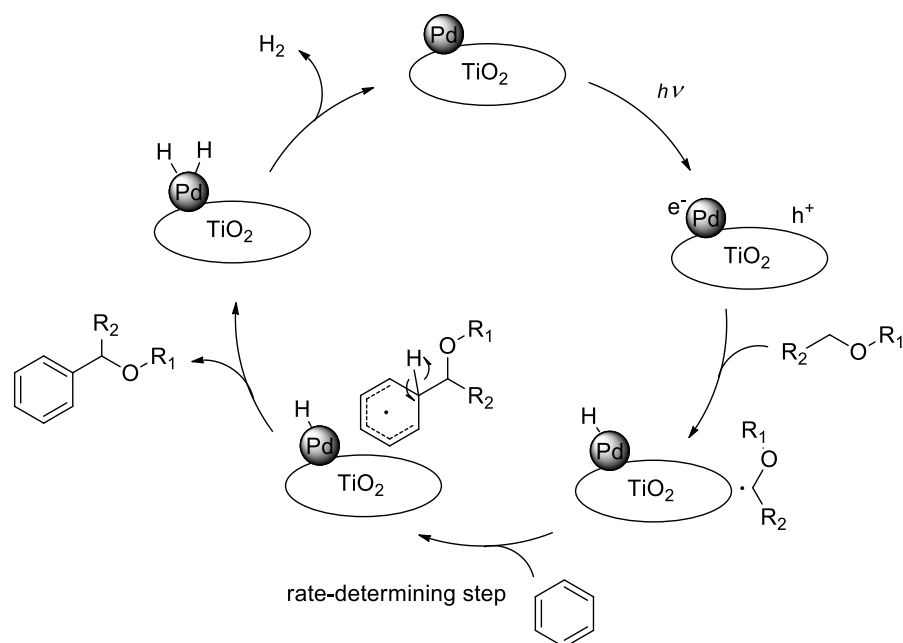


Entry	Substrate	Product	Pd(II)/MWCNT (TOF, h <sup>-1</sup> )	Pd(OAc) <sub>2</sub> (TOF, h <sup>-1</sup> )
1			90%, 3 h (16.48)	88%, 3 h (5.74)
2			80%, 24 h (1.62)	80%, 24 h (0.64)
3			27%, 12 h	49%, 12 h
4			32%, 24 h	75%, 24 h

**Table 4.** N-chelating directed C-H functionalization/C-C bond formation of aromatic substrates with diphenyliodonium salts, catalyzed by oxidized Pd NPs supported on MWCNTs.

Pd NPs have also been proposed to catalyze C-C bond formation through C(sp<sup>3</sup>)-H activation, which proceeded through a radical. In 2016, Yoshida and co-workers designed different bifunctional metal NPs/TiO<sub>2</sub> photocatalysts for the C(sp<sup>3</sup>)-H functionalization of ethers with benzene at the  $\alpha$ -position.<sup>168</sup> The most active catalytic system in the reaction was that based on PdNPs /TiO<sub>2</sub>, and it was selected to perform mechanistic studies. The authors proposed that under UV light irradiation ( $\lambda=365 \pm 20$  nm), an excited electron was generated that would be localized at the Pd NP, giving its corresponding hole at the TiO<sub>2</sub> support (see Scheme 11). The hole would activate the  $\alpha$ -C-H bond of the ether to give an  $\alpha$ -oxoalkyl radical. Alternatively, the Pd NPs that are electron-rich would interact with anti-bonding  $\pi^*$  molecular orbital of benzene, activating it towards C-C bond formation. Based on a kinetic isotope effect, it was proposed that the reaction proceeded through an intermediate bearing an sp<sup>3</sup>-like carbon center in the aromatic ring, the formation of which would be the rate-limiting step. Further generation of the reaction product and formation of hydrogen would restart the catalytic cycle.

**Scheme 11.** Proposed radical mechanism for the C-H functionalization of ethers with benzene catalyzed by PdNPs/TiO<sub>2</sub>. Irradiation with light generates a hole in the support, which assists the formation of an alkyl-ether radical. This specie would react with benzene, which was previously activated by interaction of the  $\pi$ -cloud with the Pd NP. The active species regenerate through reductive elimination and formation of H<sub>2</sub>.



Summarizing, although Pd NPs have been widely used as catalysts in C-H functionalization, especially in arylation of aromatic compounds, the reaction mechanism and the nature of the active species have not been precisely determined. Key issue remains that the reactions may be catalyzed

by leached Pd species. However, several observations suggest that C2 arylation of indoles may occur at the surface of the PdNPs, which must be previously oxidized.

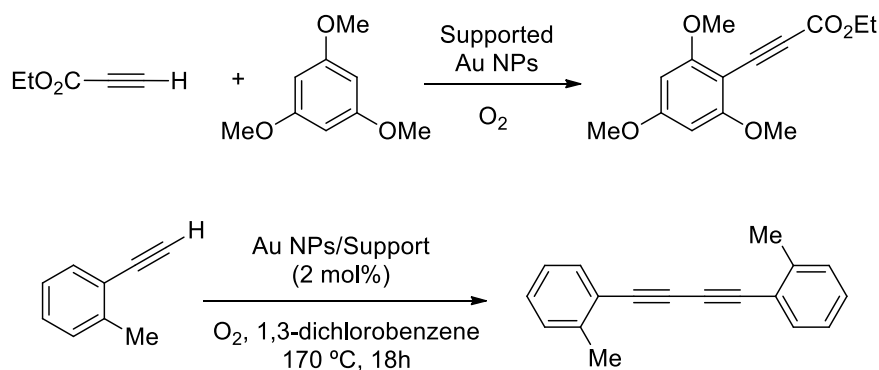
### 3.2.2. Au NPs in the C-H functionalization of C(sp)-H bonds and beyond.

There is a controversy about whether C(sp)-H activation may be considered as a C-H activation or as an acid-base reaction. Textbooks prefer the last mechanism; as proposed by Hartwig, the acidity of alkynyl C-H bond makes it possible to form M-alkynyl complexes after deprotonation of the alkyne with relatively weak bases.<sup>169</sup> In addition, M-C bonds in alkynyl complexes are stronger than those in alkyl or aryl complexes. Thus, although C(sp)-H cleavage formally involves an activation of a C-H bond, we prefer to consider such reactions as C-H functionalization rather than as C-H activation. However, it is common to find in the literature the “C-H activation” terminology for C(sp)-H cleavage, so they will be briefly discussed herein.

Supported gold NPs are well-known catalysts for the C(sp)-H activation of terminal alkynes.<sup>170-171</sup> In many cases, it has been proposed that the reactions are catalyzed by support-stabilized Au(III) species, following an Au(I)/Au(III) catalytic cycle as for homogeneous processes. Such catalysts have been used for instance in three-component coupling reactions of alkyne, aldehyde, and amine by Zhang and Corma,<sup>172</sup> or in cycloisomerization/oxidative dimerization of aryl propargyl ethers by the group of Stratakis.<sup>173</sup> As an example, in 2013, Corma and co-workers observed that the reactivity of supported Au NPs was dependent upon presence or absence of O<sub>2</sub>.<sup>174</sup> Thus, under O<sub>2</sub> atmosphere, the oxidative arene alkynylation of trimethoxybenzene was observed (see Scheme 12). Since it is known that Au NPs can dissociate molecular oxygen to generate reactive species,<sup>175</sup> the authors proposed that oxygen atoms would assist C(sp)-H functionalization by trapping the protons generated in the reaction to give a Au<sup>+</sup>-alkynyl moiety. Then, after coordination of the arene to the Au<sup>+</sup> species, the molecule is deprotonated by the OH<sup>-</sup> to give a Au(I)-aryl moiety, followed by C-C coupling between the aryl and alkynyl groups. The heterogeneous nature of the catalyst was demonstrated after hot filtration experiments, indicating that C-H functionalization might take place at the surface of the NPs. It was also proposed that the mechanism involved an Au(0)/Au(I) catalytic cycle instead of the classical Au(I)/Au(III). Later, the same group performed a theoretical and experimental study in order to elucidate the role of oxygen in the aerobic homocoupling of alkynes (Glaser) catalyzed by Au NPs supported on CeO<sub>2</sub> (see Scheme 12).<sup>148</sup> The dissociation of oxygen at the surface of the NP was the rate limiting step of the reaction. By DFT calculations, it was shown that C-H activation/deprotonation occurred at the surface of the NPs, and that the alkyne could adsorb on Au(0) atoms, as well as on cationic Au<sup>δ+</sup> and Au<sup>+</sup> sites. The deprotonation of the alkyne was energetically possible in all systems as long as O atoms were present to assist the process, but alkynes adsorbed at Au<sup>δ+</sup> and Au<sup>+</sup> sites were more reactive than those adsorbed at Au(0) sites. This work confirmed that

the partial oxidation of the Au NPs is the key step in the C(sp)-H activation at the surface of the NPs, O<sub>2</sub> being the acceptor of both electrons and protons generated in the process.

**Scheme 12.** C(sp)-H functionalization of alkynes with trimethoxybenzene (top) and homocoupling of alkynes (below) catalyzed by supported Au NPs require the presence of oxygen. It was proposed that the role of the oxygen is to act as acceptor of both protons generated in the C-H cleavage.



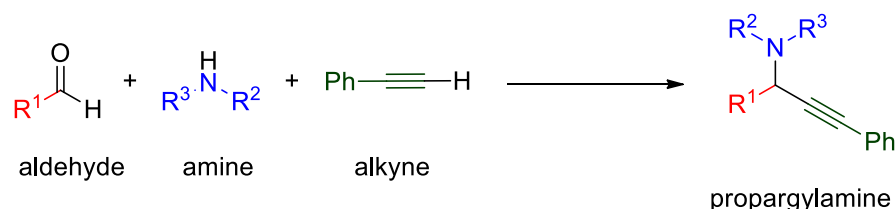
In some other cases, Au NPs in solution have been proposed to participate in the reaction either by acting as reservoir for molecular active species, Au(I) complexes generally, or by catalyzing the C(sp)-H activation at their surface, as the ability of Au NPs to react with the C(sp)-H bond of terminal alkynes is well-known.<sup>176</sup>

In addition, Au NPs have been used in alkane hydrocarboxylation by Ribeiro et al.<sup>177</sup> A mixture of Au NPs and nano-rods supported on carbon xerogels catalyze the transformation of cyclohexane to 54% cyclohexanecarboxylic acid in the presence of CO, peroxodisulfate and water. A H<sub>2</sub>O/CH<sub>3</sub>CN mixture was used as solvent, and the reaction was performed under mild conditions (50 °C) and with Au loadings of 0.2 mol%. By-products are cyclohexanol, cyclohexanone, and 1,2-cyclohexanediol. The NPs showed higher activities than HAuCl<sub>4</sub>·3H<sub>2</sub>O. In addition, the catalyst could be re-used up to seven times maintaining its performance.

Propargylamines are interesting substrates, because they are intermediates in the synthesis of biologically active compounds and drugs.<sup>178</sup> They are frequently prepared through a three-component reaction between an aldehyde, an alkyne and an amine, usually called A<sup>3</sup> coupling (see Scheme 13). This reaction has been traditionally performed using strong bases to deprotonate the alkyne reagent, typically butyllithium or organomagnesium reagents. However, during the past 10 years, catalysis by metal NPs has arisen as a better strategy to avoid the use of stoichiometric reagents and the catalysts can be recycled in some cases. In these reactions, the mechanism involves a C(sp)-H activation. Au NPs have proven to be active catalysts in the A<sup>3</sup> coupling, although more recently Cu, Fe and their respective oxides have attracted more attention due to their availability and lower costs (see section

3.2.3). Some examples of A<sup>3</sup> coupling catalyzed by Au NPs can be found in the reports of Kidway et al.;<sup>179</sup> Datta et al.;<sup>180</sup> Layek et al.;<sup>181</sup> Gholinejad et al.<sup>182</sup> or Aguilar et al.<sup>183</sup>

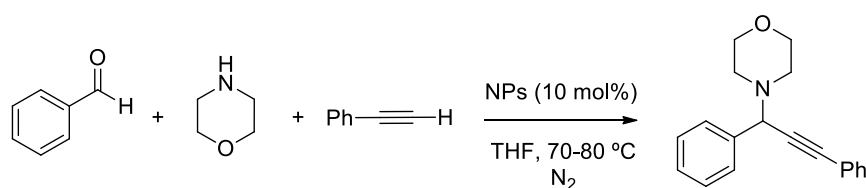
**Scheme 13.** A<sup>3</sup> coupling reaction between an aldehyde, an amine and an alkyne to give a propargylamine.



### 3.2.3. Other metal NPs in C(sp)-H activation.

Fe and Cu NPs (and their corresponding oxides) are good candidates to perform some of the catalytic C(sp)-H functionalization reactions, since these metals are cheap and abundant. In addition, some Fe oxide NPs are ferromagnetic, which is an advantage in terms of separation and recyclability.

The first example of an A<sup>3</sup> coupling between benzaldehyde, morpholine and phenylacetylene catalyzed by Cu NPs was reported by Kidway et al. in 2007 (see Table 5).<sup>184</sup> Different metal NPs were tested for this reaction, using relatively large catalyst loadings. Amongst them, Cu, Ag and Au were the most active. When performing the reaction with Cu NPs of ca. 18 nm mean size, the optimal conditions were reached using CH<sub>3</sub>CN as solvent, at 100-110°C and a catalyst loading of 15 mol%. The catalyst was recycled and reused up to five times obtaining good activities.



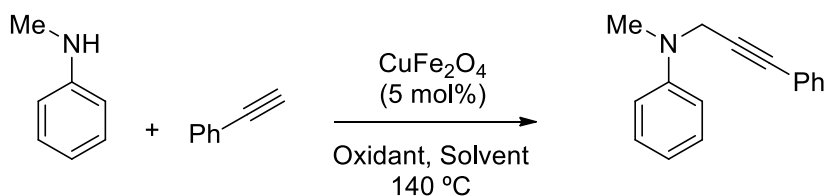
Metal	Time (h)	Yield (%)
Cu	6.5	91
Au	4	92
Ag	3.5	84
Ni	10	42



**Table 5.** A<sup>3</sup> coupling reaction between benzaldehyde, morpholine and phenylacetylene catalyzed by metal NPs. Reactions were carried out under N<sub>2</sub> atmosphere.

Sharghi et al. reported the synthesis of substituted benzofurans starting from 2-hydroxybenzaldehyde (salicylaldehyde), a secondary amine and phenylacetylene, catalyzed by copper (I) oxide nanoparticles (formally Cu<sub>2</sub>O NPs) at 100 °C in the presence of TBAB and K<sub>2</sub>CO<sub>3</sub> as base and in the absence of solvent.<sup>185</sup> In 2014, Kotadia and Soni reported the synthesis of Fe-doped titania (Fe/TiO<sub>2</sub>) and silica (SiO<sub>2</sub>) NPs between 10-15 nm by sol-gel processes.<sup>186</sup> The NPs were used in A<sup>3</sup>-coupling reactions between an aldehyde, an amine and a terminal alkyne. Fe/TiO<sub>2</sub> was the most active catalyst for the microwave-assisted reaction in absence of solvent. Bhalla and co-workers reported the use of superparamagnetic Fe<sub>3</sub>O<sub>4</sub> NPs stabilized by an organic conjugated molecule (perylene bisimide, PBI) in the A<sup>3</sup> coupling under mild conditions.<sup>187</sup> The authors proposed that activation of the C(sp)-H bond from the alkyne takes place at the surface of the Fe<sub>3</sub>O<sub>4</sub> NPs, although no further mechanistic studies were performed. In addition, the catalytic system was also active in the synthesis of propargylamines under aldehyde-free conditions using dimethylarylamine substrates, through C(sp<sup>3</sup>)-H activation of the methyl groups.

Other catalytic systems based on metal NPs for the A<sup>3</sup> coupling have been reported during the past few years. For example, Sasikala et al. reported a heterogeneous catalyst composed by La loaded CuO NPs;<sup>188</sup> Gulati et al. prepared CuO NPs supported on Fe<sub>2</sub>O<sub>3</sub> that were easily recyclable from the reaction medium.<sup>189</sup> Gupta et al. have reported the synthesis of Cu<sub>6</sub>Se<sub>4.5</sub> NPs, which were used in the preparation of propargylamines through a cross-dehydrogenative coupling between tertiary amines and terminal alkynes.<sup>190</sup> Superparamagnetic copper ferrite (CuFe<sub>2</sub>O<sub>4</sub>) NPs have been tested in the synthesis of propargylamines through three-component cross-coupling reactions between anilines and terminal alkynes using *tert*-butyl hydroperoxide (TBHP) as oxidant and source of methyl radicals in dimethylacetamide (DMA) at high temperatures (140 °C).<sup>191</sup> The presence of TBHP as oxidant in the reaction was essential for the formation of the products supporting the hypothesis of a radical mechanism (see Table 6). Similarly, the synthesis of propargylamines via C-H activation and involving three-component, amines, dichloromethane and terminal alkynes has been also catalyzed by indium oxide NPs by Rahman et al.<sup>192</sup>



Solvent	Oxidant	Conversion (%)
<i>o</i> -xylene	TBHP	48
Diglyme	TBHP	58
DMF	TBHP	88
DMA	<i>tert</i> -butylbenzoylperoxide	84
DMA	dicumyl peroxide	86
DMA	Hydrogen peroxide	0

**Table 6.** Synthesis of propargylamines catalyzed by copper ferrite ( $\text{CuFe}_2\text{O}_4$ ) NPs through three-component cross-coupling reactions between anilines and terminal alkynes. *Tert*-butyl hydroperoxide (TBHP) is used as both oxidant and source of methyl radicals.

There are a few reactions that proceed via formation of free radicals after leaching of molecular species from the NPs, such as arylation of benzoquinone<sup>193</sup> or decarboxylative coupling.<sup>194-195</sup> However, we do not consider such reactions as C-H activation catalyzed by metal NPs, so they fall out of the scope of this review.

There are also examples of C-H activation for C-C coupling that have been proposed to involve the formation of radicals by irradiation with light. Bhalla and co-workers showed that metal NPs functionalized with supramolecular ensembles of fluorescent materials exhibited good activities in photocatalytic  $\text{C}(\text{sp}^2)\text{-H}$  alkynylation of arenes with terminal alkynes, as well as in amination of arenes with activated aromatic amines.<sup>196</sup> The reactions were carried out in DMSO with  $\text{K}_2\text{CO}_3$  as a base under air using 1.0 mol % of the ensemble catalyst irradiating with a 60 W tungsten filament bulb. The aggregates of perylene bisimide (PBI) played the role of a light harvesting antenna in the  $\text{C}(\text{sp}^2)\text{-H}$  alkynylation. The Cu NPs showed higher activities than  $\text{Cu}^{2+}$  complexes. A catalytic system composed of hexaphenylbenzene and  $\text{Ag}@\text{Cu}_2\text{O}$  core-shell nanoparticles with a size of ca. 10 nm was prepared by the same group and shown to be an efficient catalysts for the formation of imidazole and benzimidazoles derivatives via visible light mediated (100 W tungsten filament bulb) C-H activation.<sup>197</sup> Analogously to the above described system, the composed material was excited in the presence of light that induced an energy transfer process which enhanced the catalytic activity of the CuO shell.

### 3.3. C-X Bond formation.

In this section we will discuss the exchange of a C-H bond by a C-X bond (X= O, N, S, etc.). By these processes, organic molecules of important added value such as ketones, alcohols and epoxides can be easily prepared from readily available sources such as alkanes or arenes. Formally, these transformations can be considered as oxidation reactions, as the valence of the C atom increased after exchange of a H by a N, an O or a halide atom. Regarding the mechanism, these reactions often involve radical species that can be provided by the metal NPs or by using classical radical agents that can exchange electrons with the metal NPs. In this sub-section we will focus on the processes carried out under mild conditions.

#### 3.3.1. Oxidative C-H activation to afford C-O bonds.

One of the most important transformations in heterogeneous catalysis that involves C-H activation is the oxidation of methane.<sup>24</sup> Catalytic C-H activation of CH<sub>4</sub> is a process that employs high temperatures, because of the high energies required in the homo- and heteroleptic cleavage of these bonds, the absence of dipole moment, or the very high value of pK<sub>a</sub>, among other reasons.<sup>198</sup> Metal NPs have been successfully used in the activation of methane at high temperatures.<sup>199</sup> Dry reforming of methane, the simultaneous activation of CH<sub>4</sub> and CO<sub>2</sub> to give a *syngas* mixture (CO + H<sub>2</sub>) is one of the most studied processes, and it can be catalyzed by metal NPs such as Pt NPs or Ni NPs or metal-oxide such as NiO NPs at temperatures that generally surpass 500 °C.<sup>200-203</sup> Very recently, Takami et al. have proposed that this reaction can be carried out at lower temperatures using plasmonic Ni photocatalysts in the presence of light (300 W Xe lamp).<sup>204</sup> There have also been other examples of C-H oxidative activation of alkanes at high temperatures that are heterogeneously catalyzed by metal NPs, such as oxidative dehydrogenation<sup>205-207</sup> or isomerization.<sup>208</sup> However, in this review we will not discuss the oxidative transformations at high temperatures and we will focus in processes carried out in the presence of solvents.

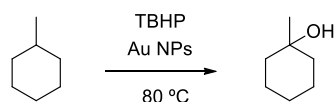
Oxidative C-H addition in solution has been mainly focused on the C(sp<sup>3</sup>)-H activation, a reaction with a high energetic barrier that usually is performed through a radical catalytic cycle and in the presence of oxidants and, in some cases, radical co-catalysts such as peroxides. It is generally accepted that NPs promote the decomposition of peroxides to give oxygen radical species, the role of which is to assist the C-H activation of the substrates.<sup>209</sup> The first evidence of the formation of surface-oxygen radical species in the oxidation of alkanes was provided by Hutchings and co-workers. In 2011, they prepared Au-Pd alloy NPs supported on carbon that were active in the oxidation of primary C-H bonds in toluene at 160 °C.<sup>210</sup> More recently it was proven that the same reaction could be carried out under milder conditions (80 °C), in the presence of 1 equivalent of *tert*-butyl hydroperoxide

(TBHP) and using Au-Pd NPs supported on TiO<sub>2</sub> as catalyst.<sup>211</sup> By solid-state electron paramagnetic resonance (EPR) experiments, the authors proposed that surface-bound oxygen radical species which were formed after reaction with TBHP, played an active role in the activation of toluene. Since then, several oxidative C-H activations catalyzed by metallic and metal-oxide NPs have been reported. As above discussed, we do not consider here reactions that do not involve interaction of the C–H bond and the metal. Thus, in the present work, we will summarize a few examples of catalytic oxidations involving the use of metal NPs focusing on processes carried out under mild conditions.

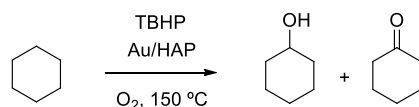
Au NPs have been widely employed in oxidative C-H activations (see Scheme 14). For instance, in 2010 Mendez et al. prepared Au NPs with an average size below 3 nm supported on Gd-doped TiO<sub>2</sub>, which were used to catalyze the methylcyclohexane mediated epoxidation of stilbene, which led to the autoxidation of methylcyclohexane to 1-methylcyclohexanol.<sup>212</sup> An alkylperoxy radical took part in the mechanism of the reaction but the specific role of the catalyst was not confirmed. In 2011, Liu et al. prepared small Au NPs (<2 nm) supported on hydroxyapatite (HAP), that were used in the oxidation of toluene at 150 °C.<sup>213</sup> Then, Donoeva et al. showed that Au NPs of less than 2 nm of size were not active for the solvent-free oxidation of cyclohexene under mild reaction conditions (65 °C), but that larger Au NPs were much more active.<sup>214</sup> The authors proposed that the role of the Au NPs was to promote the formation of cyclohexenyl radicals that would further react with dissolved oxygen.

Sarma and co-workers synthesized a ternary nano-composite based on Au NPs supported on polydopamine-reduced graphene oxide (AuNPs-pDA-rGO).<sup>215</sup> The catalyst was used in the oxidation of C-H bonds of benzylic hydrocarbons in CH<sub>3</sub>CN at 60 °C under O<sub>2</sub> atmosphere, in the presence of *N*-hydroxyphthalimide (NHPI) as co-catalyst. Liu et al. reported the use of Au NPs supported on carbon dots (AuNPs/CQDs), for electrocatalytic cyclohexane oxidation with H<sub>2</sub>O<sub>2</sub> in the presence of visible light.<sup>216</sup> The interaction between the support and AuNPs was characterized by X-ray absorption with the observation of a new peak at 1.5 Å corresponding to the Au-C bonds. Reactions were carried out at room temperature without any solvent, producing water as the only by-product. The authors proposed that light absorption by the surface plasmon resonance of the AuNPs after irradiation with green light (λ=490-590 nm), enhanced the decomposition of H<sub>2</sub>O<sub>2</sub>, providing the HO· radicals active in the oxidation of the cyclohexane. The synergy between the CQDs and the Au NPs in the presence of visible light is a key factor for this photocatalytic reaction. The effect of the wavelength on the activity and selectivity of the reaction was also studied, and the authors found that the optimal conditions were reached when irradiating with green light.

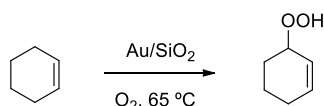
**Scheme 14.** Oxidative C-H functionalization of C(sp<sup>3</sup>)-H bonds catalyzed by Au NPs.



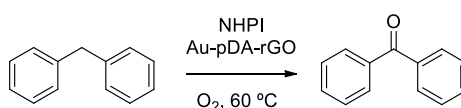
Mendez et al. *Dalton Trans.* **2010**



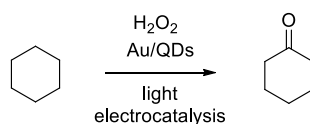
Liu et al. *ACS Catal.* **2011**



Donoeva et al. *ACS Catal.* **2013**



Majmudar et al. *ChemCatChem.* **2016**

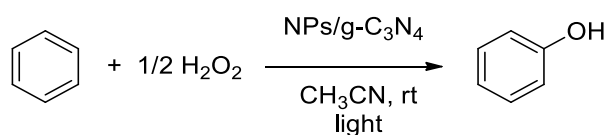


Liu et al. *ACS Catal.* **2014**

Other metal NPs have been used in oxidative C-H activation. Varma and co-workers synthesized photoactive Pd NPs supported on graphitic carbon nitride (g-C<sub>3</sub>N<sub>4</sub>), which were active in the oxidative esterification of alkyl aromatic alcohols in methanol.<sup>217</sup> Sun et al. prepared diatomite-supported manganese oxide NPs that were used in the oxyalkylation of vinylarenes.<sup>218</sup> Payra et al. reported the synthesis of poly-substituted furans catalyzed by CuO NPs of 10 nm, using TBHP oxidant agent and a 1:1 mixture of H<sub>2</sub>O/EtOH as solvent.<sup>219</sup>

Some examples of oxidative C-H activations involving bimetallic NPs have been reported during the past years. Adams et al. reported IrBi NPs that were synthesized from bimetallic molecular cluster complexes.<sup>220</sup> In a proof of concept, the authors showed that these bimetallic NPs were more active in the direct oxidation of 3-picolin to niacin with peroxyacetic acid, than their analogous monometallic NPs. Au-Pd NPs supported on MOFs (MIL-101<sup>158</sup>) have been used by Liu et al. in the esterification of alkyl aromatics with alcohols at 120 °C in the presence of O<sub>2</sub>.<sup>221</sup> More recently, Varma and co-workers have tested different photoactive catalysts based on NPs supported on g-C<sub>3</sub>N<sub>4</sub> in the hydroxylation of benzene into phenol at room temperature under visible light (20 W domestic bulb), using H<sub>2</sub>O<sub>2</sub> as oxidant (see Table 7).<sup>222</sup> CuAg NPs were found to be the most active, and more

active than monometallic Cu or Ag NPs, suggesting the presence of a synergistic effect. Non-covalent interaction between the benzene and the graphitic surface is proposed as an element that facilitates the C-H cleavage.



Entry	Catalyst (supported on g-C <sub>3</sub> N <sub>4</sub> )	Time	Conv. (%)
1	Fe <sub>2</sub> O <sub>3</sub>	12 h	15
2	Pd	12 h	43
3	Cu	12 h	39
4	Ni	12 h	20
5	Ag	12 h	32
6	FePd	12 h	70
7	PdCu	12 h	81
8	CuNi	12 h	57
9	CuAg	30 min	99

**Table 7.** Hydroxylation of benzene into phenol using H<sub>2</sub>O<sub>2</sub> as oxidant catalyzed by different mono- and bimetallic NPs.

In summary, the use of metal NPs allows performing oxidative C-H activation reactions under milder conditions than traditional heterogeneous catalysis. Special interest must be paid to catalytic systems in which the use of co-catalysts, oxidants and/or the use of light have allowed to carry out the C-H activations at room temperature. This fact, combined with the recyclability allowed by some of the catalysts, may be of potential interest for the scaling up of the processes. Although Au NPs remain as the most widely studied catalytic system for these reactions, some less costly alternatives have appeared during the past decade. However, there are still efforts needed to explore alternatives to reduce the cost of the catalysts and achieve milder reaction conditions in certain catalytic processes.

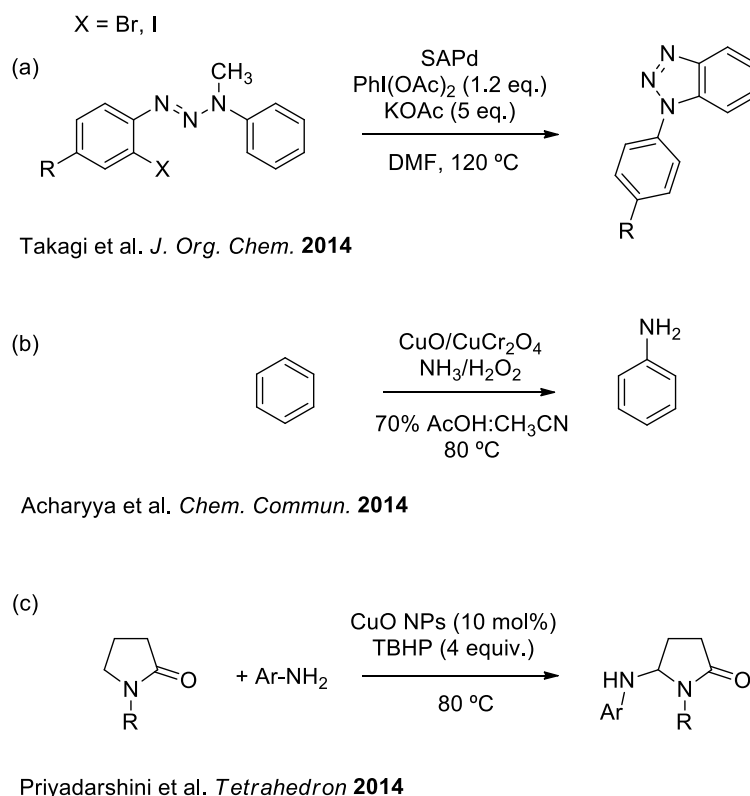
### 3.3.2 C-H bond activation in the formation of other bonds.

The synthesis of organic molecules containing C-Y bonds (Y= N, S, Se, Cl, Br, I etc.) through C-H activation and catalyzed by metal NPs has given rise to only few examples in the literature. Herein, the reactions are classified as a function of the Y-atom introduced.

### 3.3.2.1 C-H bond activation for C-N formation.

Takagi et al. reported the use of sulfur-modified gold-supported Pd NPs (SAPd) of ca. 5 nm size, which were used in the synthesis of substituted benzotriazoles via C-H activation and C-N bond formation.<sup>223</sup> The reaction proceeded through a migration/cyclization/dealkylation pathway, in which the fate of the N-methyl group is not known.<sup>224</sup> The reactions were carried out in DMF at 120 °C in the presence of KOAc and using PhI(OAc)<sub>2</sub> as oxidant (see Scheme 15a). Acharyya et al. reported the use of CuO NPs with a mean size of 10 nm, supported on CuCr<sub>2</sub>O<sub>4</sub> spinel nanoparticles (30-60 nm).<sup>225</sup> They were used for the formation of aniline through oxyamination of benzene in the presence of a H<sub>2</sub>O<sub>2</sub>/NH<sub>3</sub> mixture, using a 70% aqueous mixture of acetic acid:CH<sub>3</sub>CN as solvent and at 80 °C (see Scheme 15b). Priyadarshini et al. have reported the use of CuO nanoparticles for oxidative cross-coupling of aromatic amines with 2-pyrrolidinone (see Scheme 15c).<sup>226</sup> Whereas CuO NPs were active in the reaction, other systems such as ZnO, TiO<sub>2</sub> or NiO NPs did not give significant conversions. TBHP was used as oxidant and the reactions were performed at 80 °C using 20 mol % of CuO NPs.

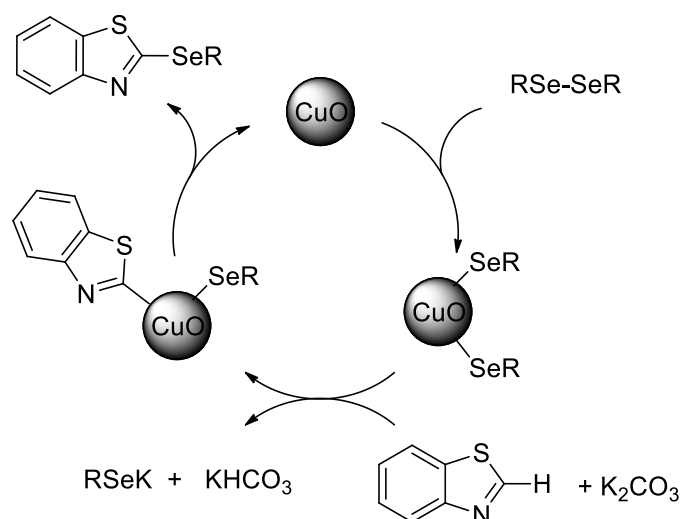
**Scheme 15.** C-N bond formation through C-H functionalization catalyzed by metal NPs. (a) Synthesis of substituted benzotriazoles catalyzed by Pd NPs. (b) Synthesis of aniline catalyzed by CuO NPs. (c) Oxidative cross-coupling of aromatic amines with 2-pyrrolidinone catalyzed by CuO NPs.



### 3.3.2.2 C-H bond activation for chalcogenation and halogenation.

In 2013, Rosario et al. reported the use of CuO NPs for the C-H activation of thiazoles.<sup>227</sup> The use of a basic agent was shown to be essential for the regeneration of the catalytic active species. The formation of the 2-(organoselenyl)thiazoles was carried out in DMF at 140 °C using 20 mol% of catalyst loading. In all cases the reaction products were obtained as a mixture together with diarylselenides, which were removed by chromatography. The addition of radical inhibitors did not hamper the reaction. Thus, the authors proposed a possible mechanism for the reaction (Scheme 16) involving a Se-Se bond activation at the surface of the NPs through an oxidative addition, followed by C-H activation of the thiazole and reductive elimination.

**Scheme 16.** C2 functionalization of thiazoles with arylselenides catalyzed by CuO NPs. The mechanism involved Se-Se bond activation.



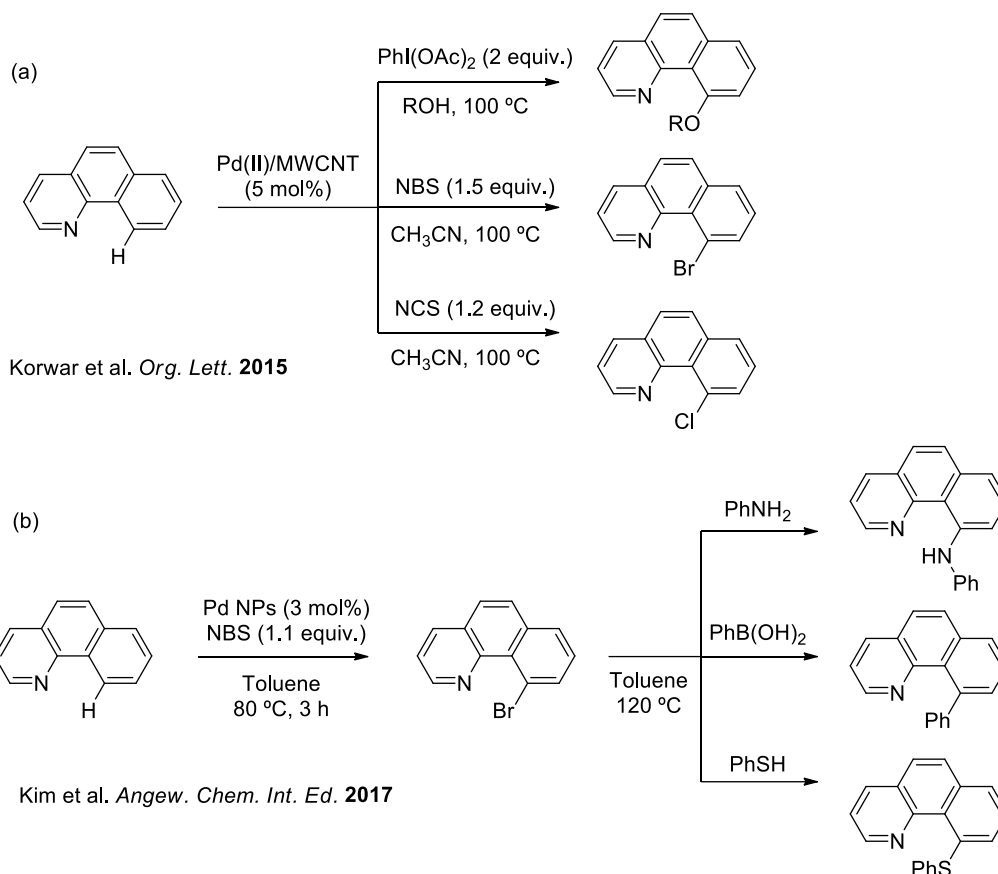
Cu NPs were employed by Mohan et al. in the synthesis of alkynyl sulfides and alkynyl selenides via C-H functionalization of alkynes under O<sub>2</sub> in DMSO, using Na<sub>2</sub>CO<sub>3</sub> as base, at 70 °C with 0.5 mol % of catalyst loadings.<sup>228</sup> Similar to the above suggested mechanism, the authors proposed that the reaction was initiated by S-S or Se-Se activation of the disulfide or diselenide reagent on the surface of the NPs, followed by metallation of the alkyne and reductive elimination. The role of the oxygen was to regenerate the disulfide or the diselenide. Fe<sub>3</sub>O<sub>4</sub> NPs supported on charcoal, (0.5 mol% Fe<sub>3</sub>O<sub>4</sub>/C) were also studied by the same group in the cross coupling reactions between alkynes and diselenides to obtain alkynyl selenides.<sup>229</sup>

Pd NPs have been used in halogenation reactions through C-H activation. In 2015, Korwar et al. expanded the application of their catalytic system composed of Pd NPs supported on multiwalled carbon nanotubes Pd(II)/MWCNT (see Section 3.1.1).<sup>230</sup> The catalyst showed high activity in the selective N-chelation-directed C-H activation for C-O, C-Cl and C-Br bond formation (see Scheme



17a). The authors showed that halogenation reactions were faster with the Pd(II)/MWCNT system than with Pd(OAc)<sub>2</sub>. An interesting advantage of halogenation reactions is that further C-X activation by Pd can allow tandem processes through lower energetic pathways than direct C-H activation. Kim et al. prepared Pd NPs of 3.5 nm by decomposition of [Pd(acac)<sub>2</sub>] in the presence of oleylamine and trioctylphosphine.<sup>231</sup> By the controlled oxidation of the NPs with PhICl<sub>2</sub> in benzene at 120 °C, Pd(IV) surface species containing oxide and chloride ligands were formed, that were characterized by XPS.<sup>232</sup> Interestingly, further treatment of the oxidized NPs with H<sub>2</sub> allowed regenerating the initial reduced Pd NPs, which maintained their morphology. The oxidized Pd NPs containing Pd(IV) species at their surface were active in C-H halogenation but, after the completion of the reaction, Pd(0) species were regenerated. Thus, the catalysts were used in tandem reactions that combined C-H halogenation by Pd(IV) species with further cross coupling performed by Pd(0), to allow C-N, C-C and C-S bond formation (see Scheme 17b). The heterogeneous nature of the C-H halogenation was proposed after a hot filtration experiment and a mercury poisoning test.

**Scheme. 17.** Halogenation of arenes through C-H activation catalyzed by Pd NPs. (a) N-chelation-directed C-H activation for C-O, C-Cl and C-Br bond formation catalyzed by oxidized Pd NPs supported on MWCNTs. (b) Tandem reactions combining C-H activation/halogenation, followed by further cross coupling reaction to allow C-N, C-C and C-S bond formation, catalyzed by oxidized Pd NPs.



Pascanu et al. reported the use of Pd NPs supported on MOFs (Pd@MOF) as catalysts in the selective halogenation of aromatic derivatives via C-H activation.<sup>233</sup> Pd NPs with a mean size of around 2 nm were immobilized into two porous MOFs of different nature, [Pd@MIL-88B-NH<sub>2</sub> (Fe-MOF), and Pd@MIL-101-NH<sub>2</sub> (Cr-MOF)]. Both systems were good catalysts for the halogenation of a wide range of aromatic substrates containing directing groups such as pyridine or amides, under mild reaction conditions. NCS, NBS or *N*-iodosuccinimide (NIS) were used as halogen sources. The authors proposed that the mechanism involved a rapid leaching-deposition of Pd.

#### 4. Si-H activation by metal NPs.

Hydrosilanes are useful precursors for the preparation of many different silicon containing molecules.<sup>234-236</sup> Transformation of hydrosilanes into value-added molecules generally involves the  $\sigma$ -activation of a Si-H bond. The higher basicity of the Si-H bonds in comparison with H-H or C-H bonds makes them a stronger  $\sigma$ -donor. Also, the higher accessibility of the  $\sigma^*$ -orbital makes hydrosilanes more  $\pi$ -acceptor and as result Si(sp<sup>3</sup>)-H bonds are easier to activate than C(sp<sup>3</sup>)-H bonds. The different substituents in the Si moiety can affect the activation of the Si-H bond, and it is well-known that electron-withdrawing groups facilitate the bond dissociation. Apart from its own interest, an advantage of the comprehensive study of reactions that imply activation of hydrosilanes by transition metals is that hydrosilanes, which undergo Si-H activation more easily than alkanes, can be used as a model for C-H activation reactions.

Catalytic activation of hydrosilanes by homogeneous organometallic complexes has been widely studied. Traditionally, oxidative addition of Si-H has been performed on Pt organometallic complexes such as the Karstedt's catalyst [Platinum(0)-1,3-divinyl-1,1,3,3-tetramethyldisiloxane].<sup>237</sup> However, during the last years some evidences have shown that metal NPs can afford Si-H activation in a heterogeneous process, i.e. taking place at their surface. For instance, Pelzer and co-workers prepared Ru NPs by decomposition of Ru(COD)(COT) under a H<sub>2</sub> atmosphere in the presence of *n*-octylsilane as ligand.<sup>238-239</sup> Solid state <sup>13</sup>C NMR characterization demonstrated the formation of naked silicon atoms and alkylsilane ligands that were coordinated to the surface of the NPs, as a result of the activation of the  $\sigma$ -Si-H bond, followed by Si-C cleavage at the surface of the Ru NPs. In another work from Pelzer, Basset and co-workers,<sup>240</sup> Pt NPs of 2 nm size were prepared by decomposition [Pt(dba)<sub>2</sub>] under 3 bar of H<sub>2</sub> using *n*-octylsilane as ligand. After characterization of the NPs by Infrared Spectroscopy, Transmission Electron Microscopy-Energy Dispersive X-Ray Spectroscopy (TEM-EDX) and X-Ray Photoelectron Spectroscopy (XPS), the authors proposed that silicon alkyl species were coordinated to the surface.

A new interest in studying the catalytic performance of metal NPs in reactions involving  $\sigma$ -Si-H activation has evolved in recent years. In this section, the role of metal NPs as active species in hydrosilylation and in silane oxidation, two reactions that start from the  $\sigma$ -activation of the Si-H bond, will be discussed.

#### 4.1. Hydrosilylation.

Organosilicon molecules are important as polymers, sealants, adhesives, coatings, and agents for surface treatments, and as synthetic intermediates in organic and medicinal chemistry.<sup>241-243</sup> The main route for their preparation consists of the hydrosilylation of unsaturated organic compounds, an organic addition reaction that in many cases is catalyzed by transition-metal complexes in the homogeneous phase.<sup>234-236,244</sup> Although the reaction can be catalyzed by several metals, Pt-based catalysts have been the most widely investigated due to their good activities and their regio- and stereospecificity.<sup>245-247</sup> Moreover, Karstedt's<sup>248</sup> catalyst (an alkene-stabilized Pt(0) complex) and Speier's<sup>249</sup> catalyst (H<sub>2</sub>PtCl<sub>6</sub>) are air-stable catalysts that have been commonly used in industry due to their activity, selectivity and broad scope. In contrast to the widely studied homogeneous catalysts for hydrosilylation reactions, the development of catalysts based on metal NPs has not been deeply explored because of their low performance compared to homogeneous complexes, which in most cases is related to agglomeration of the NPs to give inactive bulk metal.<sup>250</sup> Actually, Speier's catalyst replaced Pt/C because it was orders of magnitude faster.

Although non-noble metals such as Fe,<sup>251</sup> Co<sup>252</sup> and Ni<sup>253</sup> have attracted increasing attention during the last years as less costly alternatives, Pt still remains the most often used catalyst.<sup>250</sup> Given

the high market price of platinum, it is important to improve the performance and reduce the metal losses during the hydrosilylation catalytic process. Thus, a better understanding of the reaction mechanism has been a main goal for researchers in the field. The nature of the active species in Pt catalyzed hydrosilylation of multiple bonds has been a controversial subject during the past forty years. For instance, after extensive studies, Lewis and co-workers considered that homogeneous Pt(0) complexes were the active species in the hydrosilylation of C-C multiple bonds,<sup>254</sup> and it was not until the last years when the debates have been reopened (see discussion below), suggesting that both Pt NPs formed in the activation of the Karstedt's catalyst and homogeneous species can be responsible for the catalytic activity.<sup>255</sup> The absence of heterogeneous catalysts for industrial applications, together with discussion about hydrosilylation mechanism, has motivated development of new catalytic systems based on metal NPs. This can also be useful to researchers in the nano-catalysis field to achieve a better understanding of Si-H activation. Furthermore, NPs present some advantages over metallic complexes as they can be more easily immobilised on a support allowing separation from the reaction medium and enhancing recyclability in the case of liquid products. Recently, new efforts have been done to synthesize metal NPs that are promising catalytic systems for hydrosilylation. In this review, we describe some examples of hydrosilylation catalyzed by NPs either dispersed in solution or after immobilisation on a support.

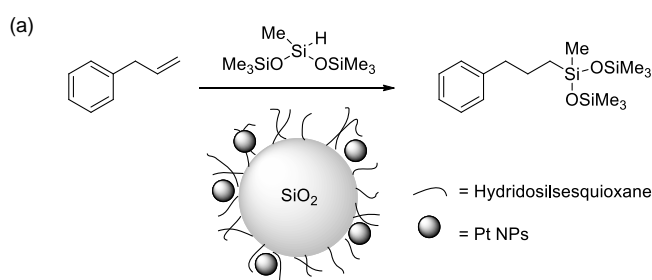
#### **4.1.1. Platinum NPs as catalysts for hydrosilylation of C-C multiple bonds.**

Several heterogeneous catalysts have been employed for the hydrosilylation of alkenes and/or alkynes: platinum on carbon (Pt/C),<sup>256-258</sup> platinum on silica (Pt/SiO<sub>2</sub>),<sup>259</sup> platinum on titania (Pt/TiO<sub>2</sub>),<sup>260</sup> platinum oxide supported on magnetite<sup>261</sup> or non-supported platinum oxide,<sup>262-264</sup> among others. Pt/C as a catalyst for the hydrosilylation of alkenes and alkynes was first reported by Wagner in 1953,<sup>256-257</sup> but further observations by Speier et al. demonstrated that the stereochemistry of the addition of silanes to different terminal alkynes using Pt/C or chloroplatinic acid was very similar,<sup>249</sup> suggesting that the operating mechanism in both cases might involve Pt NPs. It was not until 2002, when Boudjouk and co-workers evidenced the formation of Pt NPs of 2-5 nm by High-Resolution Electron Microscopy (HREM) when Pt/C was used in the hydrosilylation of alkynes.<sup>258</sup> Several observations suggested that formation of Pt NPs was a key step in hydrosilylation catalyzed by Pt(0) in homogeneous phase.<sup>237</sup> For example, the extensive work of Lewis and co-workers on this subject showed that Pt NPs were formed during the Karstedt's catalyzed hydrosilylation of alkenes, which likely played a role in the catalytic reaction.<sup>265-267</sup> However, after a more detailed mechanistic study, Lewis proposed that monoatomic Pt(0) species were the real catalytic active species, and that the formation of Pt NPs was a consequence of the aggregation of these unprotected species.<sup>254</sup> Then, in 2006, Finney and Finke reported on the nature of active species in hydrogenation reactions catalyzed

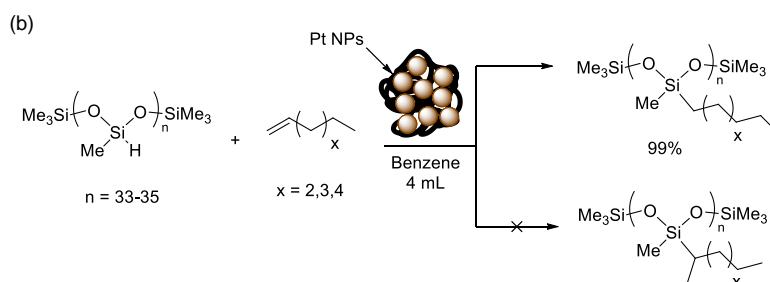
by Pt(II) complexes.<sup>268</sup> In the same work, the authors discussed the controversial nature of the active species in hydrosilylation catalyzed by Pt(COD)Cl<sub>2</sub>. The authors concluded that the nature of the active species in hydrosilylation was not clear and more mechanistic studies were needed.

The first examples of hydrosilylation catalyzed by *pre-formed* nanoparticles involved the stabilization of Pt NPs by siloxane derivatives. In 1997, Brook and co-workers designed a heterogeneous catalyst after reaction of Karstedt's complex with silica particles modified with a hydrogen silsesquioxane layer at their surface.<sup>269</sup> Thus, Pt NPs of around 2.0 nm were formed and were linked to the silica surface by siloxane groups which prevented the NPs from coalescing. The catalyst could be used in the hydrosilylation of alkenes and alkynes without agglomeration of the NPs even after removing the solvent (see Scheme 18a). In addition, the supported catalyst was recycled several times without losing its activity. In 2005, Chauhan et al.<sup>270</sup> reported the hydrosilylation of a poly-(methylhydro)siloxane (PMHS) polymer containing Si-H moieties with alkenes with different steric and electronic features, catalyzed by Pt NPs of ca. 2.0 nm supported on PMHS (see Scheme 18b). The polymer stabilized the NPs preventing their coalescence and allowing the recycling of the catalyst up to 6 times without loss of activity. Characterization of the hydrosilylated polymer by <sup>13</sup>C and <sup>29</sup>Si Nuclear Magnetic Resonance (NMR) confirmed the good regioselectivity of the Pt NPs towards the anti-Markovnikov reaction product, i.e. 1-alkylsilanes. In addition, regioselectivity of the Pt NPs remained unaffected when different functional groups were present in the alkenes such as carbonyl, ether, epoxide or hydroxyl. This is of importance since hydrosilylation of functionalized olefins can be frequently accompanied by side reactions such as ring opening polymerization or hydrosilylation of carbonyl groups. Monitoring the reaction by UV-vis analysis led the authors to propose that Pt(0) molecular species were not taking part in the reaction mechanism, and that Pt NPs were the real catalyst of the process. Recently, Chauhan et al. have reported a similar catalytic system involving Pt NPs supported on a cross-linked polysiloxane, and they expanded the scope of the catalyst towards hydrosilylation of alkynes containing different functional groups.<sup>271</sup> Although the regio- and stereoselectivity was similar to those given by molecular complexes, the system represents an improvement compared to homogeneous catalysts in terms of catalyst recovery and recyclability.

**Scheme 18.** (a) First example of hydrosilylation catalyzed by Pt NPs stabilized by a hydridosilsesquioxane layer at the surface of SiO<sub>2</sub> (b) Pt NPs catalyzed regioselective hydrosilylation of PMHS.



Brook et al. *Inorg. Chim. Acta* **1997**



Chauhan, et al. *J. Am. Chem. Soc.* **2005**

In 2013, Bai et al. prepared Pt NPs of 4-5 nm stabilized by polyethylene glycol functionalized with 4-aminobenzoic acid (PEG-AMV) with different Pt wt% content.<sup>272</sup> The Pt NPs were prepared by *in situ* reduction of  $\text{H}_2\text{PtCl}_6$  in the presence of the polymer in EtOH. The catalysts were used in the hydrosilylation of terminal alkenes in the absence of solvent. The catalytic system could be recycled up to ten times still exhibiting good activities in the hydrosilylation of 1-octene with  $(\text{EtO})_3\text{SiH}$ . However, the catalyst was less efficient in the activation of more challenging silanes such as  $\text{Et}_3\text{SiH}$ , although it should be noted that very low catalyst loadings of 0.025 mol% of Pt were used. In the same year, Ciriminna et al. reported a new sol-gel entrapped hybrid catalyst containing Pt(0) NPs of 4-6 nm, which was called “SilicaCat Pt(0),” that was employed as a heterogeneous catalyst for the hydrosilylation of alkenes. The catalyst was prepared by reduction of  $\text{K}_2\text{PtCl}_4$  with sodium borohydride in the presence of an organically modified silicate (ORMOSILs) porous matrix (see Figure 15).<sup>273</sup> After optimization of the reaction conditions, the catalytic system was tested in the hydrosilylation of different terminal alkenes at room temperature or at 65 °C. The Pt loadings were of 0.5-1.0 mol%, and the selectivity varied from moderate to good depending on the substrate. The catalyst presented very low values of Pt leaching at the end of the reaction, which is an important factor for the potential industrial application of hydrosilylation catalysts (see Table 8). Higher leaching values were observed for acrolein diethyl acetal (entry 2 in Table 8) and were attributed to the presence of the chelating group displaying a higher coordinative capacity. The catalyst selectivity was retained after 3 reaction cycles, but a decrease of the conversion was observed after the second run. This effect was attributed to the pore blockage by the organic substrate, as sonication in  $\text{CH}_2\text{Cl}_2$  restored the initial activity.

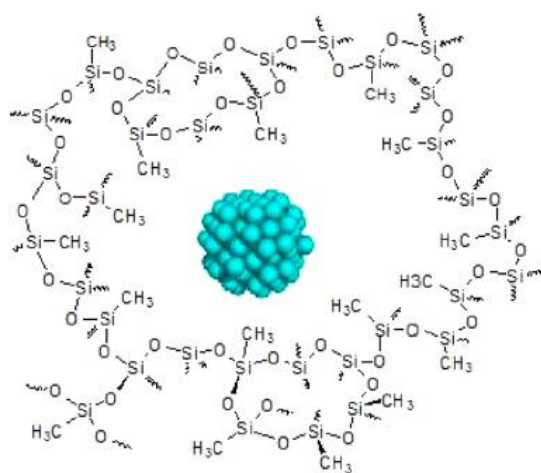


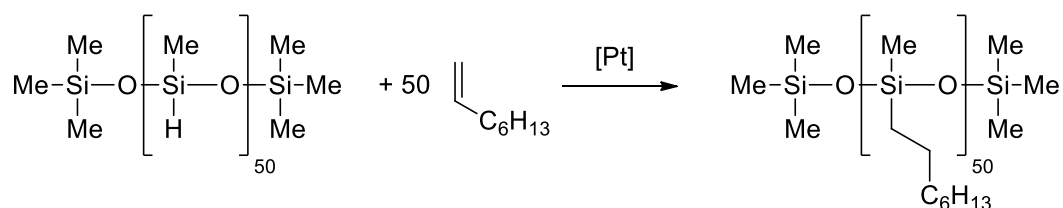
**Figure 15.** Schematic representation of the Pt NPs encapsulated in the ORMOSIL of the SiliaCat Pt(0) catalyst. Reprinted with permission from ref 273. Copyright 2013 American Chemical Society.

Entry	Substrate	Catalyst (mol%)	T (°C)	Time (h)	Conv. (%)	Select. Linear (%)	Pt leaching (mg/kg)
1	<chem>C5H11CH=CH2</chem>	1	22	5	88	98	-
			60	5	99	99	-
2	<chem>CH2=CHCOEt</chem>	1	65	1	100	100	25
		0.5	65	3	100	100	9
3	<chem>CH2=CHCH2CH2COCH3</chem>	0.5	0.5	3	100	100	-

**Table 8.** Catalytic Hydrosilylation of functionalized alkenes with triethoxysilane over SiliaCat Pt(0) under different reaction conditions. In all cases, a 30% molar excess of silane was used and toluene (15 mL in entry 1 and 0.5 M in substrate in entries 2-3) was added as solvent. Pt leaching was determined by ICP-OES. The result for leaching is given in mg of Pt per kg of pure product.

Although all the examples of alkene hydrosilylation discussed hereabove suggested an active role of the Pt NPs in the Si-H activation, the systems presented TON values near 1000, contrasting with the values obtained at industrial scale with homogeneous catalysts that are of about  $10^5$ . This is probably related to the presence of the stabilizing support, which lowers the catalytic activity of the NPs hindering the surface accessibility. In a communication from Thieuleux, Meille and co-

workers,<sup>255</sup> monodisperse Pt NPs of 1.6-1.7 nm dispersed in solution were used in the hydrosilylation of alkenes. The NPs were synthesized by decomposition of Pt(dba)<sub>2</sub> or Karstedt's complex in presence of n-octylsilane or polymethylhydrosiloxane (PMHS) containing about 50 Si-H moieties (see Table 9) and using 4 bars of hydrogen as a reducing agent. In this work, the Pt NPs were as efficient as Karstedt's complex in the hydrosilylation of 1-octene with PMHS. Thus, very high TON and regioselectivity to the terminal product similar to Karstedt's catalyst were obtained as well as comparable proportions of 1-octene isomerization to 2-octene, a common side-reaction (see Table 9). This result clearly shows that NPs stabilized in solution may achieve activities comparable to Karstedt's complex and are not a simple consequence of the deactivation of the catalyst. Furthermore, if NPs are not stabilized by ligands, they tend to agglomerate with an observed concomitant drop in their catalytic activity. Kinetic studies performed by the authors also demonstrated that, although at short reaction times NPs are less efficient than Karstedt's complex, the activity reaches very similar values when the reaction progresses. This work is not in contradiction with the observations made by Lewis et al., who performed *in situ* experiments at very low TONs, when the active species deriving from the Karstedt's complex are homogeneous Pt(0) species, i.e. when NP formation has not yet started.



Catalyst	Pt precursor	Stabilizer	Mean diameter -(nm)	SiH conv. (TON) 7 ppm Pt	1-octene isomerization
Karstedt	-	-	-	96% (1.0×10 <sup>5</sup> )	12%
Pt(dba) <sub>2</sub>	-	-	-	98% (1.1×10 <sup>5</sup> )	12%
PtNPs1	Pt(dba) <sub>2</sub>	n-octylsilane	1.6	98% (1.1×10 <sup>5</sup> )	11%
PtNPs2	Karstedt	PMHS	1.7	97% (1.0×10 <sup>5</sup> )	11%
PtNPs3	Karstedt	n-octylsilane	1.7	99% (1.1×10 <sup>5</sup> )	11%

**Table 9.** Compared activities between the PtNPs, Karstedt's complex and Pt(dba)<sub>2</sub>. The SiH conversions were measured 30 minutes after the end of the PMHS addition.

The renaissance of the use of Pt NPs for the hydrosilylation of multiple C-C bonds is beginning to promote the development of new heterogeneous catalysts based on metal NPs. Bandare and Buchmeiser prepared Pt NPs of ca. 7 nm supported on a polymeric monolith and used it for the



hydrosilylation of olefins in continuous flow with low Pt leaching values.<sup>274</sup> Solomonz et al.<sup>275</sup> immobilized Pt NPs inside and outside of carbon nanoreactors, which were active in the hydrosilylation of acetylene and promoted the formation of aromatic products over aliphatic ones as a result of  $\pi$ - $\pi$  interactions. More recently, Thieuleux, Meille and co-workers have prepared a heterogeneous catalyst composed of Pt NPs trapped in the walls of porous mesostructured silica.<sup>276</sup> This catalyst reaches TON values comparable to those obtained by the homogeneous complexes (100,000) and no leaching was observed thanks to the physical trapping, which is of potential interest for industrial applications.

In summary, Pt NPs as active species for hydrosilylation reactions has been a topic of controversy during the past forty years, but several examples suggest that they play a role in the reaction in contrast to the opinion prevailing in the 90's. Moreover, the use of easily recyclable Pt NPs in hydrosilylation of C-C multiple bonds is a promising topic in heterogeneous catalysis. These Pt NPs are good candidates as substitutes for the homogeneous processes that take place at industrial scale with molecular complexes and which imply loss of the active platinum. This can lead to lower the costs of the preparation of the organosilicon products and enhance their purity due to the absence of Pt in the products. However, it is still not clear if the Si-H activation takes place at the surface of the NP or if Pt leached atoms are the real active species, so more focused mechanistic studies are still needed.

#### **4.1.2. Other metallic nanoparticles as catalysts for hydrosilylation of functional groups.**

##### **4.1.2.1 Au.**

Although homogeneous Au(I) complexes are similar in terms of electronic properties to Pt(0) complexes, they are not active in hydrosilylation of C-C multiple bonds and their use was restricted to the hydrosilylation of aldehydes.<sup>277</sup> Nevertheless, Au NPs have been successfully employed as active catalysts in the hydrosilylation of alkynes and other reactions that implied Si-H activation.<sup>170-171</sup> Supported Au NPs that were prepared from solvated Au atoms for the hydrosilylation of alkynes were first reported by Caporusso et al., but restricted to hydrosilylation of terminal alkynes.<sup>278-279</sup> In 2007, Corma and co-workers<sup>280</sup> showed that Au NPs of ca. 4 nm supported on CeO<sub>2</sub> could catalyze the hydrosilylation of aldehydes, ketones, imines, alkenes and alkynes. In addition, the Au/CeO<sub>2</sub> catalytic system was free of gold leaching allowing its reusability. However, by comparison with the activity of homogeneous Au(I) and Au(III) complexes also prepared in this work, the authors proposed that the active species in these reactions are likely Au(III) atoms stabilized on the surface of the support, and in this case the NPs would act as a reservoir for the active species.

To the best of our knowledge, there are only 2 examples in the literature in which Si-H activation is possibly taking place at the surface of metallic Au. In 2008, Shore and Organ<sup>281</sup> prepared Au films on the surface of borosilicate capillaries by a two-step decomposition reaction of AuCl<sub>3</sub>. These Au films were active catalysts in the hydrosilylation of terminal alkynes with triaryl- and trialkylsilanes in microwave-assisted continuous flow, showing good robustness. This fact can be used as an indication of the absence of metal leaching to give active species stabilized in solution. In addition, the authors also performed ICP-MS analysis and observed that the reaction products were free of Au. In 2013, Ishikawa et al. reported the preparation of a nanoporous gold catalyst, by selective removal of Al or Ag starting from the alloys Au<sub>20</sub>Al<sub>80</sub> or Au<sub>30</sub>Ag<sub>70</sub> respectively.<sup>282</sup> The non-supported catalyst was used in the hydrosilylation of terminal alkynes with trialkylsilanes, and it was easily recoverable by decantation at the end of the reaction. The authors performed ICP measurements and a hot filtration test to prove the absence of Au leaching from the NPs, supporting the hypothesis that Si-H activation is taking place at the surface of the solid catalyst.

Summarizing, although Au complexes are restricted to aldehyde hydrosilylation, Au NPs can be used in the hydrosilylation reactions of diverse substrates. However, Si-H activation by metallic Au has not been widely explored and it is still limited to hydrosilylation of terminal alkynes, and the homolytic or heterolytic nature of this activation is not known. It has been observed that secondary phosphine oxides (SPO) ligands may assist the heterolytic activation of H<sub>2</sub> by AuNPs, and the formation of a Au(I)-enriched surface enhances the selectivity for aldehyde hydrogenation.<sup>87</sup> Thus, the fact that no examples of alkene hydrosilylation with Au NPs have been reported so far and that selectivity for aldehydes is preferred in some cases,<sup>280</sup> suggests that the Si-H activation may well be of heterolytic nature. Several examples of supported Au NPs for the hydrosilylation of alkynes and allenes and disilylation of alkynes through Si-H and Si-Si bonds activation have been reported to date by the group of Stratakis,<sup>283-285</sup> likely involving a Au(I)-Au(III) catalytic cycle by leached species, so they fall out of the scope of this review.

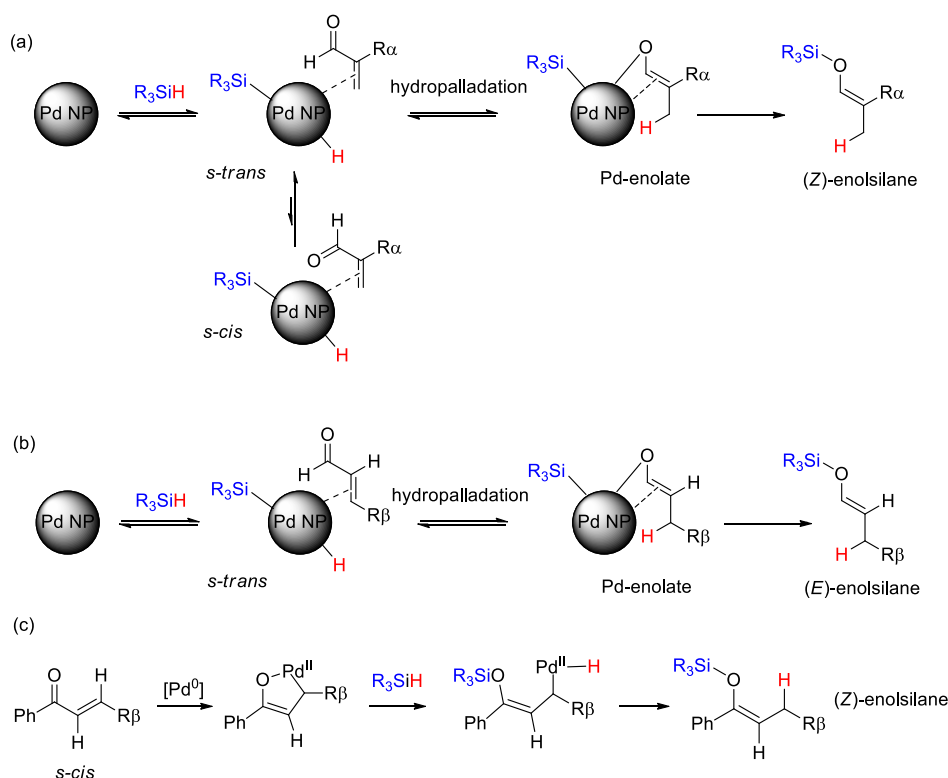
#### **4.1.2.2. Pd.**

Pd NPs in Si-H activation were first used in the hydrosilylation of alkenes by Tamura and Fujihara. In this work, Pd NPs of 2.0 nm size stabilized by chiral binaphthyl (BINAP) ligands were synthesized.<sup>286</sup> They were used in the asymmetric catalytic hydrosilylation of styrene under mild conditions, leading to high enantioselectivity values. Interestingly, whereas the Pd-BINAP NPs can catalyze this reaction, the analogous homogeneous complexes were totally inactive with diphosphine ligands.<sup>287</sup> This result may be linked to the difference in the coordination modes of the ligand between the molecular complex and the nanoparticles.

Pd complexes have been known as active catalysts in 1,4-hydrosilylation of enals.<sup>288-289</sup> Thus, Pd NPs were used in 1,4-hydrosilylation of enals and enones by Benohoud et al. in 2011.<sup>290</sup> The NPs

were generated *in situ* by reduction of PdCl<sub>2</sub> by the silane in the presence of PCy<sub>3</sub>, and they were confirmed as the active species because their removal from the reaction medium by centrifugation stopped the reaction although some Pd complex still remained in the solution. In addition, a similar stereoselectivity was observed when the reaction was carried out with pre-formed Pd NPs stabilized by PVP. The process was stereoselective for the formation of the (*Z*)- or (*E*)-enolsilane when starting from the  $\alpha$ - or  $\beta$ -substituted enals respectively (see Scheme 19a-b). A large variety of substrates were tested in the reaction, and the stereoselectivity was retained even though the sizes and morphologies of the *in situ* generated Pd NPs were not reproducible. To explain the stereoselectivity, the authors proposed that the role of the Pd NPs is to facilitate the hydropalladation in the *s-trans* conformation of the enal, a process that would be difficult with a mononuclear Pd complex due to geometric constraints, but that can be easily achieved with Pd NPs because different Pd atoms can be involved in hydrido attack and formation of the Pd-O bond. Competition experiments with Et<sub>3</sub>SiD and Ph<sub>3</sub>SiH were carried out, showing that the product presented similar deuteration degrees. The authors suggested that reversible Si-H activation by the Pd NP occurs prior to the hydrosilylation reaction. However, the fact that no hydrogenation of the alkene function was observed is somehow in contradiction with the formation of surface hydrides in the Pd NPs. It should also be noted that, in contrast to Pd NPs, selective formation of the *Z*-enolsilane was observed in the hydrosilylation of  $\beta$ -substituted enones catalyzed by molecular complexes, because in this case the mechanism likely involves the formation of a metallacyclopalladate (see Scheme 19c).<sup>289</sup>

**Scheme 19.** (a) Rationalisation of the observed stereoselectivity for  $\alpha$ -substituted enals when starting from hydrosilylated Pd NPs, (b) rationalisation of the observed stereoselectivity for  $\beta$ -substituted enals under the same conditions and (c) proposed mechanism for the homogeneously catalyzed 1,4-hydrosilylation of  $\beta$ -substituted enones.

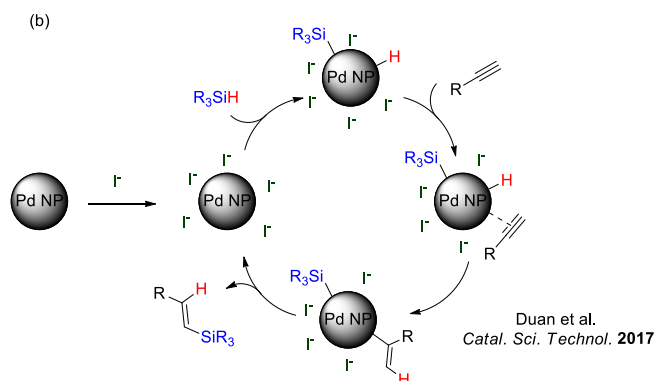
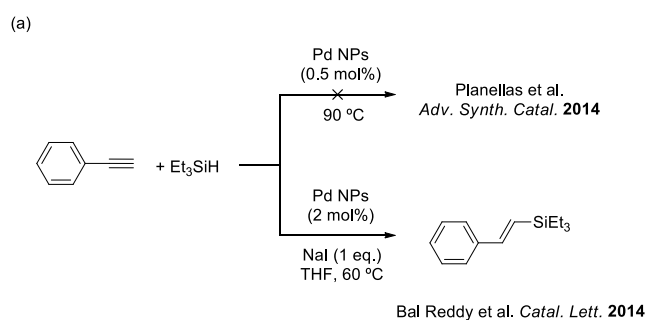


Yamada and co-workers prepared in 2014 a hybrid material made of Pd NPs and a Si-nanowire-array by reduction of  $K_2PdCl_4$  in the presence of the support.<sup>291</sup> The authors observed that the catalyst was selective toward the *cis* isomer in the 1,4-hydrosilylation of  $\alpha$ -substituted enals. This nanohybrid material was also used to carry out different reactions such as C-C coupling or chemoselective hydrogenation of C-C multiple bonds, suggesting that the operating mechanism involved Pd leached species as proposed by Reetz and de Vries.<sup>138</sup>

Pd NPs have also been used in the hydrosilylation of alkynes. In 2014, Planellas et al. reported the synthesis of Pd NPs of around 3.5 nm stabilized by a tris-imidazolium salt that were active in the hydrosilylation of internal alkynes, substrates that are less reactive than terminal acetylenes.<sup>292</sup> Moreover, phenylacetylene was unreactive towards the addition of  $Et_3SiH$  under the same reaction conditions, and it even acted as a poison for other substrates. The authors proposed that this behaviour may be attributed to the formation of  $\sigma$ -alkynyl unreactive species. The controlled addition of water to the reaction promoted the oxidation of the silane to the silanol, which probably is also catalyzed by the NPs (see section 4.2). In the same year, Bal Reddy et al. reported the use of Pd NPs of ca. 2.5 nm supported on a polystyrene resin matrix in the hydrosilylation of alkynes under air under mild reaction conditions.<sup>293</sup> The particles were recyclable up to ten times with very low metal leaching, and the slight loss of activity was attributed to the coalescence of the NPs. Interestingly, in this case the NPs were active in the hydrosilylation of phenylacetylene with  $Et_3SiH$ . After comparing the reaction conditions, we have found two remarkable differences between these two works: in the first

one, the authors performed the reaction in pure silane without addition of any extra additives, and in the second one, the reaction was carried out in THF in the presence of 1 equiv. of NaI, necessary to activate the reaction (see Scheme 20a). Although the role of NaI in the mechanism was not discussed, the differences in the reactivity of Pd NPs for the same reaction is an indication that controlling the surface properties could enable to tune the catalytic activity. Recently, Duan et al. have shed some light on this subject.<sup>294</sup> The authors prepared Pd NPs of ca. 12 nm supported on an N-O-dual doped porous carbon (Pd@N,O-Carbon) that was obtained from renewable biomass. The authors observed that addition of I<sup>-</sup> anions to the reaction medium was the key step to activate the hydrosilylation of terminal alkynes. Thus, the Pd NPs were functionalized with I<sup>-</sup> by treatment of the catalyst with tetrabutylammonium iodide (TBAI). Interestingly, these NPs exhibited a similar activity as pure Pd NPs after addition of an excess of TBAI. After these observations, the authors proposed that the role of iodide in the reaction is to increase the negative charge of the Pd atoms, as is well established for homogeneous Pd catalysts,<sup>295</sup> facilitating the oxidative addition of the hydrosilane (see Scheme 20b). Another possibility is that the role of the iodide was to prevent the C-H activation of the alkyne to give unreactive  $\sigma$ -alkynyl species as proposed by Planellas et al. Again, addition of water promoted the oxidation of silane to silanol and, as a result, the NPs were active in the semi-reduction of the alkyne due to the concomitant formation of surface hydrides (see section 4.2).

**Scheme 20.** (a) Iodide effect in the hydrosilylation of terminal alkynes catalyzed by Pd NPs and (b) mechanism proposed by Duan et al. in which the role of the I<sup>-</sup> is to increase the electron density of the Pd NP and facilitate the reaction.



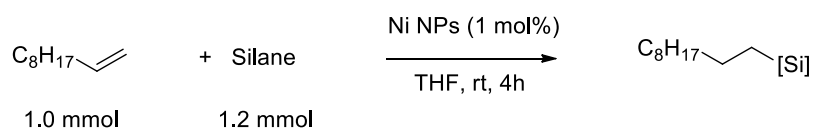
#### 4.1.2.3. Rh.

Molecular complexes of rhodium have been mainly used in hydrosilylation of alkynes<sup>296</sup> and ketones.<sup>297</sup> There are only 2 examples in the literature of Rh NPs in hydrosilylation of alkynes. In 2012, Solomonsz et al. prepared Rh and RhPt NPs embedded in a nano-reactor consisting of hollow graphitized carbon nanofibers (GNF), which were employed in the hydrosilylation of terminal alkynes.<sup>298</sup> The authors explored the role of the support in the selectivity of the reaction. Depending on the presence of aromatic substituents on the alkyne or the silane reagents,  $\pi$ - $\pi$  interactions with the support modify the preferred reaction route affecting the selectivity of the reaction. When only the alkyne was aromatic, an increase in the dehydrogenative silylation products was observed, which was proposed to be related to the high local concentration of the aromatic substrate (phenylacetylene) within the GNF cavity. When both alkyne and silane carried aromatic functions, the strong stacking interactions were sufficient to overcome local concentration effects enhancing the formation of the thermodynamically less stable terminal (Z) regioisomer. In 2015, Pleixats and co-workers synthesized Rh NPs stabilized by a nitrogen-rich PEG-matrix by reduction of  $\text{RhCl}_3$  with  $\text{NaBH}_4$  in water.<sup>299</sup> After varying the ligand to metal precursor ratio from 1:1 to 0.02:1, Rh NPs ranging from 1.6 to 32.3 nm were obtained. The NPs were tested in the hydrosilylation of internal alkynes and only the larger nano-objects of > 20 nm proved to be active catalysts in the reaction; due to the low surface coverage by stabilizing ligands the substrates can readily approach the catalyst surface. The catalyst precipitated after addition of diethyl ether allowing its recycling at the end of the reaction. This NPs system was water-resistant, and hydrosilylation could be carried out even in the presence of traces of

water without forming silanols, in contrast to what occurred with the Pd NPs prepared by the same group.<sup>292</sup> The Rh NPs were active in hydrogenation of alkynes with H<sub>2</sub>, showing that indeed no hydrogen was formed from silanes and water on Rh NPs.

#### **4.1.2.4. Ni.**

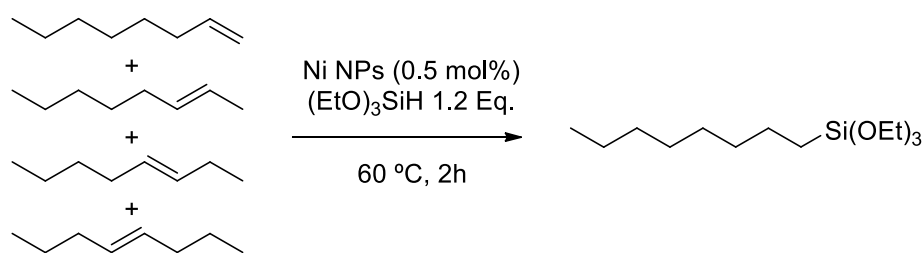
Ni is a less-costly alternative metal for hydrosilylation reactions. Although hydrosilylation of alkenes catalyzed by Ni complexes is known,<sup>253,300-301</sup> there has been only one report in which Ni catalyzed the addition of less-reactive tri-substituted silanes,<sup>302</sup> which are more interesting from the application point of view. Here we present the use of Ni NPs in hydrosilylation. Recently, Buslov et al. investigated the addition of trimethoxysilane to 1-decene catalyzed by Ni(O<sup>t</sup>Bu)<sub>2</sub>·KCl and observed the formation of a dark-brown solution that contained Ni NPs with an average size of 3.5 nm, which was proposed to be the actual catalytic active species.<sup>303</sup> These NPs were active in the hydrosilylation of terminal alkenes with (MeO)<sub>3</sub>SiH under mild conditions. The scope of silanes activated by the Ni NPs was analysed in the hydrosilylation of 1-decene (see Table 10), and the NPs were shown to be more active than pincer-type Ni<sup>II</sup> complexes prepared by the same group in the activation of triphenylsilane<sup>253</sup> (entry 8, Table 10). However, the Ni NPs were not able to activate less reactive silanes such as Et<sub>3</sub>SiH. Additionally, the Ni NPs were active catalysts in the isomerization-hydrosilylation tandem process, allowing the synthesis of single terminal alkyl silanes from mixtures of alkene isomers (see Scheme 21). This is an interesting reaction as it converts internal alkenes to terminal silanes that can be converted to terminal alcohols. It is an alternative, if costly, to the present industrial tandem route involving hydroformylation.



Entry	Silane	Yield
1	(MeO) <sub>3</sub> SiH	88
2	(EtO) <sub>3</sub> SiH	91
3	Me <sub>2</sub> (MeO)SiH	84
4	Me(EtO) <sub>2</sub> SiH	81
5	PMDS <sup>a</sup>	35
6	MD'M <sup>b</sup>	14
7	Et <sub>3</sub> SiH	6
8	Ph <sub>3</sub> SiH	43
9	Ph <sub>2</sub> SiH <sub>2</sub>	82 <sup>c</sup>

**Table 10.** Ni NPs catalyzed hydrosilylation of 1-decene with various silanes. <sup>a</sup> 1,1,3,3,3-pentamethyldisiloxane. <sup>b</sup> 1,1,1,3,5,5,5-heptamethyltrisiloxane. <sup>c</sup> 12% of didecyldiphenylsilane was formed.

**Scheme 21.** Synthesis of a terminal alkyl silane from a mixture of alkene isomers catalyzed by Ni NPs.



More recently, Galeandro-Diamant et al. have shown that pre-formed Ni silicide (Ni<sub>3</sub>Si<sub>2</sub>) NPs in solution or Ni(0) NPs supported on SiO<sub>2</sub> can be used as catalysts in the hydrosilylation of alkenes.<sup>304</sup> The selected model reaction was the hydrosilylation of triethoxyvinylsilane with triethoxysilane in a toluene solution at 120 °C using 0.2 mol% of Ni loading. The authors observed vinylsilane conversions of 60% after 600 hours when using Ni(0)/SiO<sub>2</sub> as catalyst, and of ca. 90% when using the Ni<sub>3</sub>Si<sub>2</sub> colloidal solution. In addition, they obtained several by-products resulting from hydrogenation, dehydrogenative silylation, dimerization, etc. Although conversion and selectivity were rather low, also this work demonstrates that Ni NPs can actually be used as catalysts for hydrosilylation reactions.



Another example of Ni NPs catalysing the hydrosilylation reaction was reported by García and co-workers,<sup>305</sup> who applied their well-established methodology to support metal NPs on graphene supports (Ni/G). Ni NPs of around 4.0 nm were obtained by reduction of NiCl<sub>2</sub> in ethylene glycol in the presence of the support. The Ni/G system was an active catalyst in the hydrosilylation of aliphatic and aromatic aldehydes with TON values of about 10<sup>5</sup>, whilst Cu/G NPs prepared by a similar methodology<sup>306</sup> were much less active. The Ni/G system became inactive during the reaction, but neither metallic leaching nor growth in NPs size was observed. The deactivation of the catalyst was therefore attributed to the loss of the 2D morphology of the graphene that was observed in the TEM images.

In conclusion, we have seen metal NPs not based on Pt can also catalyze hydrosilylation reactions. Ni NPs are active catalysts in this process, being a cheap alternative that will probably be further developed in the next years. In addition, with these examples in mind it is reasonable to think that hydrosilylation catalyzed by metallic complexes based on Pd, Rh or even Pt, which are more electronegative and thus more prone to reduction under the reaction conditions, may involve, at least in some cases, the formation of NPs that may be the actual catalytic active species. All the examples we have discussed herein are in agreement with the hypothesis that hydrosilylation reactions can indeed be catalyzed by metallic nanoparticles. However, there are several uncertainties about the reaction mechanism and the nature of the active species. It should be noted that in many cases the addition of salts is a pre-requisite to trigger the reaction. Thus, it is logical to think that leached species would be at least one of the active species in the catalytic cycles.

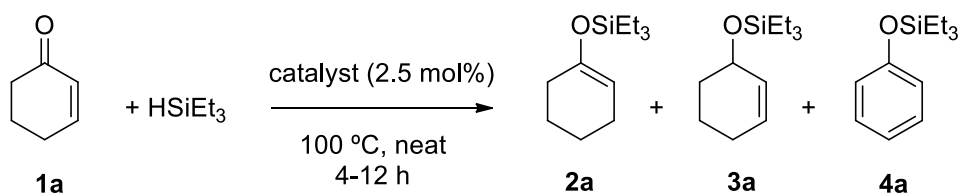
#### **4.1.3. Bimetallic NPs as new catalytic systems for hydrosilylation reactions.**

During the last years, a few examples of hydrosilylation catalyzed by bimetallic systems have been reported. Synergistic effect resulting from the combination of metals is expected as an interesting advantage of the bimetallic systems over traditional monometallic catalysts. The presence of two metallic centres with different electron densities seems to facilitate Si-H activation. This would be in agreement with a heterolytic splitting of the Si-H bond, similar to the mechanism described by Crabtree (see discussion below).<sup>307</sup>

For example, we have already shown that Solomon et al. prepared RhPt NPs embedded in a nano-reactor, which were employed in the hydrosilylation of terminal alkynes.<sup>298</sup> RhPd NPs embedded in an ionic gel were prepared by Thiot et al. in 2007. They were used in a one-pot hydrosilylation/Hiyama coupling reaction of phenylacetylene in the presence of HSiMe(OEt)<sub>2</sub> and PhI.<sup>308</sup> In the reported bimetallic system, it was proposed that Rh catalyzed the hydrosilylation and that Pd catalyzed the C-C coupling. Both metals acted without interference and moreover there was no formation of the undesired Sonogashira side product normally observed in the reaction catalyzed

by the combination of the organometallic precursors. The stereocontrol of the reaction for the formation of the trans-alkene with (>99%) was attributed to a beneficial Pd-catalyzed isomerization from the mixture of stereoisomeric (E) and (Z)-vinylsilane intermediates into the more stable (E)-vinylsilane.

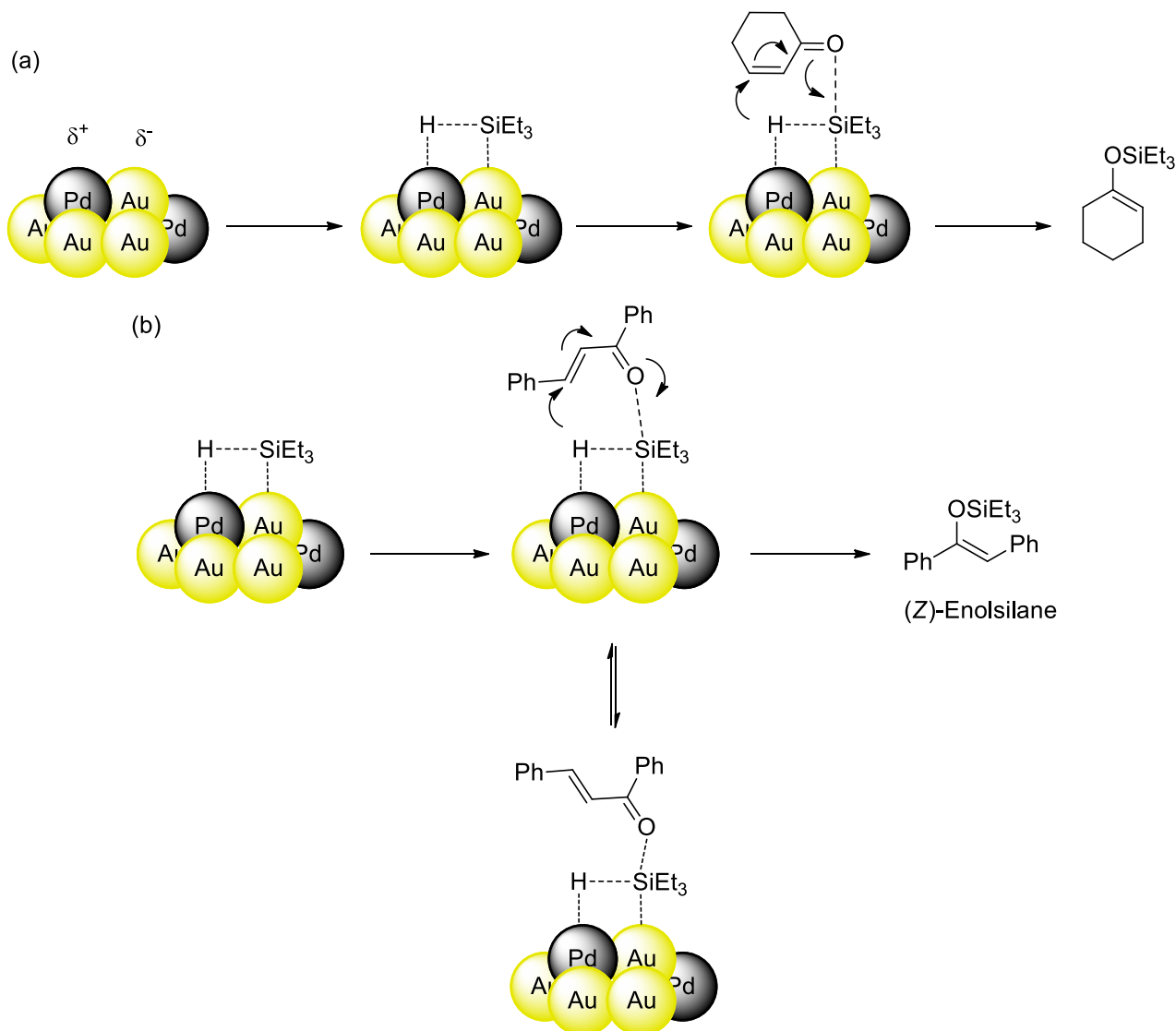
An interesting catalytic system that has been used in hydrosilylation reactions is the PdAu alloy, a good example of the synergistic effect between two different metals at the surface of a nano-catalyst. In 2014, Chen et al. prepared PdAu nanoporous catalysts (solid materials containing pores within nanometric scale) by selective removal of Al from the Au<sub>20</sub>Pd<sub>10</sub>Al<sub>70</sub> ternary alloy.<sup>309</sup> After a screening of catalysts displaying different compositions, the AuPd alloy showed a remarkable synergistic effect for the 1,4-hydrosilylation of conjugated cyclic enones with triethylsilane (see Table 11). While Au nanopore catalysts gave mixtures with the product of the hydrosilylation of the ketone group (compound **3a**) and Pd nanopore catalysts were active in dehydrogenation of the alkene to give the aromatic compound (compound **4a**), AuPd nanopores were in general more selective to 1,4-hydrosilylation. AuPd NPs deposited on TiO<sub>2</sub> were less active in this reaction. Based on the observations made in this work and the good dispersion of Au and Pd atoms at the surface of the catalyst as determined by dispersive X-Ray spectroscopy (EDS) and X-Ray photoelectron spectroscopy (XPS), the authors proposed a synergistic mechanism in which Si-H activation would afford a Pd-H bond and a Au-Si bond (see Scheme 22a). The affinity of the Si for the carbonyl oxygen would direct selective addition of the hydride to the β-position.



Entry	Catalyst (precursor alloy)	2a (%)	3a (%)	4a (%)
1	AuPdNPore-1 (Au <sub>20</sub> Pd <sub>10</sub> Al <sub>70</sub> )	92	0	4
2	AuNPore-1 + PdNPore-1	70	20	6
3	Au <sub>20</sub> Pd <sub>10</sub> Al <sub>70</sub> alloy	0	0	0
4	None	0	0	0
5	AuPdNPore-2 (Au <sub>25</sub> Pd <sub>5</sub> Al <sub>70</sub> )	87	0	5
6	AuPdNPore-3 (Au <sub>10</sub> Pd <sub>20</sub> Al <sub>70</sub> )	46	0	13
7	AuPdNPs on TiO <sub>2</sub>	47	0	4

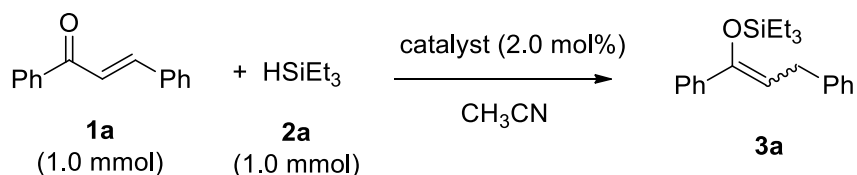
**Table 11.** Screening of various nanoporous metal catalysts in the 1,4-hydrosilylation of conjugated cyclic enones.

**Scheme 22.** (a) Proposed mechanism for the selective 1,4-hydrosilylation of conjugated cyclic enones by PdAu bimetallic alloys and (b) rationalization of the possible mechanism for the 1,4-hydrosilylation of conjugated enones by PdAu bimetallic alloys in order to explain the stereoselectivity of the process that differs from the one observed with Pd NPs.



More recently, Miura et al. have studied the activity of different PdAu alloy NPs of ca. 3 nm supported on a variety of supports in the 1,4-hydrosilylation of  $\alpha,\beta$ -unsaturated ketones and hydrosilylation of internal alkynes.<sup>310</sup> The AuPd NPs were obtained by reduction of PdCl<sub>2</sub> and HAuCl<sub>4</sub> in the desired ratio with NaBH<sub>4</sub> in the presence of PVP. Then, they were supported on Nb<sub>2</sub>O<sub>5</sub>, found to be the optimal support for the reaction. NPs with different Pd/Au ratios were prepared in order to learn how the composition affects the hydrosilylation reaction. Interestingly, while supported Au or Pd NPs were totally unreactive in the 1,4-hydrosilylation of enones, PdAu NPs show good performances under mild reaction conditions. Moreover, when varying the Pd/Au ratio by decreasing the amount of Pd atoms in the alloy, the activity of the catalyst increased (see Table 12). The authors

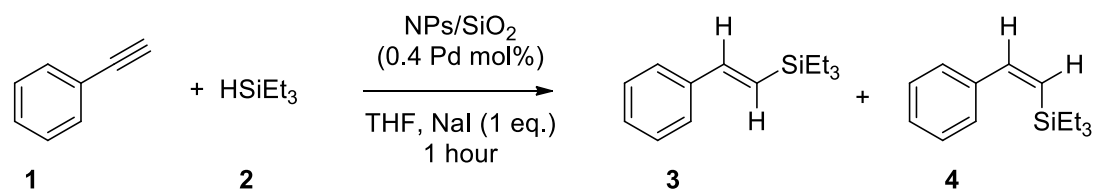
correlated the good activity of the catalyst with the presence of Pd single-sites at the surface of the catalyst. A rationale for this synergistic effect has been proposed by Chen et al. (see Scheme 22b). When a Pd atom is surrounded by Au atoms, the electron density in Pd is decreased, increasing its reactivity towards activation of the Si-H bond and formation of the Pd-H bond. A remarkable observation is that, with AuPd alloy, the *cis*-enolsilane was selectively obtained in the 1,4-hydrosilylation of different  $\beta$ -conjugated enones, in contrast to the results of Benohoud et al. with Pd NPs discussed earlier,<sup>290</sup> in which the *trans*-enolsilane was the main reaction product (Scheme 19b). This may be explained by the absence of Pd-Pd moieties at the surface of the NP in the PdAu alloy. In addition, the heterolytic cleavage of the Si-H bond by the Pd-Au bimetallic surface seems a more accurate mechanistic pathway than the one proposed by Benohoud et al., since it is in agreement with the observations made in homogeneous phase where the reaction starts by formation of a  $\eta^2$ -HSiR<sub>3</sub> complex, followed by an outer sphere nucleophilic attack and heterolytic splitting.<sup>307</sup>



Entry	Catalyst	Temp. (°C)	Time	Yield 3a (%) – Z/E ratio	
1	Pd/SiO <sub>2</sub>	75	20 min	0	-
2	Au/SiO <sub>2</sub>	75	20 min	5	99:1
3	Pd <sub>3</sub> Au <sub>1</sub> /SiO <sub>2</sub>	75	20 min	0	-
4	Pd <sub>1</sub> Au <sub>1</sub> /SiO <sub>2</sub>	75	20 min	3	89:11
6	Pd <sub>1</sub> Au <sub>3</sub> /SiO <sub>2</sub>	75	20 min	59	94:6
7	Pd <sub>1</sub> Au <sub>3</sub> /SiO <sub>2</sub>	rt	3 h	4	93:7
8	Pd <sub>1</sub> Au <sub>3</sub> /Al <sub>2</sub> O <sub>3</sub>	rt	3 h	1	-
9	Pd <sub>1</sub> Au <sub>3</sub> /CeO <sub>2</sub>	rt	3 h	6	96:6
10	Pd <sub>1</sub> Au <sub>3</sub> /ZrO <sub>2</sub>	rt	3 h	13	93:7
11	Pd <sub>1</sub> Au <sub>3</sub> /TiO <sub>2</sub>	rt	3 h	24	93:7
12	Pd <sub>1</sub> Au <sub>3</sub> /Nb <sub>2</sub> O <sub>5</sub>	rt	3 h	45	92:8
13	Pd <sub>1</sub> Au <sub>5</sub> /Nb <sub>2</sub> O <sub>5</sub>	rt	1 h	85	93:7
14	Au/Nb <sub>2</sub> O <sub>5</sub>	rt	3 h	1	-
15	Pd/Nb <sub>2</sub> O <sub>5</sub>	rt	3 h	0	-

**Table 12.** Optimization of the reaction conditions in the hydrosilylation of a  $\beta$ -unsaturated ketone catalyzed by supported PdAu NPs.

Another catalytic system that has been used in the hydrosilylation of alkynes is that of PdCu NPs supported on SiO<sub>2</sub>. In recent work from Cai and co-workers,<sup>311</sup> the authors explored the activity of catalytic systems based on PdNi, PdFe, PdCo and PdCu bimetallic NPs in the hydrosilylation of alkynes with Et<sub>3</sub>SiH (see Table 13). Similar to that observed with PdAu NPs, diluting the amount of Pd atoms in the alloy increased the catalytic activity of the NPs in the reaction. Pd<sub>1</sub>Cu<sub>2</sub>/SiO<sub>2</sub> was the most selective catalyst for the formation of the *trans*-alkene, allowing the reaction to be performed in air, mild conditions (room temperature) and with lower Pd charges (0.4 mol%) than pure Pd NPs (ca. 60 °C and ca. 2 mol% of Pd). However, the addition of NaI to activate the NPs was still necessary (see discussion above). The catalytic system was easily recoverable by simple filtration and was recycled up to 5 times maintaining its activity. The heterogeneous nature of the PdCu/SiO<sub>2</sub> catalyst was deduced from a hot filtration experiment that stopped the reaction, which was restarted after addition of the filtered catalyst. It is interesting to note that alloying Pd NPs with an earth-abundant metal such as Cu, not only increases the performance of the catalyst but also lowers the cost of the catalyst, which can also be of interest for applications.



Entry	Catalyst	T (°C)	Ratio (1 vs 2)	Yield (%)	3/4
1 <sup>a</sup>	Pd	40	1:5	24	77/23
2 <sup>b</sup>	Ni	40	1:5	<5	90/10
4	Pd <sub>1</sub> Ni <sub>2</sub>	20	1:2	98	87/13
7	Pd <sub>1</sub> Fe <sub>2</sub>	20	1:2	98	87/13
8	Pd <sub>1</sub> Co <sub>2</sub>	20	1:2	99	88/12
9 <sup>c</sup>	Pd <sub>1</sub> Cu <sub>2</sub>	20	1:2	98	98/2
10 <sup>c,d</sup>	Cu	20	1:2	-	-
11 <sup>c</sup>	Pd+Cu	20	1:2	31	86/14

**Table 13.** Optimization of the bimetallic catalytic system supported on SiO<sub>2</sub> for the hydrosilylation of phenylacetylene with triethylsilane. <sup>a</sup> 0.4 mol% of Pd NPs was used as catalyst. <sup>b</sup> 1.6 mol% of Ni NPs was used as catalyst. <sup>c</sup> Reaction was performed under air. <sup>d</sup> 1.6 mol% of Cu NPs was used as catalyst.

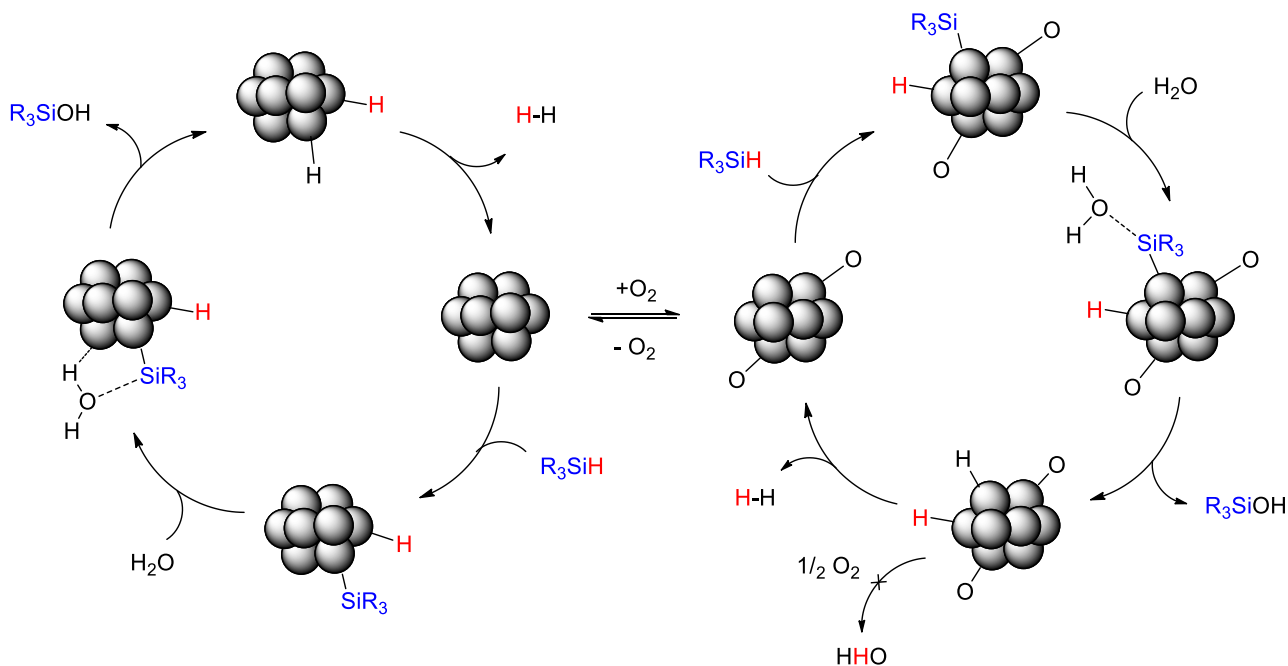
## 4.2. Silane oxidation.

Silanols are compounds containing Si-OH groups, and they are useful molecules for the synthesis of silicon-based polymers as well as in organic synthesis.<sup>243,312-313</sup> For instance, they have been used as nucleophilic agents in C-C cross-coupling reactions,<sup>314</sup> organo-catalysts for activation of carbonyl compounds<sup>315</sup> or guiding groups for C-H activation.<sup>316</sup> Silanols can be obtained by several methods, one of them being the oxidation of silanes through Si-H activation.<sup>317</sup> Alternatively, activation of Si-H bonds forming silanols and further alcoholysis or aminolysis can lead to the formation of silyl ethers or silazane derivatives, which are also interesting in organic synthesis.

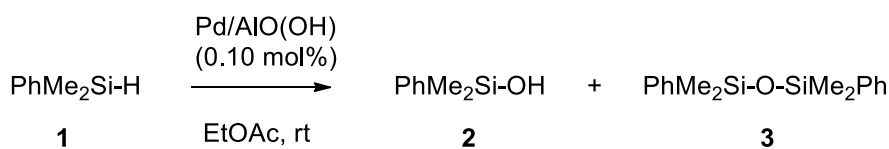
### 4.2.1. Silanol formation catalyzed by metal NPs.

Metal NPs can catalyze the oxidation of silanes to silanols at their surface in a highly exothermic reaction. The reaction is usually carried out with water, which acts as nucleophilic agent attacking the Si atom coordinated at the surface of the NP. As mentioned above, in the hydrosilylation of internal alkynes catalyzed by Pd NPs, the presence of water led to the formation of the corresponding silanol with the concomitant formation of surface-adsorbed hydride. Under these conditions, selective hydrogenation of alkynes into alkenes was observed instead of alkyne hydrosilylation.<sup>292,294</sup> Moreover, the catalytic oxidation of silanes to form the silanols is often accelerated by air.<sup>318</sup> The generally accepted mechanism for the oxidation of silanes by water catalyzed by metal NPs is shown in Scheme 23. In a first step, there is an activation of the Si-H bond to give surface adsorbed hydride and silyl moieties. Then, there is a nucleophilic attack of the oxygen atom of water to the Si atom, to give the silanol product and surface adsorbed hydride. Finally, a reductive elimination of the hydride at the surface of the NPs restarts the catalytic cycle. When the reaction is carried out in the presence of molecular oxygen, it could be imagined that it forms water with the surface hydrogens, but yet formation of hydrogen is observed. In fact, by computational and kinetic studies, Kamachi et al. have proposed that in the case of clean and oxygen covered Pd(111) surface, the role of oxygen atoms is to promote the desorption of H<sub>2</sub> without formation of OH<sup>-</sup> and H<sub>2</sub>O.<sup>319</sup> Kamachi et al. proposed that in the case of Pd(111) surface, a backside attack of a molecule of water with inversion of configuration at the silyl group is most favored in energy (see also Scheme 23). This attack explains the inversion of configuration at the Si center, as retention of the configuration would be expected if the mechanism evolved by reductive elimination between surface-adsorbed silyl and hydroxide groups. It should be indicated that the mechanism accepted for silane oxidation contrasts with the one proposed by Crabtree for silane alcoholysis catalyzed by Ir(III) and Pd(II) complexes in homogeneous phase. Here the reaction starts by formation of a  $\eta^2$ -HSiR<sub>3</sub> complex, followed by an outer sphere nucleophilic attack of ROH and heterolytic splitting.<sup>307</sup>

**Scheme 23.** Generally accepted mechanism for the oxidation of silanes to silanols with water catalyzed by metal NPs. The reaction can be carried out in absence (left) or the presence (right) of molecular oxygen, which participates in the reaction regenerating the catalytically active species.



In 2012, Park and co-workers reported the use of different catalytic systems in the oxidation of tri-substituted silanes with water. The most active one consisted of Pd NPs of 2-3 nm supported on a fibrous aluminium oxyhydroxide matrix (boehmite) [PdNPs/AlO(OH)].<sup>320</sup> The NPs were prepared by a sol-gel process starting from Pd(PPh<sub>3</sub>)<sub>4</sub>, and they were active in the oxidation of a wide range of silanes with good selectivity towards the formation of the silanol. Under anaerobic dry conditions the reaction did not occur, but it was notably improved in the presence of both water and oxygen (see Table 14).



Entry	Oxidant	t (min)	2 (%)	3 (%)
1	air	40	70	30
2	O <sub>2</sub>	10	32	68
3	Ar	180	3	<1
4	air + H <sub>2</sub> O (1 equiv.)	10	79	21
5	air + H <sub>2</sub> O (3 equiv.)	10	98	2
6	Ar + H <sub>2</sub> O (3 equiv.)	20	97	3

**Table 14.** Catalytic oxidation of dimethylphenylsilane with water catalyzed by PdNPs/AlO(OH).

Gold is also a well-known catalyst for the oxidation of silanes to silanols in water (see Scheme 24). The first example of Au NPs as catalysts for this reaction was provided by Kaneda's group in 2009.<sup>321</sup> In this work, Au NPs of 3.0 nm supported on hydroxyapatite (AuNPs/HAP) were synthesized by reduction of HAuCl<sub>4</sub> with KBH<sub>4</sub>. The NPs were active in the oxidation of triethylsilane with water under air at 80 °C with relatively high catalyst loadings (ca. 1 mol%), and they showed to be more selective towards the formation of the desired silanol than Au<sub>2</sub>O<sub>3</sub> and HAuCl<sub>4</sub>. The scope of AuNPs/HAP in the oxidation of silanes was explored and concerned a wide range of silanes with different electronic and steric properties. In 2015, the same group studied the role of O<sub>2</sub> in this reaction catalyzed by AuNPs/HAP, and determined that the oxygen acted not as a stoichiometric reagent but as an activator of the NPs.<sup>322</sup> Hence, the reaction stopped upon removing air and introducing Ar into the reaction but the activity was recovered when air was introduced again. In 2010, Yamamoto, Asao and co-workers used the above described nanoporous gold catalyst (see section 2.1.2) in the oxidation of silanes in water.<sup>323</sup> The catalyst was prepared by selective removal of Ag from a Au<sub>30</sub>Ag<sub>70</sub> alloy. This catalyst operated at room temperature with a catalyst loading of 1 mol% and it was easily recycled from the reaction medium. It was also active in the oxidation of several trialkylsilanes. Duan and co-workers prepared Au NPs of around 2.5 nm that were dispersed in a poly(ionic liquid) and were anchored onto the porous walls of organosilica SBA-15.<sup>324</sup> The recyclable catalyst was active in the oxidation of silanes in neat water with a catalyst loading of 0.4 mol% at 40 °C under air.

Other supports have helped to enhance the activity of Au NPs in the reaction. For instance, Au NPs supported on carbon nanotubes (CNTs) are more active than supported Au/HAP NPs and nanoporous gold. Doris and co-workers reported the first nanotube-based hybrid system for this reaction in 2011 (Au/CNT),<sup>325</sup> using Au NPs of 3 nm. The catalyst was easily reusable and operated at room temperature with low catalyst loadings (0.01 mol%). Oxidation of alkyl and aryl silanes was

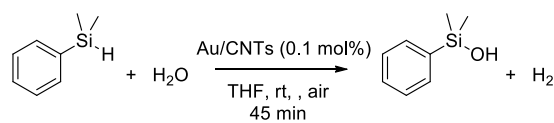


carried out in air with high yields and very good selectivity towards the formation of the silanol. The nanohybrid material was more active in the reaction (TOF  $7.2 \cdot 10^4 \text{ h}^{-1}$ ) than Au NPs of 3 nm dispersed in solution under the same reaction conditions, showing that the support plays a role in the reaction, probably stabilizing the Au oxidized species by charge-transfer processes.<sup>326</sup> Later on, in 2014, Liu et al. supported Au NPs of 1-1.5 nm on oxidized carbon nanotubes (o-CNTs), which displayed comparable activities.<sup>327</sup> The catalyst was stable and recoverable several times without observation of metal leaching or loss of activity.

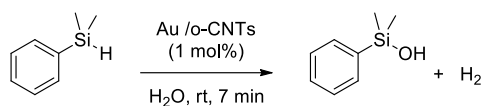
More recently, da Silva et al. have prepared 3 nm Au NPs/PVP supported on MnO<sub>2</sub> nanowires that could operate at room temperature with very low catalyst loadings (0.001-0.0002 mol% of Au), allowing good values of TOF ( $5.9 \cdot 10^5 \text{ h}^{-1}$ ).<sup>328</sup> However, the scope of the catalyst towards the activation of trialkylsilanes was not deeply explored in this work. The particles were obtained by classical reduction of HAuCl<sub>4</sub> with NaBH<sub>4</sub>, and they conserved their morphology and catalytic activity after 10 reaction cycles. The authors attributed the enhancement of the activity of this system compared to other supported NPs to cooperative effects between the support and the Au NPs, which would lead to high concentration of reactive Au<sup>δ+</sup> species at the surface.

Pt NPs have been also applied in this reaction, but to the best of our knowledge there is only one example reported by Chauhan et al (see Scheme 24).<sup>329</sup> The NPs were prepared by decomposition of PtMe<sub>2</sub>(COD) with poly(methylhydro)siloxane (PMHS), as described in section 4.1. Interestingly, the Pt NPs were selective towards the oxidation of silanes containing alkenes or alkynes moieties when 2 equivalents of water were present in the reaction, and no hydrosilylation at all was observed. Ag NPs display lower performances in the oxidation of silanes. Ag NPs obtained by reduction of AgNO<sub>3</sub> with NaBH<sub>4</sub> supported on HAP have been used in the oxidation of phenylsilanes by Kaneda's group, although high catalyst loadings were used (3 mol%) to complete the reaction at room temperature in 15 min (see Scheme 24).<sup>330</sup> Ag nanoporous catalysts have also been used in the reaction, but were found less efficient than Ag/HAP and higher catalyst loadings were required (10 mol%).<sup>331</sup>

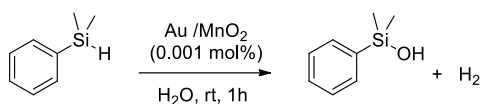
**Scheme 24.** Silanol formation through catalytic oxidation of organosilanes by supported Au, Pt or Ag NPs.



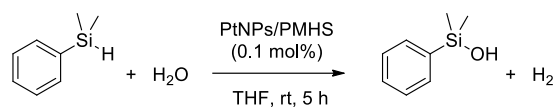
John et al. *Angew. Chem., Int. Ed.* **2011**



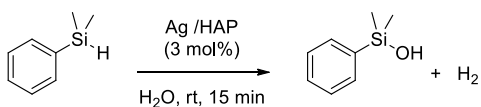
Liu et al. *J. Mater. Chem. A.* **2014**



da Silva et al. *Appl. Catal. B.* **2016**



Chauhan et al. *Appl. Organometal. Chem.* **2009**



Mitsudome et al. *Angew. Chem., Int. Ed.* **2008**

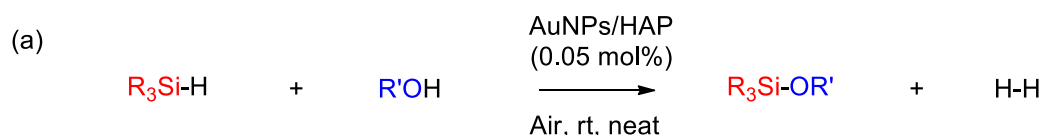
In conclusion, metal NPs have emerged as good catalysts for silane oxidation to give silanols because of their good activities, selectivities and recyclability from the reaction medium after deposition on a support. In addition, the reaction is enhanced in the presence of air facilitating the operability of the process, which in our opinion makes metal NPs very interesting for scaled-up industrial processes.

#### 4.2.2. Other catalytic reactions involving oxidation of silanes.

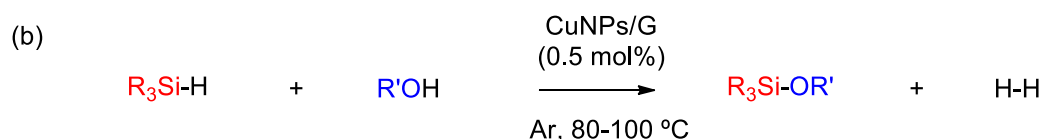
Silyl ethers can be obtained by reaction of chlorosilanes or disilazanes with alcohols in the presence of a base. However, these reagents are corrosive and air-sensitive, and stoichiometric amounts of salts are obtained as by-products in the reaction. Thus, an alternative to its preparation is the catalytic dehydrogenative etherification of silanes with alcohols, analogous to the formation of silanols, in which the only by-product is molecular hydrogen (see Scheme 25). Several homogeneous catalysts have been used in this reaction based on different metals such as Au,<sup>332</sup> Rh,<sup>333</sup> Pt,<sup>334</sup> or Zn.<sup>335</sup>

Since then, supported metal NPs have also been used as efficient catalyst for this reaction, whose main advantage is that in most of the cases they can be easily recycled from the reaction medium. Some selected examples are the work of Kaneda's and Garcia's groups. Kaneda and co-workers studied this reaction catalyzed by different metal NPs supported on HAP.<sup>336</sup> Among all the systems studied Au/HAP was the most active catalyst using low loadings (0.005 mol%, Scheme 25a). García and co-workers showed that Cu NPs of 10-25 nm supported on graphene materials are efficient catalysts for the dehydrogenative coupling of silanes and alcohols (Scheme 25b).<sup>306</sup> Similarly, the dehydrogenative coupling of hydrosilanes with primary or secondary amines can allow the synthesis of silyl amines (see Scheme 25c). García and co-workers performed this catalytic process using Pd NPs supported on graphene (PdNPs/G), whilst analogous Cu and Ni NPs supported on G were inactive.<sup>337</sup>

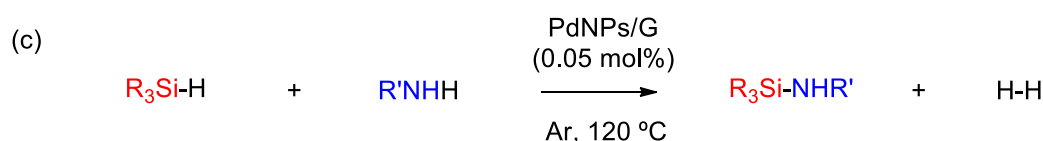
**Scheme 25.** Catalytic conditions for the dehydrogenative etherification of silanes with alcohols catalyzed by (a) Au/HAP and (b) Cu/G. (c) Catalytic conditions for the dehydrogenative amination of silanes with amines catalyzed by Pd/G.



Mitsudome et al. *Chem. Eur. J.*; **2013**



Blandez et al. *Angew. Chem.*; **2014**

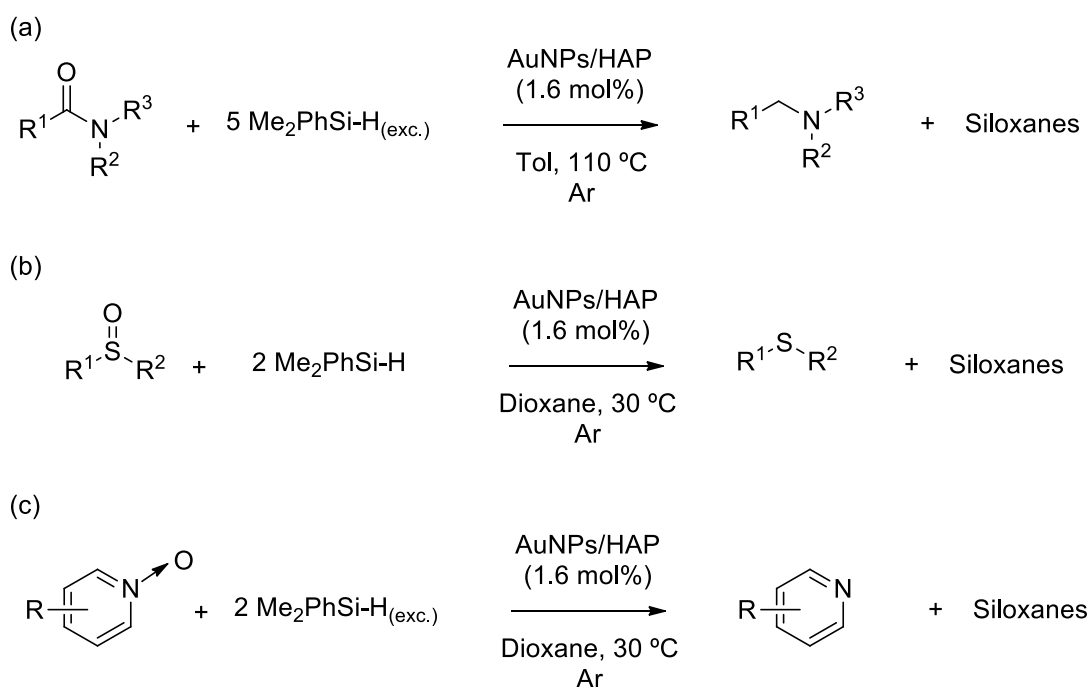


Blandez et al. *Catal. Sci. Technol.*; **2015**

Another interesting reaction that implies Si-H activation and that can be catalyzed by metal NPs is the deoxygenation reaction. Kaneda's group tested the AuNPs/HAP system in the deoxygenation of amides, sulfoxides and pyridine *N*-oxides (see Scheme 26).<sup>338</sup> The NPs were selective towards the reduction of such groups, while other organic groups such as alkenes or esters were unreactive. The AuNPs were more active than the previous systems based on homogeneous or heterogenized Fe, Ru, Os or Zn complexes, and they were easily recyclable without any loss in efficiency. By IR

spectroscopy, the authors confirmed the interaction between the Au NPs and the Si-H bond, while the C=O stretching band of the amide substrates was unaffected after treatment of the catalyst with this molecule. This indicates that the reaction starts probably with Si-H activation, like in the silanol formation. In 2014, Taori and Buchmeiser studied the reaction mechanism of the deoxygenation of DMF to give trimethylamine catalyzed by Pt NPs.<sup>339</sup> The authors confirmed that the reaction starts by Si-H activation of two silane molecules, and that it evolves by a concerted double-reduction of DMF by two hydride groups coordinated at the surface. This “dual effect” that was already proposed for homogeneous catalysts was governed by steric factors in the Pt NPs studied in this work.

**Scheme 26.** General conditions for the catalytic deoxygenation of (a) amides, (b) sulfoxides and (c) pyridine *N*-oxides catalyzed by AuNPs/HAP.



## 5. Conclusions.

This literature survey shows that activation and coordination processes of  $\sigma$ -bonds occur similarly on molecular complexes and on nanoparticles.  $\text{H}_2$  can coordinate and dissociate on nanoparticles in a way very similar to what is observed on molecular species. C-H bonds can be activated through mechanisms that resemble those found in molecular chemistry. The difference lies in the richness brought by the number of active surface atoms which allow *inter alia* the fast diffusion of hydrides on nanoparticles, the easy reduction of aromatic rings and, thanks to the formation of a 4-membered ring, the enantiospecific H/D exchange in amino-acids. Productive C-H functionalization is still less advanced than in molecular chemistry although tremendous progresses

have been achieved for the past few years. Concerning silanes, the detection of coordinated Si-H bonds is not documented although upon interacting with nanoparticles, silanes give rise to Si species linked to the surface in various coordination modes. It has now been established that hydrosilylation can be catalyzed by nanoparticles after years of controversies, although, so far, no specific reactivity is clearly observed with nanoparticles. However, one advantage of nanoparticles is the possibility to produce bimetallic species in which synergies can be observed or which are able to isolate active atoms like Pd in PdAu nanoparticles. To conclude, most of the literature reported in this review is recent and there is no doubt that the field of  $\sigma$ -bond activation using nanoparticles will continue to develop at an increasing rate. Whereas  $\sigma$ -H<sub>2</sub> is well understood for some systems such as Ru NPs, future directions in this field will probably be focused on characterization of more complex systems (i.e. Pd NPs containing subsurface hydrides), understanding of ligand effects, or physical activation of the reaction (i.e. irradiation with light). C-H functionalization faces bigger challenges, as in many cases the active species remain unknown. Thus, we believe that this target must be addressed before advances can be made in the rational design of catalytic systems based on metal NPs. Finally, the recent development on hydrosilylation catalyzed by metallic NPs will likely play an important role in the heterogenization of this reaction, as this reaction continues to be performed in homogeneous phase at industrial scale.

## 6. Acknowledgements.

The authors thank ERC Advanced Grant (MONACAT 2015-694159) and IDEX/Chaires d'attractivité de l'Université Fédérale de Toulouse Midi-Pyrénées for financial support. D. Bouzouita is a participant in the EU Isotopics consortium. The ISOTOPICS project has received funding from the European Union Horizon2020 research and innovation program under the Marie Skłodowska-Curie grant agreement N88675071.

## 7. Bibliography.

- (1) Calvin, M. *Homogeneous catalytic hydrogenation*. *J. Am. Chem. Soc.* **1939**, *61*, 2230-2234.
- (2) Vaska, L.; DiLuzio, J. W. *Activation of hydrogen by a transition metal complex at normal conditions leading to a stable molecular dihydride*. *J. Am. Chem. Soc.* **1962**, *84*, 679-680.
- (3) Jardine, F. H.; Osborn, J. A.; Wilkinson, G.; Young, J. F. *Homogeneous catalytic hydrogenation and hydroformylation of acetylenic compounds*. *Chem. Ind.* **1965**, 560.
- (4) Wasserman, H. J.; Kubas, G. J.; Ryan, R. R. *Molecular hydrogen complexes of the transition metals. 2. Preparation, structure, and reactivity of W(CO)<sub>3</sub>(PCy<sub>3</sub>)<sub>2</sub> and W(CO)<sub>3</sub>(P-iso-Pr<sub>3</sub>)<sub>2</sub>,  $\eta^2$ -H<sub>2</sub> complex precursors exhibiting metal...hydrogen-carbon interaction*. *J. Am. Chem. Soc.* **1986**, *108*, 2294-2301.
- (5) Kubas, G. J. *Activation of dihydrogen and coordination of molecular H<sub>2</sub> on transition metals*. *J. Organomet. Chem.* **2014**, *751*, 33-49.

- (6) Kubas, G. J. *Metal-dihydrogen and  $\sigma$ -bond coordination: the consummate extension of the Dewar-Chatt-Duncanson model for metal-olefin  $\pi$  bonding*. *J. Organomet. Chem.* **2001**, 635, 37-68.
- (7) Crabtree, R. H. *Dihydrogen Complexation*. *Chem. Rev.* **2016**, 116, 8750-8769.
- (8) Heinekey, D. M.; Oldham, W. J., Jr. *Coordination chemistry of dihydrogen*. *Chem. Rev.* **1993**, 93, 913-926.
- (9) Kubas, G. J. *Dihydrogen complexes as prototypes for the coordination chemistry of saturated molecules*. *Proc. Natl. Acad. Sci. U. S. A.* **2007**, 104, 6901-6907.
- (10) Alcaraz, G.; Grellier, M.; Sabo-Etienne, S. *Bis  $\sigma$ -Bond Dihydrogen and Borane Ruthenium Complexes: Bonding Nature, Catalytic Applications, and Reversible Hydrogen Release*. *Acc. Chem. Res.* **2009**, 42, 1640-1649.
- (11) Schubert, U.  *$\eta^2$  Coordination of silicon-hydrogen  $\sigma$  bonds to transition metals*. *Adv. Organomet. Chem.* **1990**, 30, 151-187.
- (12) Luo, X.-L.; Kubas, G. J.; Burns, C. J.; Bryan, J. C.; Unkefer, C. J. *Synthesis of the First Examples of Transition Metal  $\eta^2$ -SiH<sub>4</sub> Complexes, cis-Mo( $\eta^2$ -SiH<sub>4</sub>)(CO)(R<sub>2</sub>PC<sub>2</sub>H<sub>4</sub>PR<sub>2</sub>)<sub>2</sub>, and Evidence for an Unprecedented Tautomeric Equilibrium between an  $\eta^2$ -SiH<sub>4</sub> Complex and a Hydridosilyl Species: A Model for Methane Coordination and Activation*. *J. Am. Chem. Soc.* **1995**, 117, 1159-1160.
- (13) Crabtree, R. H. *The organometallic chemistry of alkanes*. *Chem. Rev.* **1985**, 85, 245-269.
- (14) Geftakis, S.; Ball, G. E. *Direct Observation of a Transition Metal Alkane Complex, CpRe(CO)<sub>2</sub>(cyclopentane), Using NMR Spectroscopy*. *J. Am. Chem. Soc.* **1998**, 120, 9953-9954.
- (15) Brookhart, M.; Green, M. L. H.; Wong, L. L. *Carbon-hydrogen-transition metal bonds*. *Prog. Inorg. Chem.* **1988**, 36, 1-124.
- (16) Brookhart, M.; Green, M. L. H. *Carbon-hydrogen-transition metal bonds*. *J. Organomet. Chem.* **1983**, 250, 395-408.
- (17) Scherer, W.; McGrady, G. S. *Agostic interactions in d<sup>0</sup> metal alkyl complexes*. *Angew. Chem., Int. Ed.* **2004**, 43, 1782-1806.
- (18) Mahmudov, K. T.; Gurbanov, A. V.; Guseinov, F. I.; Guedes da Silva, M. F. C. *Noncovalent interactions in metal complex catalysis*. *Coord. Chem. Rev.* **2019**, 387, 32-46.
- (19) Hall, C.; Perutz, R. N. *Transition Metal Alkane Complexes*. *Chem. Rev.* **1996**, 96, 3125-3146.
- (20) Crabtree, R. H.; Lei, A. *Introduction: CH Activation*. *Chem. Rev.* **2017**, 117, 8481-8482.
- (21) Sabatier, P. *Hydrogenation and Dehydrogenation by Catalysis*. *Ber. Dtsch. Chem. Ges.* **1911**, 44, 1984-2001.
- (22) Hagen, C. M.; Widegren, J. A.; Maitlis, P. M.; Finke, R. G. *Is It Homogeneous or Heterogeneous Catalysis? Compelling Evidence for Both Types of Catalysts Derived from [Rh( $\eta^5$ -C<sub>5</sub>Me<sub>5</sub>)Cl<sub>2</sub>]<sub>2</sub> as a Function of Temperature and Hydrogen Pressure*. *J. Am. Chem. Soc.* **2005**, 127, 4423-4432.
- (23) Zaera, F. *The Surface Chemistry of Metal-Based Hydrogenation Catalysis*. *ACS Catal.* **2017**, 7, 4947-4967.
- (24) Pla, D.; Gomez, M. *Metal and Metal Oxide Nanoparticles: A Lever for C-H Functionalization*. *ACS Catal.* **2016**, 6, 3537-3552.
- (25) Kubas, G. J.; Ryan, R. R.; Swanson, B. I.; Vergamini, P. J.; Wasserman, H. J. *Characterization of the first examples of isolable molecular hydrogen complexes, M(CO)<sub>3</sub>(PR<sub>3</sub>)<sub>2</sub>(H<sub>2</sub>) (M = molybdenum or tungsten; R = Cy or isopropyl). Evidence for a side-on bonded dihydrogen ligand*. *J. Am. Chem. Soc.* **1984**, 106, 451-452.
- (26) Kubas, G. J.; Editor *Metal Dihydrogen and  $\sigma$ -Bond Complexes: Structure, Theory and Reactivity*; Kluwer Academic/Plenum Publishers, 2001.
- (27) Gutmann, T.; del Rosal, I.; Chaudret, B.; Poteau, R.; Limbach, H.-H.; Buntkowsky, G. *From Molecular Complexes to Complex Metallic Nanostructures - <sup>2</sup>H Solid-State NMR Studies of Ruthenium-Containing Hydrogenation Catalysts*. *ChemPhysChem* **2013**, 14, 3026-3033.
- (28) Akbayrak, S.; Erdek, P.; Ozkar, S. *Hydroxyapatite supported ruthenium(0) nanoparticles catalyst in hydrolytic dehydrogenation of ammonia borane: Insight to the nanoparticles formation and hydrogen evolution kinetics*. *Appl. Catal., B* **2013**, 142-143, 187-195.
- (29) Yang, X.; Cheng, F.; Liang, J.; Tao, Z.; Chen, J. *PtxNi<sub>1-x</sub> nanoparticles as catalysts for hydrogen generation from hydrolysis of ammonia borane*. *Int. J. Hydrogen Energy* **2009**, 34, 8785-8791.

- (30) Adams, B. D.; Ostrom, C. K.; Chen, S.; Chen, A. *High-Performance Pd-Based Hydrogen Spillover Catalysts for Hydrogen Storage*. *J. Phys. Chem. C* **2010**, *114*, 19875-19882.
- (31) Wang, Z.; Yang, R. T. *Enhanced Hydrogen Storage on Pt-Doped Carbon by Plasma Reduction*. *J. Phys. Chem. C* **2010**, *114*, 5956-5963.
- (32) Au, Y. S.; Ponthieu, M.; van Zwiene, R.; Zlotea, C.; Cuevas, F.; de Jong, K. P.; de Jongh, P. E. *Synthesis of Mg<sub>2</sub>Cu nanoparticles on carbon supports with enhanced hydrogen sorption kinetics*. *J. Mater. Chem. A* **2013**, *1*, 9983-9991.
- (33) Yamauchi, M.; Kobayashi, H.; Kitagawa, H. *Hydrogen Storage Mediated by Pd and Pt Nanoparticles*. *ChemPhysChem* **2009**, *10*, 2566-2576.
- (34) Martinez-Prieto, L. M.; Chaudret, B. *Organometallic Ruthenium Nanoparticles: Synthesis, Surface Chemistry, and Insights into Ligand Coordination*. *Acc. Chem. Res.* **2018**, *51*, 376-384.
- (35) Kattel, S.; Liu, P.; Chen, J. G. *Tuning Selectivity of CO<sub>2</sub> Hydrogenation Reactions at the Metal/Oxide Interface*. *J. Am. Chem. Soc.* **2017**, *139*, 9739-9754.
- (36) Delgado, J. A.; Benkirane, O.; Claver, C.; Curulla-Ferre, D.; Godard, C. *Advances in the preparation of highly selective nanocatalysts for the semi-hydrogenation of alkynes using colloidal approaches*. *Dalton Trans.* **2017**, *46*, 12381-12403.
- (37) Zang, W.; Li, G.; Wang, L.; Zhang, X. *Catalytic hydrogenation by noble-metal nanocrystals with well-defined facets: a review*. *Catal. Sci. Technol.* **2015**, *5*, 2532-2553.
- (38) Serna, P.; Corma, A. *Transforming Nano Metal Nonselective Particulates into Chemoselective Catalysts for Hydrogenation of Substituted Nitrobenzenes*. *ACS Catal.* **2015**, *5*, 7114-7121.
- (39) Kinayyigit, S.; Philippot, K. *Organometallic approach for the synthesis of noble metal nanoparticles: towards application in colloidal and supported nanocatalysis*. *RSC Catal. Ser.* **2014**, *17*, 47-82.
- (40) Alcaraz, G.; Grellier, M.; Sabo-Etienne, S. *Bis  $\sigma$ -Bond Dihydrogen and Borane Ruthenium Complexes: Bonding Nature, Catalytic Applications, and Reversible Hydrogen Release*. *Acc. Chem. Res.* **2009**, *42*, 1640-1649.
- (41) Morris, R. H. *Dihydrogen, dihydride and in between: NMR and structural properties of iron group complexes*. *Coord. Chem. Rev.* **2008**, *252*, 2381-2394.
- (42) Sabo-Etienne, S.; Chaudret, B. *Chemistry of bis(dihydrogen) ruthenium complexes and of their derivatives*. *Coord. Chem. Rev.* **1998**, *178-180*, 381-407.
- (43) Lau, C. P.; Ng, S. M.; Jia, G.; Lin, Z. *Some ruthenium hydride, dihydrogen, and dihydrogen-bonded complexes in catalytic reactions*. *Coord. Chem. Rev.* **2007**, *251*, 2223-2237.
- (44) Ratovelomanana-Vidal, V.; Genet, J.-P. *Enantioselective ruthenium-mediated hydrogenation: developments and applications*. *J. Organomet. Chem.* **1998**, *567*, 163-172.
- (45) Favier, I.; Lavedan, P.; Massou, S.; Teuma, E.; Philippot, K.; Chaudret, B.; Gomez, M. *Hydrogenation Processes at the Surface of Ruthenium Nanoparticles: A NMR Study*. *Top. Catal.* **2013**, *56*, 1253-1261.
- (46) Novio, F.; Monahan, D.; Coppel, Y.; Antorrena, G.; Lecante, P.; Philippot, K.; Chaudret, B. *Surface Chemistry on Small Ruthenium Nanoparticles: Evidence for Site Selective Reactions and Influence of Ligands*. *Chem. - Eur. J.* **2014**, *20*, 1287-1297.
- (47) Gutmann, T.; Walaszek, B.; Xu, Y.; Waechtler, M.; del Rosal, I.; Gruenberg, A.; Poteau, R.; Axet, R.; Lavigne, G.; Chaudret, B., et al. *Hydrido-Ruthenium Cluster Complexes as Models for Reactive Surface Hydrogen Species of Ruthenium Nanoparticles. Solid-State 2H NMR and Quantum Chemical Calculations*. *J. Am. Chem. Soc.* **2010**, *132*, 11759-11767.
- (48) del Rosal, I.; Gutmann, T.; Walaszek, B.; Gerber, I. C.; Chaudret, B.; Limbach, H.-H.; Buntkowsky, G.; Poteau, R. *2H NMR calculations on polynuclear transition metal complexes: on the influence of local symmetry and other factors*. *Phys. Chem. Chem. Phys.* **2011**, *13*, 20199-20207.
- (49) Pelzer, K.; Vidoni, O.; Philippot, K.; Chaudret, B.; Colliere, V. *Organometallic synthesis of size-controlled polycrystalline ruthenium nanoparticles in the presence of alcohols*. *Adv. Funct. Mater.* **2003**, *13*, 118-126.

- (50) Lara, P.; Rivada-Wheelaghan, O.; Conejero, S.; Poteau, R.; Philippot, K.; Chaudret, B. *Ruthenium Nanoparticles Stabilized by N-Heterocyclic Carbenes: Ligand Location and Influence on Reactivity*. *Angew. Chem., Int. Ed.* **2011**, *50*, 12080-12084.
- (51) González-Gálvez, D.; Nolis, P.; Philippot, K.; Chaudret, B.; van Leeuwen, P. W. N. M. *Phosphine-Stabilized Ruthenium Nanoparticles: The Effect of the Nature of the Ligand in Catalysis*. *ACS Catal.* **2012**, *2*, 317-321.
- (52) Gonzalez-Gomez, R.; Cusinato, L.; Bijani, C.; Coppel, Y.; Lecante, P.; Amiens, C.; del Rosal, I.; Philippot, K.; Poteau, R. *Carboxylic acid-capped ruthenium nanoparticles: experimental and theoretical case study with ethanoic acid*. *Nanoscale* **2019**, *11*, 9392-9409.
- (53) Pan, C.; Pelzer, K.; Philippot, K.; Chaudret, B.; Dassenoy, F.; Lecante, P.; Casanove, M.-J. *Ligand-Stabilized Ruthenium Nanoparticles: Synthesis, Organization, and Dynamics*. *J. Am. Chem. Soc.* **2001**, *123*, 7584-7593.
- (54) Pery, T.; Pelzer, K.; Buntkowsky, G.; Philippot, K.; Limbach, H.-H.; Chaudret, B. *Direct NMR evidence for the presence of mobile surface hydrides on ruthenium nanoparticles*. *ChemPhysChem* **2005**, *6*, 605-607.
- (55) Garcia-Anton, J.; Axet, M. R.; Jansat, S.; Philippot, K.; Chaudret, B.; Pery, T.; Buntkowsky, G.; Limbach, H.-H. *Reactions of olefins with ruthenium hydride nanoparticles: NMR characterization, hydride titration, and room-temperature C-C bond activation*. *Angew. Chem., Int. Ed.* **2008**, *47*, 2074-2078.
- (56) Berthoud, R.; Delichere, P.; Gajan, D.; Lukens, W.; Pelzer, K.; Basset, J.-M.; Candy, J.-P.; Coperet, C. *Hydrogen and oxygen adsorption stoichiometries on silica supported ruthenium nanoparticles*. *J. Catal.* **2008**, *260*, 387-391.
- (57) Gutel, T.; Santini, C. C.; Philippot, K.; Padua, A.; Pelzer, K.; Chaudret, B.; Chauvin, Y.; Basset, J.-M. *Organized 3D-alkyl imidazolium ionic liquids could be used to control the size of in situ generated ruthenium nanoparticles?* *J. Mater. Chem.* **2009**, *19*, 3624-3631.
- (58) Campbell, P. S.; Santini, C. C.; Bouchu, D.; Fenet, B.; Philippot, K.; Chaudret, B.; Padua, A. A. H.; Chauvin, Y. *A novel stabilisation model for ruthenium nanoparticles in imidazolium ionic liquids: in situ spectroscopic and labelling evidence*. *Phys Chem Chem Phys* **2010**, *12*, 4217-4223.
- (59) Adamczyk, A.; Xu, Y.; Walaszek, B.; Roelofs, F.; Pery, T.; Pelzer, K.; Philippot, K.; Chaudret, B.; Limbach, H.-H.; Breitzke, H., et al. *Solid State and Gas Phase NMR Studies of Immobilized Catalysts and Catalytic Active Nanoparticles*. *Top. Catal.* **2008**, *48*, 75-83.
- (60) Walaszek, B.; Xu, Y.; Adamczyk, A.; Breitzke, H.; Pelzer, K.; Limbach, H.-H.; Huang, J.; Li, H.; Buntkowsky, G. *2H-solid-state-NMR study of hydrogen adsorbed on catalytically active ruthenium coated mesoporous silica materials*. *Solid State Nucl. Magn. Reson.* **2009**, *35*, 164-171.
- (61) del Rosal, I.; Mercy, M.; Gerber, I. C.; Poteau, R. *Ligand-Field Theory-Based Analysis of the Adsorption Properties of Ruthenium Nanoparticles*. *ACS Nano* **2013**, *7*, 9823-9835.
- (62) Schroeder, F.; Esken, D.; Cokoja, M.; van den Berg, M. W. E.; Lebedev, O. I.; Van Tendeloo, G.; Walaszek, B.; Buntkowsky, G.; Limbach, H.-H.; Chaudret, B., et al. *Ruthenium Nanoparticles inside Porous [Zn4O(bdc)3] by Hydrogenolysis of Adsorbed [Ru(cod)(cot)]: A Solid-State Reference System for Surfactant-Stabilized Ruthenium Colloids*. *J. Am. Chem. Soc.* **2008**, *130*, 6119-6130.
- (63) Truflandier, L. A.; Del Rosal, I.; Chaudret, B.; Poteau, R.; Gerber, I. C. *Where does Hydrogen Adsorb on Ru Nanoparticles? A Powerful Joint 2H MAS-NMR/DFT Approach*. *ChemPhysChem* **2009**, *10*, 2939-2942.
- (64) Bumüller, D.; Hehn, A.-S.; Waldt, E.; Ahlrichs, R.; Kappes, M. M.; Schooss, D. *Ruthenium Cluster Structure Change Induced by Hydrogen Adsorption: Ru19*. *J. Phys. Chem. C* **2017**, *121*, 10645-10652.
- (65) Limbach, H.-H.; Pery, T.; Rothermel, N.; Chaudret, B.; Gutmann, T.; Buntkowsky, G. *Gas phase 1H NMR studies and kinetic modeling of dihydrogen isotope equilibration catalyzed by Ru-nanoparticles under normal conditions: dissociative vs. associative exchange*. *Phys. Chem. Chem. Phys.* **2018**, *20*, 10697-10712.
- (66) Luo, X. L.; Crabtree, R. H. *Solution equilibrium between classical and nonclassical polyhydride tautomers [ReH4(CO)L3]+ and [ReH2(η2-H2)(CO)L3]+ (L = PMe2Ph)*. *Equilibrium isotope effects*



- and an intermediate trihydrogen complex in intramolecular site exchange of dihydrogen and hydride ligands. *J. Am. Chem. Soc.* **1990**, *112*, 6912-6918.
- (67) Rothermel, N.; Roether, T.; Ayvali, T.; Martinez-Prieto, L. M.; Philippot, K.; Limbach, H.-H.; Chaudret, B.; Gutmann, T.; Buntkowsky, G. *Reactions of D<sub>2</sub> with 1,4-Bis(diphenylphosphino)butane-Stabilized Metal Nanoparticles-A Combined Gas-phase NMR, GC-MS and Solid-state NMR Study.* *ChemCatChem* **2019**, *11*, 1465-1471.
- (68) Novio, F.; Philippot, K.; Chaudret, B. *Location and Dynamics of CO Co-ordination on Ru Nanoparticles: A Solid State NMR Study.* *Catal. Lett.* **2010**, *140*, 1-7.
- (69) Cusinato, L.; Martinez-Prieto, L. M.; Chaudret, B.; del Rosal, I.; Poteau, R. *Theoretical characterization of the surface composition of ruthenium nanoparticles in equilibrium with syngas.* *Nanoscale* **2016**, *8*, 10974-10992.
- (70) Chen, H.-Y. T.; Tosoni, S.; Pacchioni, G. *Hydrogen Adsorption, Dissociation, and Spillover on Ru<sub>10</sub> Clusters Supported on Anatase TiO<sub>2</sub> and Tetragonal ZrO<sub>2</sub> (101) Surfaces.* *ACS Catal.* **2015**, *5*, 5486-5495.
- (71) Fernandez, C.; Bion, N.; Gaigneaux, E. M.; Duprez, D.; Ruiz, P. *Kinetics of hydrogen adsorption and mobility on Ru nanoparticles supported on alumina: Effects on the catalytic mechanism of ammonia synthesis.* *J. Catal.* **2016**, *344*, 16-28.
- (72) Karim, W.; Spreafico, C.; Kleibert, A.; Gobrecht, J.; Vande Vondele, J.; Ekinci, Y.; van Bokhoven, J. A. *Catalyst support effects on hydrogen spillover.* *Nature* **2017**, *541*, 68-71.
- (73) Prins, R. *Hydrogen Spillover. Facts and Fiction.* *Chem. Rev.* **2012**, *112*, 2714-2738.
- (74) Doyle, A. M.; Shaikhutdinov, S. K.; Jackson, S. D.; Freund, H.-J. *Hydrogenation on metal surfaces: Why are nanoparticles more active than single crystals?* *Angew. Chem., Int. Ed.* **2003**, *42*, 5240-5243.
- (75) Yamauchi, M.; Ikeda, R.; Kitagawa, H.; Takata, M. *Nanosize Effects on Hydrogen Storage in Palladium.* *J. Phys. Chem. C* **2008**, *112*, 3294-3299.
- (76) Bardhan, R.; Hedges, L. O.; Pint, C. L.; Javey, A.; Whitlam, S.; Urban, J. J. *Uncovering the intrinsic size dependence of hydriding phase transformations in nanocrystals.* *Nat. Mater.* **2013**, *12*, 905-912.
- (77) Syrenova, S.; Wadell, C.; Nugroho, F. A. A.; Gschneidner, T. A.; Diaz Fernandez, Y. A.; Nalin, G.; Switlik, D.; Westerlund, F.; Antosiewicz, T. J.; Zhdanov, V. P., et al. *Hydride formation thermodynamics and hysteresis in individual Pd nanocrystals with different size and shape.* *Nat. Mater.* **2015**, *14*, 1236-1244.
- (78) Zlotea, C.; Campesi, R.; Cuevas, F.; Leroy, E.; Dibandjo, P.; Volkringer, C.; Loiseau, T.; Ferey, G.; Latroche, M. *Pd Nanoparticles Embedded into a Metal-Organic Framework: Synthesis, Structural Characteristics, and Hydrogen Sorption Properties.* *J. Am. Chem. Soc.* **2010**, *132*, 2991-2997.
- (79) Greeley, J.; Mavrikakis, M. *Surface and Subsurface Hydrogen: Adsorption Properties on Transition Metals and Near-Surface Alloys.* *J. Phys. Chem. B* **2005**, *109*, 3460-3471.
- (80) Armbruester, M.; Behrens, M.; Cinquini, F.; Foettinger, K.; Grin, Y.; Haghofner, A.; Kloetzer, B.; Knop-Gericke, A.; Lorenz, H.; Ota, A., et al. *How to Control the Selectivity of Palladium-based Catalysts in Hydrogenation Reactions: The Role of Subsurface Chemistry.* *ChemCatChem* **2012**, *4*, 1048-1063.
- (81) Ludwig, W.; Savara, A.; Dostert, K.-H.; Schauer mann, S. *Olefin hydrogenation on Pd model supported catalysts: New mechanistic insights.* *J. Catal.* **2011**, *284*, 148-156.
- (82) Wilde, M.; Fukutani, K.; Naschitzki, M.; Freund, H. J. *Hydrogen absorption in oxide-supported palladium nanocrystals.* *Phys. Rev. B: Condens. Matter Mater. Phys.* **2008**, *77*, 113412/113411-113412/113414.
- (83) Neyman, K. M.; Schauer mann, S. *Hydrogen Diffusion into Palladium Nanoparticles: Pivotal Promotion by Carbon.* *Angew. Chem., Int. Ed.* **2010**, *49*, 4743-4746.
- (84) Aleksandrov, H. A.; Kozlov, S. M.; Schauer mann, S.; Vayssilov, G. N.; Neyman, K. M. *How Absorbed Hydrogen Affects the Catalytic Activity of Transition Metals.* *Angew. Chem., Int. Ed.* **2014**, *53*, 13371-13375.

- (85) Kozlov, S. M.; Aleksandrov, H. A.; Neyman, K. M. *Adsorbed and Subsurface Absorbed Hydrogen Atoms on Bare and MgO(100)-Supported Pd and Pt Nanoparticles*. *J. Phys. Chem. C* **2014**, *118*, 15242-15250.
- (86) Kozlov, S. M.; Aleksandrov, H. A.; Neyman, K. M. *Energetic Stability of Absorbed H in Pd and Pt Nanoparticles in a More Realistic Environment*. *J. Phys. Chem. C* **2015**, *119*, 5180-5186.
- (87) Cano, I.; Huertos, M. A.; Chapman, A. M.; Buntkowsky, G.; Gutmann, T.; Groszewicz, P. B.; van Leeuwen, P. W. N. M. *Air-Stable Gold Nanoparticles Ligated by Secondary Phosphine Oxides as Catalyst for the Chemoselective Hydrogenation of Substituted Aldehydes: a Remarkable Ligand Effect*. *J. Am. Chem. Soc.* **2015**, *137*, 7718-7727.
- (88) Almora-Barrios, N.; Cano, I.; van Leeuwen, P. W. N. M.; Lopez, N. *Concerted Chemoselective Hydrogenation of Acrolein on Secondary Phosphine Oxide Decorated Gold Nanoparticles*. *ACS Catal.* **2017**, *7*, 3949-3954.
- (89) Cano, I.; Martinez-Prieto, L. M.; Chaudret, B.; van Leeuwen, P. W. N. M. *Iridium versus Iridium: Nanocluster and Monometallic Catalysts Carrying the Same Ligand Behave Differently*. *Chem. - Eur. J.* **2017**, *23*, 1444-1450.
- (90) Rojas, H.; Diaz, G.; Martinez, J. J.; Castaneda, C.; Gomez-Cortes, A.; Arenas-Alatorre, J. *Hydrogenation of  $\alpha,\beta$ -unsaturated carbonyl compounds over Au and Ir supported on SiO<sub>2</sub>*. *J. Mol. Catal. A: Chem.* **2012**, *363-364*, 122-128.
- (91) Mukherjee, S.; Libisch, F.; Large, N.; Neumann, O.; Brown, L. V.; Cheng, J.; Lassiter, J. B.; Carter, E. A.; Nordlander, P.; Halas, N. J. *Hot Electrons Do the Impossible: Plasmon-Induced Dissociation of H<sub>2</sub> on Au*. *Nano Lett.* **2013**, *13*, 240-247.
- (92) Mukherjee, S.; Zhou, L.; Goodman, A. M.; Large, N.; Ayala-Orozco, C.; Zhang, Y.; Nordlander, P.; Halas, N. J. *Hot-Electron-Induced Dissociation of H<sub>2</sub> on Gold Nanoparticles Supported on SiO<sub>2</sub>*. *J. Am. Chem. Soc.* **2014**, *136*, 64-67.
- (93) Zhou, L.; Zhang, C.; McClain, M. J.; Manjavacas, A.; Krauter, C. M.; Tian, S.; Berg, F.; Everitt, H. O.; Carter, E. A.; Nordlander, P., et al. *Aluminum Nanocrystals as a Plasmonic Photocatalyst for Hydrogen Dissociation*. *Nano Lett.* **2016**, *16*, 1478-1484.
- (94) Gol'dshleger, N. F.; Tyabin, M. B.; Shilov, A. E.; Shteinman, A. A. *Activation of saturated hydrocarbons. Deuterium-hydrogen exchange in solutions of transition metal complexes*. *Zh. Fiz. Khim.* **1969**, *43*, 2174-2175.
- (95) Gol'dshleger, N. F.; Es'kova, V. V.; Shilov, A. E.; Shteinman, A. A. *Reactions of alkanes in solutions of platinum chloride complexes*. *Zh. Fiz. Khim.* **1972**, *46*, 1353-1354.
- (96) Sakakura, T.; Tanaka, M. *Efficient catalytic carbon-hydrogen activation of alkanes: regioselective carbonylation of the terminal methyl group of n-pentane by RhCl(CO)(PMe<sub>3</sub>)<sub>2</sub>*. *J. Chem. Soc., Chem. Commun.* **1987**, 758-759.
- (97) Tang, X.; Jia, X.; Huang, Z. *Challenges and opportunities for alkane functionalisation using molecular catalysts*. *Chem. Sci.* **2018**, *9*, 288-299.
- (98) Shilov, A. E.; Shul'pin, G. B. *Activation of C-H bonds by metal complexes*. *Chem. Rev.* **1997**, *97*, 2879-2932.
- (99) Arockiam, P. B.; Bruneau, C.; Dixneuf, P. H. *Ruthenium(II)-Catalyzed C-H Bond Activation and Functionalization*. *Chem. Rev.* **2012**, *112*, 5879-5918.
- (100) Dyker, G.; Editor *Handbook of C-H Transformations: Applications in Organic Synthesis, Volume 2*; Wiley-VCH Verlag GmbH & Co. KGaA: Weinheim, 2005.
- (101) Goldberg, K. I.; Goldman, A. S. *Large-Scale Selective Functionalization of Alkanes*. *Acc. Chem. Res.* **2017**, *50*, 620-626.
- (102) Perutz, R. N.; Sabo-Etienne, S. *The  $\sigma$ -CAM mechanism:  $\sigma$  complexes as the basis of  $\sigma$ -bond metathesis at late-transition-metal centers*. *Angew. Chem., Int. Ed.* **2007**, *46*, 2578-2592.
- (103) Labinger, J. A.; Bercaw, J. E. *Understanding and exploiting C-H bond activation*. *Nature* **2002**, *417*, 507-514.
- (104) Shilov, A. E.; Shul'pin, G. B. *Activation and catalytic reactions of saturated hydrocarbons in the presence of metal complexes*; Springer: Dordrecht, 2001.

- (105) Chatt, J.; Davidson, J. M. *The tautomerism of arene and ditertiary phosphine complexes of ruthenium(0), and the preparation of new types of hydrido-complexes of ruthenium(II)*. *Journal of the Chemical Society* **1965**, 843-855.
- (106) Janowicz, A. H.; Bergman, R. G. *Carbon-hydrogen activation in completely saturated hydrocarbons: direct observation of  $M + R-H \rightarrow M(R)(H)$* . *J. Am. Chem. Soc.* **1982**, *104*, 352-354.
- (107) Murai, S.; Kakiuchi, F.; Sekine, S.; Tanaka, Y.; Kamatani, A.; Sonoda, M.; Chatani, N. *Efficient catalytic addition of aromatic carbon-hydrogen bonds to olefins*. *Nature* **1993**, *366*, 529-531.
- (108) Grellier, M.; Vendier, L.; Chaudret, B.; Albinati, A.; Rizzato, S.; Mason, S.; Sabo-Etienne, S. *Synthesis, Neutron Structure, and Reactivity of the Bis(dihydrogen) Complex  $RuH_2(\eta^2-H_2)_2(PCy_3)_2$  Stabilized by Two Tricyclopentylphosphines*. *J. Am. Chem. Soc.* **2005**, *127*, 17592-17593.
- (109) Guari, Y.; Castellanos, A.; Sabo-Etienne, S.; Chaudret, B.  *$RuH_2(H_2)_2(PCy_3)_2$ : a room temperature catalyst for the Murai reaction*. *J. Mol. Catal. A: Chem.* **2004**, *212*, 77-82.
- (110) Atzrodt, J.; Derdau, V.; Fey, T.; Zimmermann, J. *The renaissance of H/D exchange*. *Angew. Chem., Int. Ed.* **2007**, *46*, 7744-7765.
- (111) Atzrodt, J.; Derdau, V.; Kerr, W. J.; Reid, M. *Deuterium- and Tritium-Labelled Compounds: Applications in the Life Sciences*. *Angew. Chem., Int. Ed.* **2018**, *57*, 1758-1784.
- (112) Phillips, D. H.; Potter, G. A.; Horton, M. N.; Hewer, A.; Crofton-Sleigh, C.; Jarman, M.; Venitt, S. *Reduced genotoxicity of [D5-ethyl]-tamoxifen implicates  $\alpha$ -hydroxylation of the ethyl group as a major pathway of tamoxifen activation to a liver carcinogen*. *Carcinogenesis* **1994**, *15*, 1487-1492.
- (113) Marcus, D. M.; McLachlan, K. A.; Wildman, M. A.; Ehresmann, J. O.; Kletnieks, P. W.; Haw, J. F. *Experimental Evidence from H/D Exchange Studies for the Failure of Direct C-C Coupling Mechanisms in the Methanol-to-Olefin Process Catalyzed by HSAPO-34*. *Angew. Chem., Int. Ed.* **2006**, *45*, 3133-3136.
- (114) Stokvis, E.; Rosing, H.; Beijnen, J. H. *Stable isotopically labeled internal standards in quantitative bioanalysis using liquid chromatography/mass spectrometry: necessity or not?* *Rapid Commun. Mass Spectrom.* **2005**, *19*, 401-407.
- (115) Atzrodt, J.; Derdau, V.; Kerr, W. J.; Reid, M. *C-H Functionalization for Hydrogen Isotope Exchange*. *Angew. Chem., Int. Ed.* **2017**, *57*, 3022-3047.
- (116) Junk, T.; Catallo, W. J. *Preparative supercritical deuterium exchange in arenes and heteroarenes*. *Tetrahedron Lett.* **1996**, *37*, 3445-3448.
- (117) Heys, R. *Investigation of iridium hydride complex  $[IrH_2(Me_2CO)_2(PPh_3)_2]BF_4$  as a catalyst of hydrogen isotope exchange of substrates in solution*. *J. Chem. Soc., Chem. Commun.* **1992**, 680-681.
- (118) Hesk, D.; Das, P. R.; Evans, B. *Deuteration of acetanilides and other substituted aromatics using  $[Ir(COD)(Cy_3P)(Py)]PF_6$  as catalyst*. *J. Labelled Compd. Radiopharm.* **1995**, *36*, 497-502.
- (119) Neubert, L.; Michalik, D.; Baehn, S.; Imm, S.; Neumann, H.; Atzrodt, J.; Derdau, V.; Holla, W.; Beller, M. *Ruthenium-Catalyzed Selective  $\alpha,\beta$ -Deuteration of Bioactive Amines*. *J. Am. Chem. Soc.* **2012**, *134*, 12239-12244.
- (120) Bai, W.; Lee, K.-H.; Tse, S. K. S.; Chan, K. W.; Lin, Z.; Jia, G. *Ruthenium-Catalyzed Deuteration of Alcohols with Deuterium Oxide*. *Organometallics* **2015**, *34*, 3686-3698.
- (121) Khaskin, E.; Milstein, D. *Simple and Efficient Catalytic Reaction for the Selective Deuteration of Alcohols*. *ACS Catal.* **2013**, *3*, 448-452.
- (122) Chen, S.; Song, G.; Li, X. *Chelation-assisted rhodium hydride-catalyzed regioselective H/D exchange in arenes*. *Tetrahedron Lett.* **2008**, *49*, 6929-6932.
- (123) Yang, H.; Dormer, P. G.; Rivera, N. R.; Hoover, A. J. *Palladium(II)-Mediated C-H Tritiation of Complex Pharmaceuticals*. *Angew. Chem., Int. Ed.* **2018**, *57*, 1883-1887.
- (124) Hickman, A. J.; Cismesia, M. A.; Sanford, M. S. *Structure Activity Relationship Study of Diimine Pt(II) Catalysts for H/D Exchange*. *Organometallics* **2012**, *31*, 1761-1766.
- (125) Derdau, V.; Atzrodt, J.; Zimmermann, J.; Kroll, C.; Brueckner, F. *Hydrogen-Deuterium Exchange Reactions of Aromatic Compounds and Heterocycles by  $NaBD_4$ -Activated Rhodium, Platinum and Palladium Catalysts*. *Chem. - Eur. J.* **2009**, *15*, 10397-10404.

- (126) Jere, F. T.; Miller, D. J.; Jackson, J. E. *Stereoretentive C-H Bond Activation in the Aqueous Phase Catalytic Hydrogenation of Amino Acids to Amino Alcohols*. *Org. Lett.* **2003**, *5*, 527-530.
- (127) Ott, L. S.; Cline, M. L.; Deetlefs, M.; Seddon, K. R.; Finke, R. G. *Nanoclusters in Ionic Liquids: Evidence for N-Heterocyclic Carbene Formation from Imidazolium-Based Ionic Liquids Detected by <sup>2</sup>H NMR*. *J. Am. Chem. Soc.* **2005**, *127*, 5758-5759.
- (128) Sullivan, J. A.; Flanagan, K. A.; Hain, H. *Selective H-D exchange catalyzed by aqueous phase and immobilized Pd nanoparticles*. *Catal. Today* **2008**, *139*, 154-160.
- (129) Pieters, G.; Taglang, C.; Bonnefille, E.; Gutmann, T.; Puente, C.; Berthet, J.-C.; Dugave, C.; Chaudret, B.; Rousseau, B. *Regioselective and Stereospecific Deuteration of Bioactive Aza Compounds by the Use of Ruthenium Nanoparticles*. *Angew. Chem., Int. Ed.* **2014**, *53*, 230-234.
- (130) Taglang, C.; Martinez-Prieto, L. M.; del Rosal, I.; Maron, L.; Poteau, R.; Philippot, K.; Chaudret, B.; Perato, S.; Sam Lone, A.; Puente, C., et al. *Enantiospecific C-H activation using ruthenium nanocatalysts*. *Angew. Chem., Int. Ed.* **2015**, *54*, 10474-10477.
- (131) Bresó-Femenia, E.; Godard, C.; Claver, C.; Chaudret, B.; Castellón, S. *Selective catalytic deuteration of phosphorus ligands using ruthenium nanoparticles: a new approach to gain information on ligand coordination*. *Chem. Commun.* **2015**, *51*, 16342-16345.
- (132) Garbaskas, M. F.; Kasper, J. S.; Lewis, L. N. *The synthesis and structure of bis{2-[(diphenoxyphosphino)oxy]phenyl-C,P}bis(triphenylphosphite-P)ruthenium, [cyclic] [(C<sub>6</sub>H<sub>5</sub>O)<sub>2</sub>POC<sub>6</sub>H<sub>4</sub>]<sub>2</sub>Ru[P(OC<sub>6</sub>H<sub>5</sub>)<sub>3</sub>]<sub>2</sub>*. *J. Organomet. Chem.* **1984**, *276*, 241-248.
- (133) Bhatia, S.; Spahlinger, G.; Boukhumseen, N.; Boll, Q.; Li, Z.; Jackson, J. E. *Stereoretentive H/D Exchange via an Electroactivated Heterogeneous Catalyst at sp<sup>3</sup> C-H Sites Bearing Amines or Alcohols*. *Eur. J. Org. Chem.* **2016**, *2016*, 4230-4235.
- (134) Martínez-Prieto, L. M.; Baquero, E. A.; Pieters, G.; Flores, J. C.; de Jesús, E.; Nayral, C.; Delpech, F.; van Leeuwen, P. W. N. M.; Lippens, G.; Chaudret, B. *Monitoring of nanoparticle reactivity in solution: interaction of l-lysine and Ru nanoparticles probed by chemical shift perturbation parallels regioselective H/D exchange*. *Chem. Comm.* **2017**, *53*, 5850-5853.
- (135) Rothermel, N.; Bouzouita, D.; Roether, T.; de Rosal, I.; Tricard, S.; Poteau, R.; Gutmann, T.; Chaudret, B.; Limbach, H.-H.; Buntkowsky, G. *Surprising Differences of Alkane C-H Activation Catalyzed by Ruthenium Nanoparticles: Complex Surface-Substrate Recognition?* *ChemCatChem* **2018**, *10*, 4243-4247.
- (136) Palazzolo, A.; Feuillastre, S.; Pfeifer, V.; Garcia-Argote, S.; Bouzouita, D.; Tricard, S.; Chollet, C.; Marcon, E.; Buisson, D.-A.; Cholet, S., et al. *Efficient Access to Deuterated and Tritiated Nucleobase Pharmaceuticals and Oligonucleotides using Hydrogen-Isotope Exchange*. *Angew. Chem., Int. Ed.* **2019**, *58*, 4891-4895.
- (137) Fang, P.-P.; Jutand, A.; Tian, Z.-Q.; Amatore, C. *Au-Pd Core-Shell Nanoparticles Catalyze Suzuki-Miyaura Reactions in Water through Pd Leaching*. *Angew. Chem., Int. Ed.* **2011**, *50*, 12184-12188, S12184/12181-S12184/12185.
- (138) Reetz, M. T.; de Vries, J. G. *Ligand-free Heck reactions using low Pd-loading*. *Chem. Commun.* **2004**, 1559-1563.
- (139) Lohr, T. L.; Piers, W. E.; Parvez, M. *Arene C-H bond activation across Pt(II)-OH bonds: catalyzed vs. uncatalyzed pathways*. *Chem. Sci.* **2013**, *4*, 770-775.
- (140) Djakovitch, L.; Felpin, F.-X. *Direct C sp<sup>2</sup>-H and C sp<sup>3</sup>-H arylation enabled by heterogeneous palladium catalysts*. *ChemCatChem* **2014**, *6*, 2175-2187.
- (141) Deprez, N. R.; Sanford, M. S. *Synthetic and Mechanistic Studies of Pd-Catalyzed C-H Arylation with Diaryliodonium Salts: Evidence for a Bimetallic High Oxidation State Pd Intermediate*. *J. Am. Chem. Soc.* **2009**, *131*, 11234-11241.
- (142) Kalyani, D.; Deprez, N. R.; Desai, L. V.; Sanford, M. S. *Oxidative C-H Activation/C-C Bond Forming Reactions: Synthetic Scope and Mechanistic Insights*. *J. Am. Chem. Soc.* **2005**, *127*, 7330-7331.
- (143) Neal, L. M.; Hagelin-Weaver, H. E. *C-H Activation and C-C coupling of 4-methylpyridine using palladium supported on nanoparticle alumina*. *J. Mol. Catal. A: Chem.* **2008**, *284*, 141-148.

- (144) Tang, D.-T. D.; Collins, K. D.; Ernst, J. B.; Glorius, F. *Pd/C as a Catalyst for Completely Regioselective C-H Functionalization of Thiophenes under Mild Conditions*. *Angew. Chem., Int. Ed.* **2014**, *53*, 1809-1813.
- (145) Tang, D.-T. D.; Collins, K. D.; Glorius, F. *Completely Regioselective Direct C-H Functionalization of Benzo[b]thiophenes Using a Simple Heterogeneous Catalyst*. *J. Am. Chem. Soc.* **2013**, *135*, 7450-7453.
- (146) Sehnal, P.; Taylor, R. J. K.; Fairlamb, I. J. S. *Emergence of palladium(IV) chemistry in synthesis and catalysis*. *Chem. Rev.* **2010**, *110*, 824-889.
- (147) Engle, K. M.; Wang, D.-H.; Yu, J.-Q. *Ligand-Accelerated C-H Activation Reactions: Evidence for a Switch of Mechanism*. *J. Am. Chem. Soc.* **2010**, *132*, 14137-14151.
- (148) Boronat, M.; Laursen, S.; Leyva-Perez, A.; Oliver-Meseguer, J.; Combata, D.; Corma, A. *Partially oxidized gold nanoparticles: A catalytic base-free system for the aerobic homocoupling of alkynes*. *J. Catal.* **2014**, *315*, 6-14.
- (149) Lane, B. S.; Brown, M. A.; Sames, D. *Direct Palladium-Catalyzed C-2 and C-3 Arylation of Indoles: A Mechanistic Rationale for Regioselectivity*. *J. Am. Chem. Soc.* **2005**, *127*, 8050-8057.
- (150) Garcia-Cuadrado, D.; de Mendoza, P.; Braga, A. A. C.; Maseras, F.; Echavarren, A. M. *Proton-Abstraction Mechanism in the Palladium-Catalyzed Intramolecular Arylation: Substituent Effects*. *J. Am. Chem. Soc.* **2007**, *129*, 6880-6886.
- (151) Zinovyeva, V. A.; Vorotyntsev, M. A.; Bezverkhyy, I.; Chaumont, D.; Hierso, J.-C. *Highly Dispersed Palladium-Polypyrrole Nanocomposites: In-Water Synthesis and Application for Catalytic Arylation of Heteroaromatics by Direct C-H Bond Activation*. *Adv. Funct. Mater.* **2011**, *21*, 1064-1075.
- (152) Ehlers, P.; Petrosyan, A.; Baumgard, J.; Jopp, S.; Steinfeld, N.; Ghochikyan, T. V.; Saghyan, A. S.; Fischer, C.; Langer, P. *Synthesis of 2,5-Diarylpyrroles by Ligand-Free Palladium-Catalyzed CH Activation of Pyrroles in Ionic Liquids*. *ChemCatChem* **2013**, *5*, 2504-2511.
- (153) Gniewek, A.; Trzeciak, A. M.; Ziolkowski, J. J.; Kepinski, L.; Wrzyszczyk, J.; Tylus, W. *Pd-PVP colloid as catalyst for Heck and carbonylation reactions: TEM and XPS studies*. *J. Catal.* **2005**, *229*, 332-343.
- (154) Yang, F.; Feng, A.; Wang, C.; Dong, S.; Chi, C.; Jia, X.; Zhang, L.; Li, Y. *Graphene oxide/carbon nanotubes-Fe<sub>3</sub>O<sub>4</sub> supported Pd nanoparticles for hydrogenation of nitroarenes and C-H activation*. *RSC Adv.* **2016**, *6*, 16911-16916.
- (155) Williams, T. J.; Reay, A. J.; Whitwood, A. C.; Fairlamb, I. J. S. *A mild and selective Pd-mediated methodology for the synthesis of highly fluorescent 2-arylated tryptophans and tryptophan-containing peptides: a catalytic role for Pd<sup>0</sup> nanoparticles?* *Chem. Commun.* **2014**, *50*, 3052-3054.
- (156) Williams, T. J.; Fairlamb, I. J. S. *A key role for iodobenzene in the direct C-H bond functionalization of benzoxazoles using PhI(OAc)<sub>2</sub> mediated by a Pd(OAc)<sub>2</sub>/1,10-phenanthroline catalyst system: in situ formation of well-defined Pd nanoparticles*. *Tetrahedron Lett.* **2013**, *54*, 2906-2908.
- (157) Baumann, C. G.; De Ornellas, S.; Reeds, J. P.; Storr, T. E.; Williams, T. J.; Fairlamb, I. J. S. *Formation and propagation of well-defined Pd nanoparticles (PdNPs) during C-H bond functionalization of heteroarenes: are nanoparticles a moribund form of Pd or an active catalytic species?* *Tetrahedron* **2014**, *70*, 6174-6187.
- (158) Férey, G.; Mellot-Draznieks, C.; Serre, C.; Millange, F.; Dutour, J.; Surblé, S.; Margiolaki, I. *A Chromium Terephthalate-Based Solid with Unusually Large Pore Volumes and Surface Area*. *Science* **2005**, *309*, 2040-2042.
- (159) Huang, Y.; Lin, Z.; Cao, R. *Palladium Nanoparticles Encapsulated in Metal-Organic Framework as Efficient Heterogeneous Catalysts for Direct C2 Arylation of Indoles*. *Chem. - Eur. J.* **2011**, *17*, 12706-12712.
- (160) Wang, L.; Yi, W.-b.; Cai, C. *Fluorous silica gel-supported perfluoro-tagged palladium nanoparticles: an efficient and reusable catalyst for direct C-2 arylation of indoles*. *Chemical Communications* **2011**, *47*, 806-808.

- (161) Huang, Y.; Ma, T.; Huang, P.; Wu, D.; Lin, Z.; Cao, R. *Direct C-H Bond Arylation of Indoles with Aryl Boronic Acids Catalyzed by Palladium Nanoparticles Encapsulated in Mesoporous Metal-Organic Framework*. *ChemCatChem* **2013**, *5*, 1877-1883.
- (162) Malmgren, J.; Nagendiran, A.; Tai, C.-W.; Baeckvall, J.-E.; Olofsson, B. *C-2 Selective Arylation of Indoles with Heterogeneous Nanopalladium and Diaryliodonium Salts*. *Chem. - Eur. J.* **2014**, *20*, 13531-13535.
- (163) Duan, L.; Fu, R.; Zhang, B.; Shi, W.; Chen, S.; Wan, Y. *An Efficient Reusable Mesoporous Solid-Based Pd Catalyst for Selective C2 Arylation of Indoles in Water*. *ACS Catal.* **2016**, *6*, 1062-1074.
- (164) Mondloch, J. E.; Bury, W.; Fairen-Jimenez, D.; Kwon, S.; DeMarco, E. J.; Weston, M. H.; Sarjeant, A. A.; Nguyen, S. T.; Stair, P. C.; Snurr, R. Q., et al. *Vapor-Phase Metalation by Atomic Layer Deposition in a Metal-Organic Framework*. *J. Am. Chem. Soc.* **2013**, *135*, 10294-10297.
- (165) Huang, Y.-B.; Shen, M.; Wang, X.; Huang, P.; Chen, R.; Lin, Z.-J.; Cao, R. *Water-medium C-H activation over a hydrophobic perfluoroalkane-decorated metal-organic framework platform*. *J. Catal.* **2016**, *333*, 1-7.
- (166) Deraedt, C.; Ye, R.; Ralston, W. T.; Toste, F. D.; Somorjai, G. A. *Dendrimer-Stabilized Metal Nanoparticles as Efficient Catalysts for Reversible Dehydrogenation/Hydrogenation of N-Heterocycles*. *J. Am. Chem. Soc.* **2017**, *139*, 18084-18092.
- (167) Korwar, S.; Burkholder, M.; Gilliland, S. E.; Brinkley, K.; Gupton, B. F.; Ellis, K. C. *Chelation-directed C-H activation/C-C bond forming reactions catalyzed by Pd(II) nanoparticles supported on multiwalled carbon nanotubes*. *Chem. Commun.* **2017**, *53*, 7022-7025.
- (168) Tyagi, A.; Matsumoto, T.; Kato, T.; Yoshida, H. *Direct C-H bond activation of ethers and successive C-C bond formation with benzene by a bifunctional palladium-titania photocatalyst*. *Catal. Sci. Technol.* **2016**, *6*, 4577-4583.
- (169) Hartwig, J. F. *Organotransition Metal Chemistry: From Bonding to Catalysis*; University Science Books: Sausalito, California, 2010.
- (170) Zhang, Y.; Cui, X.; Shi, F.; Deng, Y. *Nano-Gold Catalysis in Fine Chemical Synthesis*. *Chem. Rev.* **2012**, *112*, 2467-2505.
- (171) Stratakis, M.; Garcia, H. *Catalysis by Supported Gold Nanoparticles: Beyond Aerobic Oxidative Processes*. *Chem. Rev.* **2012**, *112*, 4469-4506.
- (172) Zhang, X.; Corma, A. *Supported gold(III) catalysts for highly efficient three-component coupling reactions*. *Angew. Chem., Int. Ed.* **2008**, *47*, 4358-4361.
- (173) Efe, C.; Lykakis, I. N.; Stratakis, M. *Gold nanoparticles supported on TiO<sub>2</sub> catalyze the cycloisomerization/oxidative dimerization of aryl propargyl ethers*. *Chem. Commun.* **2011**, *47*, 803-805.
- (174) Leyva-Perez, A.; Oliver-Meseguer, J.; Cabrero-Antonino, J. R.; Rubio-Marques, P.; Serna, P.; Al-Resayes, S. I.; Corma, A. *Reactivity of Electron-Deficient Alkynes on Gold Nanoparticles*. *ACS Catal.* **2013**, *3*, 1865-1873.
- (175) Boronat, M.; Corma, A. *Molecular approaches to catalysis*. *J. Catal.* **2011**, *284*, 138-147.
- (176) Zhang, S.; Chandra, K. L.; Gorman, C. B. *Self-Assembled Monolayers of Terminal Alkynes on Gold*. *J. Am. Chem. Soc.* **2007**, *129*, 4876-4877.
- (177) Ribeiro, A. P. d. C.; Martins, L. M. D. R. d. S.; Carabineiro, S. A. C.; Figueiredo, J. L.; Pombeiro, A. J. L. *Gold nanoparticles deposited on surface modified carbon xerogels as reusable catalysts for cyclohexane C-H activation in the presence of CO and water*. *Molecules* **2017**, *22*, 603/601-603/612.
- (178) Nilsson, B. M.; Vargas, H. M.; Ringdahl, B.; Hacksell, U. *Phenyl-substituted analogs of oxotremorine as muscarinic antagonists*. *J. Med. Chem.* **1992**, *35*, 285-294.
- (179) Kidwai, M.; Bansal, V.; Kumar, A.; Mozumdar, S. *The first Au-nanoparticles catalyzed green synthesis of propargylamines via a three-component coupling reaction of aldehyde, alkyne and amine*. *Green Chem.* **2007**, *9*, 742-745.

- (180) Datta, K. K. R.; Subba Reddy, B. V.; Ariga, K.; Vinu, A. *Gold Nanoparticles Embedded in a Mesoporous Carbon Nitride Stabilizer for Highly Efficient Three-Component Coupling Reaction*. *Angew. Chem., Int. Ed.* **2010**, *49*, 5961-5965.
- (181) Layek, K.; Chakravarti, R.; Lakshmi Kantam, M.; Maheswaran, H.; Vinu, A. *Nanocrystalline magnesium oxide stabilized gold nanoparticles: an advanced nanotechnology based recyclable heterogeneous catalyst platform for the one-pot synthesis of propargylamines*. *Green Chem.* **2011**, *13*, 2878-2887.
- (182) Gholinejad, M.; Hamed, F.; Najera, C. *Gold Nanoparticles Supported on Polyacrylamide Containing a Phosphorus Ligand as an Efficient Heterogeneous Catalyst for Three-Component Synthesis of Propargylamines in Water*. *Synlett* **2016**, *27*, 1193-1201.
- (183) Aguilar, D.; Contel, M.; Urriolabeitia, E. P. *Mechanistic Insights into the One-Pot Synthesis of Propargylamines from Terminal Alkynes and Amines in Chlorinated Solvents Catalyzed by Gold Compounds and Nanoparticles*. *Chem. - Eur. J.* **2010**, *16*, 9287-9296.
- (184) Kidwai, M.; Bansal, V.; Mishra, N. K.; Kumar, A.; Mozumdar, S. *Copper-nanoparticle-catalyzed A3 coupling via C-H activation*. *Synlett* **2007**, 1581-1584.
- (185) Sharghi, H.; Shiri, P.; Aberi, M. *A solvent-free and one-pot strategy for eco-compatible synthesis of substituted benzofurans from various salicylaldehydes, secondary amines, and nonactivated alkynes catalyzed by copper(I) oxide nanoparticles*. *Synthesis* **2014**, *46*, 2489-2498.
- (186) Kotadia, D. A.; Soni, S. S. *Stable mesoporous Fe/TiO<sub>2</sub> nanoparticles: A recoverable catalyst for solvent-free synthesis of propargyl amine via C-H activation*. *Appl. Catal., A* **2014**, *488*, 231-238.
- (187) Kaur, S.; Kumar, M.; Bhalla, V. *Aggregates of perylene bisimide stabilized superparamagnetic Fe<sub>3</sub>O<sub>4</sub> nanoparticles: an efficient catalyst for the preparation of propargylamines and quinolines via C-H activation*. *Chem. Commun.* **2015**, *51*, 16327-16330.
- (188) Sasikala, R.; Rani, S. K.; Easwaramoorthy, D.; Karthikeyan, K. *Lanthanum loaded CuO nanoparticles: synthesis and characterization of a recyclable catalyst for the synthesis of 1,4-disubstituted 1,2,3-triazoles and propargylamines*. *RSC Adv.* **2015**, *5*, 56507-56517.
- (189) Gulati, U.; Rajesh, U. C.; Rawat, D. S. *CuO/Fe<sub>2</sub>O<sub>3</sub> NPs: robust and magnetically recoverable nanocatalyst for decarboxylative A<sub>3</sub> and KA<sub>2</sub> coupling reactions under neat conditions*. *Tetrahedron Lett.* **2016**, *57*, 4468-4472.
- (190) Gupta, S.; Joshi, H.; Jain, N.; Singh, A. K. *Cu<sub>6</sub>Se<sub>4.5</sub> Nanoparticles from a single source precursor: Recyclable and efficient catalyst for cross-dehydrogenative coupling of tertiary amines with terminal alkynes*. *J. Mol. Catal. A: Chem.* **2016**, *423*, 135-142.
- (191) Nguyen, A. T.; Pham, L. T.; Phan, N. T. S.; Truong, T. *Efficient and robust superparamagnetic copper ferrite nanoparticle-catalyzed sequential methylation and C-H activation: aldehyde-free propargylamine synthesis*. *Catal. Sci. Technol.* **2014**, *4*, 4281-4288.
- (192) Rahman, M.; Bagdi, A. K.; Majee, A.; Hajra, A. *Nano indium oxide catalyzed efficient synthesis of propargylamines via C-H and C-Cl bond activations*. *Tetrahedron Lett.* **2011**, *52*, 4437-4439.
- (193) Honraedt, A.; Le Callonnec, F.; Le Grogneec, E.; Fernandez, V.; Felpin, F.-X. *C-H Arylation of Benzoquinone in Water through Aniline Activation: Synergistic Effect of Graphite-Supported Copper Oxide Nanoparticles*. *J. Org. Chem.* **2013**, *78*, 4604-4609.
- (194) Priyadarshini, S.; Joseph, P. J. A.; Kantam, M. L. *Copper catalyzed cross-coupling reactions of carboxylic acids: an expedient route to amides, 5-substituted  $\gamma$ -lactams and  $\alpha$ -acyloxy esters*. *RSC Adv.* **2013**, *3*, 18283-18287.
- (195) Yang, H.; Yan, H.; Sun, P.; Zhu, Y.; Lu, L.; Liu, D.; Rong, G.; Mao, J. *Iron-catalyzed direct alkenylation of sp<sup>3</sup>(C-H) bonds via decarboxylation of cinnamic acids under ligand-free conditions*. *Green Chemistry* **2013**, *15*, 976-981.
- (196) Kaur, S.; Kumar, M.; Bhalla, V. *Supramolecular ensemble of PBI derivative and copper nanoparticles: a light harvesting antenna for photocatalytic C(sp<sup>2</sup>)-H functionalization*. *Green Chem.* **2016**, *18*, 5870-5883.
- (197) Chopra, R.; Kumar, M.; Bhalla, V. *Development of a supramolecular ensemble of an AIEE active hexaphenylbenzene derivative and Ag@Cu<sub>2</sub>O core-shell NPs: an efficient photocatalytic system for C-H activation*. *Chem. Commun.* **2016**, *52*, 10179-10182.

- (198) Schwarz, H. *Chemistry with Methane: Concepts Rather than Recipes*. *Angew. Chem., Int. Ed.* **2011**, *50*, 10096-10115.
- (199) Latimer, A. A.; Kulkarni, A. R.; Aljama, H.; Montoya, J. H.; Yoo, J. S.; Tsai, C.; Abild-Pedersen, F.; Studt, F.; Noerskov, J. K. *Understanding trends in C-H bond activation in heterogeneous catalysis*. *Nat. Mater.* **2017**, *16*, 225-229.
- (200) Vines, F.; Lykhach, Y.; Staudt, T.; Lorenz, M. P. A.; Papp, C.; Steinrueck, H.-P.; Libuda, J.; Neyman, K. M.; Goerling, A. *Methane Activation by Platinum: Critical Role of Edge and Corner Sites of Metal Nanoparticles*. *Chem. - Eur. J.* **2010**, *16*, 6530-6539.
- (201) Wang, H.; Blaylock, D. W.; Dam, A. H.; Liland, S. E.; Rout, K. R.; Zhu, Y.-A.; Green, W. H.; Holmen, A.; Chen, D. *Steam methane reforming on a Ni-based bimetallic catalyst: density functional theory and experimental studies of the catalytic consequence of surface alloying of Ni with Ag*. *Catal. Sci. Technol.* **2017**, *7*, 1713-1725.
- (202) Zhao, Y.; Liu, B.; Amin, R. *CO<sub>2</sub> Reforming of CH<sub>4</sub> over MgO-Doped Ni/MAS-24 with Microporous ZSM-5 Structure*. *Ind. Eng. Chem. Res.* **2016**, *55*, 6931-6942.
- (203) Liu, Z.; Grinter, D. C.; Lustemberg, P. G.; Nguyen-Phan, T.-D.; Zhou, Y.; Luo, S.; Waluyo, I.; Crumlin, E. J.; Stacchiola, D. J.; Zhou, J., et al. *Dry Reforming of Methane on a Highly-Active Ni-CeO<sub>2</sub> Catalyst: Effects of Metal-Support Interactions on C-H Bond Breaking*. *Angew. Chem., Int. Ed.* **2016**, *55*, 7455-7459.
- (204) Takami, D.; Ito, Y.; Kawaharasaki, S.; Yamamoto, A.; Yoshida, H. *Low temperature dry reforming of methane over plasmonic Ni photocatalysts under visible light irradiation*. *Sustainable Energy Fuels* **2019**, Ahead of Print.
- (205) Lingampalli, S. R.; Gupta, U.; Gautam, U. K.; Rao, C. N. R. *Oxidation of Toluene and Other Examples of C-H Bond Activation by CdO<sub>2</sub> and ZnO<sub>2</sub> Nanoparticles*. *ChemPlusChem* **2013**, *78*, 837-842.
- (206) Tyo, E. C.; Yin, C.; Di Vece, M.; Qian, Q.; Kwon, G.; Lee, S.; Lee, B.; DeBartolo, J. E.; Seifert, S.; Winans, R. E., et al. *Oxidative Dehydrogenation of Cyclohexane on Cobalt Oxide (Co<sub>3</sub>O<sub>4</sub>) Nanoparticles: The Effect of Particle Size on Activity and Selectivity*. *ACS Catal.* **2012**, *2*, 2409-2423.
- (207) Sobota, M.; Nikiforidis, I.; Amende, M.; Zanon, B. S.; Staudt, T.; Hoefert, O.; Lykhach, Y.; Papp, C.; Hieringer, W.; Laurin, M., et al. *Dehydrogenation of Dodecahydro-N-ethylcarbazole on Pd/Al<sub>2</sub>O<sub>3</sub> Model Catalysts*. *Chem. - Eur. J.* **2011**, *17*, 11542-11552.
- (208) An, K.; Alayoglu, S.; Musselwhite, N.; Na, K.; Somorjai, G. A. *Designed catalysts from Pt nanoparticles supported on macroporous oxides for selective isomerization of n-hexane*. *J. Am. Chem. Soc.* **2014**, *136*, 6830-6833.
- (209) Dimitratos, N.; Lopez-Sanchez, J. A.; Hutchings, G. J. *Selective liquid phase oxidation with supported metal nanoparticles*. *Chem. Sci.* **2012**, *3*, 20-44.
- (210) Kesavan, L.; Tiruvalam, R.; Ab Rahim, M. H.; bin Saiman, M. I.; Enache, D. I.; Jenkins, R. L.; Dimitratos, N.; Lopez-Sanchez, J. A.; Taylor, S. H.; Knight, D. W., et al. *Solvent-Free Oxidation of Primary Carbon-Hydrogen Bonds in Toluene Using Au-Pd Alloy Nanoparticles*. *Science* **2011**, *331*, 195-199.
- (211) bin Saiman, M. I.; Brett, G. L.; Tiruvalam, R.; Forde, M. M.; Sharples, K.; Thetford, A.; Jenkins, R. L.; Dimitratos, N.; Lopez-Sanchez, J. A.; Murphy, D. M., et al. *Involvement of Surface-Bound Radicals in the Oxidation of Toluene Using Supported Au-Pd Nanoparticles*. *Angew. Chem., Int. Ed.* **2012**, *51*, 5981-5985.
- (212) Mendez, V.; Guillois, K.; Daniele, S.; Tuel, A.; Caps, V. *Aerobic methylcyclohexane-promoted epoxidation of stilbene over gold nanoparticles supported on Gd-doped titania*. *Dalton Trans.* **2010**, *39*, 8457-8463.
- (213) Liu, Y.; Tsunoyama, H.; Akita, T.; Xie, S.; Tsukuda, T. *Aerobic oxidation of cyclohexane catalyzed by size-controlled Au clusters on hydroxyapatite: size effect in the sub-2 nm regime*. *ACS Catal.* **2011**, *1*, 2-6.
- (214) Donoeva, B. G.; Ovoshchnikov, D. S.; Golovko, V. B. *Establishing a Au Nanoparticle Size Effect in the Oxidation of Cyclohexene Using Gradually Changing Au Catalysts*. *ACS Catal.* **2013**, *3*, 2986-2991.



- (215) Majumdar, B.; Bhattacharya, T.; Sarma, T. K. *Gold Nanoparticle-Polydopamine-Reduced Graphene Oxide Ternary Nanocomposite as an Efficient Catalyst for Selective Oxidation of Benzylic C(sp<sup>3</sup>)-H Bonds Under Mild Conditions*. *ChemCatChem* **2016**, *8*, 1825-1835.
- (216) Liu, R.; Huang, H.; Li, H.; Liu, Y.; Zhong, J.; Li, Y.; Zhang, S.; Kang, Z. *Metal Nanoparticle/Carbon Quantum Dot Composite as a Photocatalyst for High-Efficiency Cyclohexane Oxidation*. *ACS Catal.* **2014**, *4*, 328-336.
- (217) Verma, S.; Nasir Baig, R. B.; Nadagouda, M. N.; Varma, R. S. *Photocatalytic C-H activation and oxidative esterification using Pd@g-C<sub>3</sub>N<sub>4</sub>*. *Catal. Today* **2017**, *309*, 248-252.
- (218) Sun, H.; Zhang, Y.; Guo, F.; Zha, Z.; Wang, Z. *Regioselective Oxyalkylation of Vinylarenes Catalyzed by Diatomite-Supported Manganese Oxide Nanoparticles*. *J. Org. Chem.* **2012**, *77*, 3563-3569.
- (219) Payra, S.; Saha, A.; Guchhait, S.; Banerjee, S. *Direct CuO nanoparticle-catalyzed synthesis of poly-substituted furans via oxidative C-H/C-H functionalization in aqueous medium*. *RSC Adv.* **2016**, *6*, 33462-33467.
- (220) Adams, R. D.; Chen, M.; Elpitiya, G.; Potter, M. E.; Raja, R. *Iridium-Bismuth Cluster Complexes Yield Bimetallic Nano-Catalysts for the Direct Oxidation of 3-Picoline to Niacin*. *ACS Catal.* **2013**, *3*, 3106-3110.
- (221) Liu, H.; Chen, G.; Jiang, H.; Li, Y.; Luque, R. *From alkyl aromatics to aromatic esters: efficient and selective C-H activation promoted by a bimetallic heterogeneous catalyst*. *ChemSusChem* **2012**, *5*, 1892-1896.
- (222) Verma, S.; Nasir Baig, R. B.; Nadagouda, M. N.; Varma, R. S. *Hydroxylation of Benzene via C-H Activation Using Bimetallic CuAg@g-C<sub>3</sub>N<sub>4</sub>*. *ACS Sustainable Chem. Eng.* **2017**, *5*, 3637-3640.
- (223) Takagi, K.; Al-Amin, M.; Hoshiya, N.; Wouters, J.; Sugimoto, H.; Shiro, Y.; Fukuda, H.; Shuto, S.; Arisawa, M. *Palladium-Nanoparticle-Catalyzed 1,7-Palladium Migration Involving C-H Activation, Followed by Intramolecular Amination: Regioselective Synthesis of N1-Arylbenzotriazoles and an Evaluation of Their Inhibitory Activity toward Indoleamine 2,3-Dioxygenase*. *J. Org. Chem.* **2014**, *79*, 6366-6371.
- (224) Zhou, J.; He, J.; Wang, B.; Yang, W.; Ren, H. *1,7-palladium migration via C-H activation, followed by intramolecular amination: regioselective synthesis of benzotriazoles*. *J. Am. Chem. Soc.* **2011**, *133*, 6868-6870.
- (225) Acharyya, S. S.; Ghosh, S.; Bal, R. *Direct catalytic oxyamination of benzene to aniline over Cu(II) nanoclusters supported on CuCr<sub>2</sub>O<sub>4</sub> spinel nanoparticles via simultaneous activation of C-H and N-H bonds*. *Chem. Commun.* **2014**, *50*, 13311-13314.
- (226) Priyadarshini, S.; Amal Joseph, P. J.; Lakshmi Kantam, M. *Copper catalyzed oxidative cross-coupling of aromatic amines with 2-pyrrolidinone: a facile synthesis of N-aryl-γ-amino-γ-lactams*. *Tetrahedron* **2014**, *70*, 6068-6074.
- (227) Rosario, A. R.; Casola, K. K.; Oliveira, C. E. S.; Zeni, G. *Copper Oxide Nanoparticle-Catalyzed Chalcogenation of the Carbon-Hydrogen Bond in Thiazoles: Synthesis of 2-(Organochalcogen)thiazoles*. *Adv. Synth. Catal.* **2013**, *355*, 2960-2966.
- (228) Mohan, B.; Hwang, S.; Woo, H.; Park, K. H. *Copper Nanoparticle Catalyzed Formation of C-S Bonds through Activation of S-S and C-H Bonds: An Easy Route to Alkynyl Sulfides*. *Synthesis* **2015**, *47*, 3741-3745.
- (229) Mohan, B.; Park, J. C.; Park, K. H. *Mechanochemical Synthesis of Active Magnetite Nanoparticles Supported on Charcoal for Facile Synthesis of Alkynyl Selenides by C-H Activation*. *ChemCatChem* **2016**, *8*, 2345-2350.
- (230) Korwar, S.; Brinkley, K.; Siamaki, A. R.; Gupton, B. F.; Ellis, K. C. *Selective N-Chelation-Directed C-H Activation Reactions Catalyzed by Pd(II) Nanoparticles Supported on Multiwalled Carbon Nanotubes*. *Org. Lett.* **2015**, *17*, 1782-1785.
- (231) Kim, K.; Jung, Y.; Lee, S.; Kim, M.; Shin, D.; Byun, H.; Cho, S. J.; Song, H.; Kim, H. *Directed C-H Activation and Tandem Cross-Coupling Reactions Using Palladium Nanocatalysts with Controlled Oxidation*. *Angew. Chem., Int. Ed.* **2017**, *56*, 6952-6956.

- (232) Kim, M.; Lee, S.; Kim, K.; Shin, D.; Kim, H.; Song, H. *A highly Lewis-acidic Pd(IV) surface on Pd@SiO<sub>2</sub> nanocatalysts for hydroalkoxylation reactions*. *Chem. Commun.* **2014**, 50, 14938-14941.
- (233) Pascanu, V.; Carson, F.; Solano, M. V.; Su, J.; Zou, X.; Johansson, M. J.; Martin-Matute, B. *Selective Heterogeneous C-H Activation/Halogenation Reactions Catalyzed by Pd@MOF Nanocomposites*. *Chem. - Eur. J.* **2016**, 22, 3729-3737.
- (234) Corey, J. Y.; Braddock-Wilking, J. *Reactions of Hydrosilanes with Transition-Metal Complexes: Formation of Stable Transition-Metal Silyl Compounds*. *Chem. Rev.* **1999**, 99, 175-292.
- (235) Corey, J. Y. *Reactions of Hydrosilanes with Transition Metal Complexes*. *Chem. Rev.* **2016**, 116, 11291-11435.
- (236) Corey, J. Y. *Reactions of hydrosilanes with transition metal complexes and characterization of the products*. *Chem. Rev.* **2011**, 111, 863-1071.
- (237) van Leeuwen, P. W. N. M. *Homogeneous Catalysis: Understanding the Art*; Springer, 2004.
- (238) Pelzer, K.; Candy, J. P.; Bergeret, G.; Basset, J. M. *Ru nanoparticles stabilized by organosilane fragments: Influence of the initial Si/Ru ratio and thermal stability*. *Eur. Phys. J. D* **2007**, 43, 197-200.
- (239) Pelzer, K.; Laleu, B.; Lefebvre, F.; Philippot, K.; Chaudret, B.; Candy, J. P.; Basset, J. M. *New Ru Nanoparticles Stabilized by Organosilane Fragments*. *Chem. Mater.* **2004**, 16, 4937-4941.
- (240) Pelzer, K.; Haevecker, M.; Boualleg, M.; Candy, J.-P.; Basset, J.-M. *Stabilization of 200-Atom Platinum Nanoparticles by Organosilane Fragments*. *Angew. Chem., Int. Ed.* **2011**, 50, 5170-5173.
- (241) Dobbs, A. P.; Chio, F. K. I.; *8.25 Hydrometallation Group 4 (Si, Sn, Ge, and Pb) A2 - Knochel, Paul in Comprehensive Organic Synthesis II (Second Edition)*; Elsevier: Amsterdam, 2014, p 964-998.
- (242) Marciniak, B.; Maciejewski, H.; Pietraszuk, C.; Pawluc, P. *Hydrosilylation. A Comprehensive Review on Recent Advances*; Springer: Berlin, 2009.
- (243) Jeon, M.; Han, J.; Park, J. *Catalytic Synthesis of Silanols from Hydrosilanes and Applications*. *ACS Catal.* **2012**, 2, 1539-1549.
- (244) Marciniak, B. *Catalysis by transition metal complexes of alkene silylation-recent progress and mechanistic implications*. *Coord. Chem. Rev.* **2005**, 249, 2374-2390.
- (245) Rooke, D. A.; Ferreira, E. M. *Platinum-catalyzed hydrosilylations of internal alkynes: harnessing substituent effects to achieve high regioselectivity*. *Angew. Chem., Int. Ed.* **2012**, 51, 3225-3230.
- (246) Silbestri, G. F.; Flores, J. C.; de Jesús, E. *Water-Soluble N-Heterocyclic Carbene Platinum(0) Complexes: Recyclable Catalysts for the Hydrosilylation of Alkynes in Water at Room Temperature*. *Organometallics* **2012**, 31, 3355-3360.
- (247) Ortega-Moreno, L.; Peloso, R.; Maya, C.; Suarez, A.; Carmona, E. *Platinum(0) olefin complexes of a bulky terphenylphosphine ligand. Synthetic, structural and reactivity studies*. *Chem. Commun.* **2015**, 51, 17008-17011.
- (248) Hitchcock, P. B.; Lappert, M. F.; Warhurst, N. J. W. *Synthesis and structure of a rac-tris(divinylsiloxane)diplatinum(0) complex and its reaction with maleic anhydride*. *Angew. Chem., Int. Ed.* **1991**, 30, 438-439.
- (249) Speier, J. L.; Webster, J. A.; Barnes, G. H. *The addition of silicon hydrides to olefinic double bonds. II. The use of Group VIII metal catalysts*. *J. Am. Chem. Soc.* **1957**, 79, 974-979.
- (250) Troegel, D.; Stohrer, J. *Recent advances and actual challenges in late transition metal catalyzed hydrosilylation of olefins from an industrial point of view*. *Coord. Chem. Rev.* **2011**, 255, 1440-1459.
- (251) Tondreau, A. M.; Atienza, C. C. H.; Weller, K. J.; Nye, S. A.; Lewis, K. M.; Delis, J. G. P.; Chirik, P. J. *Iron Catalysts for Selective Anti-Markovnikov Alkene Hydrosilylation Using Tertiary Silanes*. *Science* **2012**, 335, 567-570.
- (252) Sun, J.; Deng, L. *Cobalt Complex-Catalyzed Hydrosilylation of Alkenes and Alkynes*. *ACS Catal.* **2016**, 6, 290-300.

- (253) Buslov, I.; Becouse, J.; Mazza, S.; Montandon-Clerc, M.; Hu, X. *Chemoselective Alkene Hydrosilylation Catalyzed by Nickel Pincer Complexes*. *Angew. Chem., Int. Ed.* **2015**, *54*, 14523-14526.
- (254) Stein, J.; Lewis, L. N.; Gao, Y.; Scott, R. A. *In Situ Determination of the Active Catalyst in Hydrosilylation Reactions Using Highly Reactive Pt(0) Catalyst Precursors*. *J. Am. Chem. Soc.* **1999**, *121*, 3693-3703.
- (255) Galeandro-Diamant, T.; Zanota, M.-L.; Sayah, R.; Veyre, L.; Nikitine, C.; de Bellefon, C.; Marrot, S.; Meille, V.; Thieuleux, C. *Platinum nanoparticles in suspension are as efficient as Karstedt's complex for alkene hydrosilylation*. *Chem. Commun.* **2015**, *51*, 16194-16196.
- (256) Wagner, G. H. *Organosilicon compounds*, US2632013, 1953
- (257) Wagner, G. H. *Reactions of silanes with aliphatic unsaturated compounds*, US2637738, 1953
- (258) Chauhan, M.; Hauck, B. J.; Keller, L. P.; Boudjouk, P. *Hydrosilylation of alkynes catalyzed by platinum on carbon*. *J. Organomet. Chem.* **2002**, *645*, 1-13.
- (259) Jimenez, R.; Martinez-rosales, J. M.; Cervantes, J. *The activity of Pt/SiO<sub>2</sub> catalysts obtained by the sol-gel method in the hydrosilylation of 1-alkynes*. *Can. J. Chem.* **2003**, *81*, 1370-1375.
- (260) Alonso, F.; Buitrago, R.; Moglie, Y.; Ruiz-Martinez, J.; Sepulveda-Escribano, A.; Yus, M. *Hydrosilylation of alkynes catalysed by platinum on titania*. *J. Organomet. Chem.* **2010**, *696*, 368-372.
- (261) Cano, R.; Yus, M.; Ramon, D. J. *Impregnated Platinum on Magnetite as an Efficient, Fast, and Recyclable Catalyst for the Hydrosilylation of Alkynes*. *ACS Catal.* **2012**, *2*, 1070-1078.
- (262) Sabourault, N.; Mignani, G.; Wagner, A.; Mioskowski, C. *Platinum Oxide (PtO<sub>2</sub>): A Potent Hydrosilylation Catalyst*. *Org. Lett.* **2002**, *4*, 2117-2119.
- (263) Hamze, A.; Provot, O.; Brion, J.-D.; Alami, M. *Regiochemical aspects of the platinum oxide catalyzed hydrosilylation of alkynes*. *Synthesis* **2007**, 2025-2036.
- (264) Putzien, S.; Louis, E.; Nuyken, O.; Kuehn, F. E. *PtO<sub>2</sub> as a "self-dosing" hydrosilylation catalyst*. *Catal. Sci. Technol.* **2012**, *2*, 725-729.
- (265) Lewis, L. N. *On the mechanism of metal colloid catalyzed hydrosilylation: proposed explanations for electronic effects and oxygen cocatalysis*. *J. Am. Chem. Soc.* **1990**, *112*, 5998-6004.
- (266) Lewis, L. N.; Uriarte, R. J. *Hydrosilylation catalyzed by metal colloids: a relative activity study*. *Organometallics* **1990**, *9*, 621-625.
- (267) Lewis, L. N. *Chemical catalysis by colloids and clusters*. *Chem. Rev.* **1993**, *93*, 2693-2730.
- (268) Finney, E. E.; Finke, R. G. *Is it homogeneous Pt(II) or heterogeneous Pt(0)<sub>n</sub> catalysis? Evidence that Pt(1,5-COD)Cl<sub>2</sub> and Pt(1,5-COD)(CH<sub>3</sub>)<sub>2</sub> plus H<sub>2</sub> form heterogeneous, nanocluster plus bulk-metal Pt(0) hydrogenation catalysts*. *Inorg. Chim. Acta* **2006**, *359*, 2879-2887.
- (269) Brook, M. A.; Ketelson, H. A.; LaRonde, F. J.; Pelton, R. *Pt<sub>0</sub> compounds bound in a silsesquioxane layer: active hydrosilylation catalysts protected by the gel*. *Inorg. Chim. Acta* **1997**, *264*, 125-135.
- (270) Chauhan, B. P. S.; Rathore, J. S. *Regioselective synthesis of multifunctional hybrid polysiloxanes achieved by Pt-nanocluster catalysis*. *J. Am. Chem. Soc.* **2005**, *127*, 5790-5791.
- (271) Chauhan, B. P. S.; Sarkar, A. *Functionalized vinylsilanes via highly efficient and recyclable Pt-nanoparticle catalyzed hydrosilylation of alkynes*. *Dalton Trans.* **2017**, *46*, 8709-8715.
- (272) Bai, Y.; Zhang, S.; Deng, Y.; Peng, J.; Li, J.; Hu, Y.; Li, X.; Lai, G. *Use of functionalized PEG with 4-aminobenzoic acid stabilized platinum nanoparticles as an efficient catalyst for the hydrosilylation of alkenes*. *J. Colloid Interface Sci.* **2013**, *394*, 428-433.
- (273) Ciriminna, R.; Pandarus, V.; Gingras, G.; Beland, F.; Pagliaro, M. *Closing the Organosilicon Synthetic Cycle: Efficient Heterogeneous Hydrosilylation of Alkenes over SiliaCat Pt(0)*. *ACS Sustainable Chem. Eng.* **2013**, *1*, 249-253.
- (274) Bandari, R.; Buchmeiser, M. R. *Polymeric monolith supported Pt-nanoparticles as ligand-free catalysts for olefin hydrosilylation under batch and continuous conditions*. *Catal. Sci. Technol.* **2012**, *2*, 220-226.

- (275) Solomonsz, W. A.; Rance, G. A.; Harris, B. J.; Khlobystov, A. N. *Competitive hydrosilylation in carbon nanoreactors: probing the effect of nanoscale confinement on selectivity*. *Nanoscale* **2013**, *5*, 12200-12205.
- (276) Galeandro-Diamant, T.; Sayah, R.; Zanota, M.-L.; Marrot, S.; Veyre, L.; Thieuleux, C.; Meille, V. *Pt nanoparticles immobilized in mesostructured silica: a non-leaching catalyst for 1-octene hydrosilylation*. *Chem. Commun.* **2017**, *53*, 2962-2965.
- (277) Ito, H.; Yajima, T.; Tateiwa, J.-i.; Hosomi, A. *First gold complex-catalyzed selective hydrosilylation of organic compounds*. *Chem. Commun.* **2000**, 981-982.
- (278) Caporusso, A. M.; Aronica, L. A.; Schiavi, E.; Martra, G.; Vitulli, G.; Salvadori, P. *Hydrosilylation of 1-hexyne promoted by acetone solvated gold atoms derived catalysts*. *J. Organomet. Chem.* **2005**, *690*, 1063-1066.
- (279) Aronica, L. A.; Schiavi, E.; Evangelisti, C.; Caporusso, A. M.; Salvadori, P.; Vitulli, G.; Bertinetti, L.; Martra, G. *Solvated gold atoms in the preparation of efficient supported catalysts: Correlation between morphological features and catalytic activity in the hydrosilylation of 1-hexyne*. *J. Catal.* **2009**, *266*, 250-257.
- (280) Corma, A.; Gonzalez-Arellano, C.; Iglesias, M.; Sanchez, F. *Gold nanoparticles and gold(III) complexes as general and selective hydrosilylation catalysts*. *Angew. Chem., Int. Ed.* **2007**, *46*, 7820-7822.
- (281) Shore, G.; Organ, M. G. *Gold-film-catalyzed hydrosilylation of alkynes by microwave-assisted, continuous-flow organic synthesis (MACOS)*. *Chem. - Eur. J.* **2008**, *14*, 9641-9646.
- (282) Ishikawa, Y.; Yamamoto, Y.; Asao, N. *Selective hydrosilylation of alkynes with a nanoporous gold catalyst*. *Catal. Sci. Technol.* **2013**, *3*, 2902-2905.
- (283) Psyllaki, A.; Lykakis, I. N.; Stratakis, M. *Reaction of hydrosilanes with alkynes catalyzed by gold nanoparticles supported on TiO<sub>2</sub>*. *Tetrahedron* **2012**, *68*, 8724-8731.
- (284) Kidonakis, M.; Stratakis, M. *Ligandless Regioselective Hydrosilylation of Allenes Catalyzed by Gold Nanoparticles*. *Org. Lett.* **2015**, *17*, 4538-4541.
- (285) Titilas, I.; Kidonakis, M.; Gryparis, C.; Stratakis, M. *Tandem Si-Si and Si-H Activation of 1,1,2,2-Tetramethyldisilane by Gold Nanoparticles in Its Reaction with Alkynes: Synthesis of Substituted 1,4-Disila-2,5-cyclohexadienes*. *Organometallics* **2015**, *34*, 1597-1600.
- (286) Tamura, M.; Fujihara, H. *Chiral Bisphosphine BINAP-Stabilized Gold and Palladium Nanoparticles with Small Size and Their Palladium Nanoparticle-Catalyzed Asymmetric Reaction*. *J. Am. Chem. Soc.* **2003**, *125*, 15742-15743.
- (287) Uozumi, Y.; Tsuji, H.; Hayashi, T. *Cyclization of o-Allylstyrene via Hydrosilylation: Mechanistic Aspects of Hydrosilylation of Styrenes Catalyzed by Palladium-Phosphine Complexes*. *J. Org. Chem.* **1998**, *63*, 6137-6140.
- (288) Keinan, E.; Greenspoon, N. *Highly chemoselective palladium-catalyzed conjugate reduction of  $\alpha,\beta$ -unsaturated carbonyl compounds with silicon hydrides and zinc chloride cocatalyst*. *J. Am. Chem. Soc.* **1986**, *108*, 7314-7325.
- (289) Sumida, Y.; Yorimitsu, H.; Oshima, K. *Palladium-Catalyzed Preparation of Silyl Enolates from  $\alpha,\beta$ -Unsaturated Ketones or Cyclopropyl Ketones with Hydrosilanes*. *J. Org. Chem.* **2009**, *74*, 7986-7989.
- (290) Benohoud, M.; Tuokko, S.; Pihko, P. M. *Stereoselective Hydrosilylation of Enals and Enones Catalysed by Palladium Nanoparticles*. *Chem. - Eur. J.* **2011**, *17*, 8404-8413.
- (291) Yamada, Y. M. A.; Yuyama, Y.; Sato, T.; Fujikawa, S.; Uozumi, Y. *A Palladium-Nanoparticle and Silicon-Nanowire-Array Hybrid: A Platform for Catalytic Heterogeneous Reactions*. *Angew. Chem., Int. Ed.* **2014**, *53*, 127-131.
- (292) Planellas, M.; Guo, W.; Alonso, F.; Yus, M.; Shafir, A.; Pleixats, R.; Parella, T. *Hydrosilylation of internal alkynes catalyzed by tris-imidazolium salt-stabilized palladium nanoparticles*. *Adv. Synth. Catal.* **2014**, *356*, 179-188.
- (293) Bal Reddy, C.; Shil, A. K.; Guha, N. R.; Sharma, D.; Das, P. *Solid supported palladium(0) nanoparticles: an efficient heterogeneous catalyst for regioselective hydrosilylation of alkynes and Suzuki coupling of  $\beta$ -arylvinyl iodides*. *Catal. Lett.* **2014**, *144*, 1530-1536.

- (294) Duan, Y.; Ji, G.; Zhang, S.; Chen, X.; Yang, Y. *Additive-Modulated Switchable Reaction Pathway in the Addition of Alkynes with Organosilanes Catalyzed by a Supported Pd Nanoparticles: Hydrosilylation versus Semihydrogenation*. *Catal. Sci. Technol.* **2017**, *8*, 1039-1050.
- (295) Amatore, C.; Jutand, A. *Anionic Pd(0) and Pd(II) Intermediates in Palladium-Catalyzed Heck and Cross-Coupling Reactions*. *Acc. Chem. Res.* **2000**, *33*, 314-321.
- (296) Rivera, G.; Elizalde, O.; Roa, G.; Montiel, I.; Bernes, S. *Fluorinated N-heterocyclic carbenes rhodium (I) complexes and their activity in hydrosilylation of propargylic alcohols*. *J. Organomet. Chem.* **2012**, *699*, 82-86.
- (297) Monney, A.; Albrecht, M. *A chelating tetrapeptide rhodium complex comprised of a histidylidene residue: biochemical tailoring of an NHC-Rh hydrosilylation catalyst*. *Chem. Commun.* **2012**, *48*, 10960-10962.
- (298) Solomonsz, W. A.; Rance, G. A.; Suyetin, M.; La Torre, A.; Bichoutskaia, E.; Khlobystov, A. N. *Controlling the Regioselectivity of the Hydrosilylation Reaction in Carbon Nanoreactors*. *Chem. - Eur. J.* **2012**, *18*, 13180-13187.
- (299) Guo, W.; Pleixats, R.; Shafir, A.; Parella, T. *Rhodium Nanoflowers Stabilized by a Nitrogen-Rich PEG-Tagged Substrate as Recyclable Catalyst for the Stereoselective Hydrosilylation of Internal Alkynes*. *Adv. Synth. Catal.* **2015**, *357*, 89-99.
- (300) Lipschutz, M. I.; Tilley, T. D. *Synthesis and reactivity of a conveniently prepared two-coordinate bis(amido) nickel(II) complex*. *Chem. Commun.* **2012**, *48*, 7146-7148.
- (301) Srinivas, V.; Nakajima, Y.; Ando, W.; Sato, K.; Shimada, S. *(Salicylaldiminato)Ni(II)-catalysts for hydrosilylation of olefins*. *Catal. Sci. Technol.* **2015**, *5*, 2081-2084.
- (302) Srinivas, V.; Nakajima, Y.; Ando, W.; Sato, K.; Shimada, S. *Bis(acetylacetonato)Ni(II)/NaBHEt<sub>3</sub>-catalyzed hydrosilylation of 1,3-dienes, alkenes and alkynes*. *J. Organomet. Chem.* **2016**, *809*, 57-62.
- (303) Buslov, I.; Song, F.; Hu, X. *An Easily Accessed Nickel Nanoparticle Catalyst for Alkene Hydrosilylation with Tertiary Silanes*. *Angew. Chem., Int. Ed.* **2016**, *55*, 12295-12299.
- (304) Galeandro-Diamant, T.; Suleimanov, I.; Veyre, L.; Bousquie, M.; Meille, V.; Thieuleux, C. *Alkene hydrosilylation with supported and unsupported Ni nanoparticles: strong influence of the Ni environment on activity and selectivity*. *Catal. Sci. Technol.* **2019**, *9*, 1555-1558.
- (305) Blandez, J. F.; Esteve-Adell, I.; Primo, A.; Alvaro, M.; Garcia, H. *Nickel nanoparticles supported on graphene as catalysts for aldehyde hydrosilylation*. *J. Mol. Catal. A: Chem.* **2016**, *412*, 13-19.
- (306) Blandez, J. F.; Primo, A.; Asiri, A. M.; Alvaro, M.; Garcia, H. *Copper Nanoparticles Supported on Doped Graphenes as Catalyst for the Dehydrogenative Coupling of Silanes and Alcohols*. *Angew. Chem., Int. Ed.* **2014**, *53*, 12581-12586.
- (307) Luo, X. L.; Crabtree, R. H. *Homogeneous catalysis of silane alcoholysis via nucleophilic attack by the alcohol on an Ir( $\eta$ -2-HSiR<sub>3</sub>) intermediate catalyzed by [IrH<sub>2</sub>S<sub>2</sub>(PPh<sub>3</sub>)<sub>2</sub>]SbF<sub>6</sub> (S = solvent)*. *J. Am. Chem. Soc.* **1989**, *111*, 2527-2535.
- (308) Thiot, C.; Schumtz, M.; Wagner, A.; Mioskowski, C. *A one-pot synthesis of (E)-disubstituted alkenes by a bimetallic [Rh-Pd]-catalyzed hydrosilylation/Hiyama cross-coupling sequence*. *Chem. - Eur. J.* **2007**, *13*, 8971-8978.
- (309) Chen, Q.; Tanaka, S.; Fujita, T.; Chen, L.; Minato, T.; Ishikawa, Y.; Chen, M.; Asao, N.; Yamamoto, Y.; Jin, T. *The synergistic effect of nanoporous AuPd alloy catalysts on highly chemoselective 1,4-hydrosilylation of conjugated cyclic enones*. *Chem. Commun.* **2014**, *50*, 3344-3346.
- (310) Miura, H.; Endo, K.; Ogawa, R.; Shishido, T. *Supported Palladium-Gold Alloy Catalysts for Efficient and Selective Hydrosilylation under Mild Conditions with Isolated Single Palladium Atoms in Alloy Nanoparticles as the Main Active Site*. *ACS Catal.* **2017**, *7*, 1543-1553.
- (311) Zhang, J.-w.; Lu, G.-p.; Cai, C. *Regio- and stereoselective hydrosilylation of alkynes catalyzed by SiO<sub>2</sub> supported Pd-Cu bimetallic nanoparticles*. *Green Chem.* **2017**, *19*, 2535-2540.
- (312) Murugavel, R.; Voigt, A.; Walawalkar, M. G.; Roesky, H. W. *Hetero- and Metallasiloxanes Derived from Silanediols, Disilanols, Silanetriols, and Trisilanols*. *Chem. Rev.* **1996**, *96*, 2205-2236.

- (313) Li, G.; Wang, L.; Ni, H.; Pittman, C. U., Jr. *Polyhedral oligomeric silsesquioxane (POSS) polymers and copolymers: A review. J. Inorg. Organomet. Polym.* **2002**, *11*, 123-154.
- (314) Denmark, S. E.; Regens, C. S. *Palladium-Catalyzed Cross-Coupling Reactions of Organosilanols and Their Salts: Practical Alternatives to Boron- and Tin-Based Methods. Acc. Chem. Res.* **2008**, *41*, 1486-1499.
- (315) Tran, N. T.; Min, T.; Franz, A. K. *Silanediol Hydrogen Bonding Activation of Carbonyl Compounds. Chem. - Eur. J.* **2011**, *17*, 9897-9900.
- (316) Mewald, M.; Schiffner, J. A.; Oestreich, M. *A New Direction in C-H Alkenylation: Silanol as a Helping Hand. Angew. Chem., Int. Ed.* **2012**, *51*, 1763-1765.
- (317) Chandrasekhar, V.; Boomishankar, R.; Nagendran, S. *Recent Developments in the Synthesis and Structure of Organosilanols. Chem. Rev.* **2004**, *104*, 5847-5910.
- (318) Shimizu, K.-i.; Kubo, T.; Satsuma, A. *Surface Oxygen-Assisted Pd Nanoparticle Catalysis for Selective Oxidation of Silanes to Silanols. Chem. - Eur. J.* **2012**, *18*, 2226-2229.
- (319) Kamachi, T.; Shimizu, K.-i.; Yoshihiro, D.; Igawa, K.; Tomooka, K.; Yoshizawa, K. *Oxidation of Silanes to Silanols on Pd Nanoparticles: H<sub>2</sub> Desorption Accelerated by Surface Oxygen Atom. J. Phys. Chem. C* **2013**, *117*, 22967-22973.
- (320) Jeon, M.; Han, J.; Park, J. *Transformation of Silanes into Silanols using Water and Recyclable Metal Nanoparticle Catalysts. ChemCatChem* **2012**, *4*, 521-524.
- (321) Mitsudome, T.; Noujima, A.; Mizugaki, T.; Jitsukawa, K.; Kaneda, K. *Supported gold nanoparticle catalyst for the selective oxidation of silanes to silanols in water. Chem. Commun.* **2009**, 5302-5304.
- (322) Urayama, T.; Mitsudome, T.; Maeno, Z.; Mizugaki, T.; Jitsukawa, K.; Kaneda, K. *O<sub>2</sub>-enhanced catalytic activity of gold nanoparticles in selective oxidation of hydrosilanes to silanols. Chem. Lett.* **2015**, *44*, 1062-1064.
- (323) Asao, N.; Ishikawa, Y.; Hatakeyama, N.; Menggenbateer; Yamamoto, Y.; Chen, M.; Zhang, W.; Inoue, A. *Nanostructured Materials as Catalysts: Nanoporous-Gold-Catalyzed Oxidation of Organosilanes with Water. Angew. Chem., Int. Ed.* **2010**, *49*, 10093-10095.
- (324) Ma, L.; Leng, W.; Zhao, Y.; Gao, Y.; Duan, H. *Gold nanoparticles supported on the periodic mesoporous organosilica SBA-15 as an efficient and reusable catalyst for selective oxidation of silanes to silanols. RSC Adv.* **2014**, *4*, 6807-6810.
- (325) John, J.; Gravel, E.; Hagege, A.; Li, H.; Gacoin, T.; Doris, E. *Catalytic Oxidation of Silanes by Carbon Nanotube-Gold Nanohybrids. Angew. Chem., Int. Ed.* **2011**, *50*, 7533-7536.
- (326) Rahman, G. M. A.; Guldi, D. M.; Zambon, E.; Pasquato, L.; Tagmatarchis, N.; Prato, M. *Dispersible carbon nanotube/gold nanohybrids: Evidence for strong electronic interactions. Small* **2005**, *1*, 527-530.
- (327) Liu, T.; Yang, F.; Li, Y.; Ren, L.; Zhang, L.; Xu, K.; Wang, X.; Xu, C.; Gao, J. *Plasma synthesis of carbon nanotube-gold nanohybrids: efficient catalysts for green oxidation of silanes in water. J. Mater. Chem. A* **2014**, *2*, 245-250.
- (328) da Silva, A. G. M.; Kisukuri, C. M.; Rodrigues, T. S.; Candido, E. G.; de Freitas, I. C.; da Silva, A. H. M.; Assaf, J. M.; Oliveira, D. C.; Andrade, L. H.; Camargo, P. H. C. *MnO<sub>2</sub> nanowires decorated with Au ultrasmall nanoparticles for the green oxidation of silanes and hydrogen production under ultralow loadings. Appl. Catal., B* **2016**, *184*, 35-43.
- (329) Chauhan, B. P. S.; Sarkar, A.; Chauhan, M.; Roka, A. *Water as green oxidant: a highly selective conversion of organosilanes to silanols with water. Appl. Organomet. Chem.* **2009**, *23*, 385-390.
- (330) Mitsudome, T.; Arita, S.; Mori, H.; Mizugaki, T.; Jitsukawa, K.; Kaneda, K. *Supported silver-nanoparticle-catalyzed highly efficient aqueous oxidation of phenylsilanes to silanols. Angew. Chem., Int. Ed.* **2008**, *47*, 7938-7940.
- (331) Li, Z.; Zhang, C.; Tian, J.; Zhang, Z.; Zhang, X.; Ding, Y. *Highly selective oxidation of organosilanes with a reusable nanoporous silver catalyst. Catal. Commun.* **2014**, *53*, 53-56.
- (332) Ito, H.; Takagi, K.; Miyahara, T.; Sawamura, M. *Gold(I)-phosphine catalyst for the highly chemoselective dehydrogenative silylation of alcohols. Org. Lett.* **2005**, *7*, 3001-3004.

- (333) Hara, K.; Akiyama, R.; Takakusagi, S.; Uosaki, K.; Yoshino, T.; Kagi, H.; Sawamura, M. *Self-assembled monolayers of compact phosphanes with alkanethiolate pendant groups: remarkable reusability and substrate selectivity in Rh catalysis*. *Angew. Chem., Int. Ed.* **2008**, *47*, 5627-5630.
- (334) Caseri, W.; Pregosin, P. S. *Hydrosilylation chemistry and catalysis with cis-PtCl<sub>2</sub>(PhCH:CH<sub>2</sub>)<sub>2</sub>*. *Organometallics* **1988**, *7*, 1373-1380.
- (335) Mukherjee, D.; Thompson, R. R.; Ellern, A.; Sadow, A. D. *Coordinatively Saturated Tris(oxazolonyl)borato Zinc Hydride-Catalyzed Cross Dehydrocoupling of Silanes and Alcohols*. *ACS Catal.* **2011**, *1*, 698-702.
- (336) Mitsudome, T.; Yamamoto, Y.; Noujima, A.; Mizugaki, T.; Jitsukawa, K.; Kaneda, K. *Highly efficient etherification of silanes by using gold nanoparticle catalyst: remarkable effect of O<sub>2</sub>*. *Chem. - Eur. J.* **2013**, *19*, 14398-14402.
- (337) Blandez, J. F.; Esteve-Adell, I.; Alvaro, M.; Garcia, H. *Palladium nanoparticles supported on graphene as catalysts for the dehydrogenative coupling of hydrosilanes and amines*. *Catal. Sci. Technol.* **2015**, *5*, 2167-2173.
- (338) Mikami, Y.; Noujima, A.; Mitsudome, T.; Mizugaki, T.; Jitsukawa, K.; Kaneda, K. *Highly efficient gold nanoparticle catalyzed deoxygenation of amides, sulfoxides, and pyridine N-oxides*. *Chem. - Eur. J.* **2011**, *17*, 1768-1772.
- (339) Taori, V. P.; Buchmeiser, M. R. *Tandem-reduction of DMF with silanes via necklace-type transition over Pt(0) nanoparticles: deciphering the dual Si-H effect as an extension of steric effects*. *Chem. Commun.* **2014**, *50*, 14820-14823.

## 8. Biography of authors.

**Juan M. Asensio.** Juan M. Asensio obtained his degree in chemistry from the University of Alcalá (Spain). After finishing his master in Inorganic Chemistry, in 2012 he started a PhD at the University of Alcalá under the supervision of Prof. Ernesto de Jesús and Dr. Román Andrés. During his PhD, his research focused on the aqueous chemistry of Pd organometallic complexes and nanoparticles. Since 2016, he is a post-doctoral research scientist at the LPCNO of Toulouse under the supervision of Bruno Chaudret. His work focuses on the synthesis of nanoparticles for magnetically-induced catalysis as well as for catalysis in solution.

**Donia Bouzouita.** Donia Bouzouita obtained her engineering degree in chemistry in 2015 at the INSAT of Tunisia. During her master internship in the LPCNO of Toulouse, she studied the synthesis and the self-assembly of Pt nanoparticles for electronic applications. Since 2016, she is a PhD student in the LPCNO of Toulouse under the supervision of Bruno Chaudret and Simon Tricard. Her PhD focuses on the isotopic labeling of molecules with biological interest through C-H activation catalyzed by metal nanoparticles.

**Piet W. N. M. van Leeuwen.** After his PhD in Leyden University on coordination chemistry Piet van Leeuwen started with Shell Amsterdam in 1968 and worked on organometallic chemistry and catalysis. Since 1978 he was head of the section "Fundamental aspects of homogeneous catalysis". In 1990 he initiated the homogeneous catalysis group at the University of Amsterdam and moved

there full-time in 1994. From 2000 till 2005 he was a part-time professor of industrial homogeneous catalysis in Eindhoven and director of the National-Research-School-Combination-Catalysis. In 2004 he started in ICIQ in Tarragona till 2015. Then he moved to INSA-Toulouse, where he works in LPCNO. Since 2009 his work focuses on ligand effects in metal nanoparticle catalysis.

**Bruno Chaudret.** Bruno Chaudret graduated from Ecole Nationale de Chimie de Paris in 1975, obtained his PhD from Imperial College London in 1977 and his Doctorat d'Etat in 1979 from Université Paul Sabatier Toulouse. After having been director of the Laboratoire de Chimie de Coordination CNRS in Toulouse (2007-2011) and President of the Scientific Council of CNRS (2010-2018), he is currently Directeur de Recherche CNRS and director of the LPCNO. He has been a member of the French Academy of Sciences since 2005. His main research interests concerned first interactions of  $\sigma$ -bond with transition metal complexes, in particular dihydrogen complexes. Since 1990, he developed the synthesis of organometallic nanoparticles, their surface chemistry and their applications in catalysis, magnetism and micro- nano-electronics.

## Table of Content:

$\sigma$ -Bond Activation on Metal NPs

